TOWARDS SCIENTIFIC MANUFACTURING:

THE EFFECTS OF SHEAR RATE, STRAIN, AND COMPOSITION ON THE PROPERTIES OF BLENDS AND TABLETS

by

MARCOS LLUSA

A dissertation submitted to the

Graduate School-New Brunswick

Rutgers, The State University of New Jersey

In partial fulfillment of the requirements

For the degree of

Doctor of Philosophy

Graduate Program in

Chemical and Biochemical Engineering

Written under the direction of

Professor Fernando J. Muzzio

And approved by

____

____

____

____

____

New Brunswick, New Jersey

May, 2008

ABSTRACT OF THE DISSERTATION

Towards scientific manufacturing:

The Effects of Shear Rate, Strain, and Composition on the Properties of Blends and Tablets

by

MARCOS LLUSA

Dissertation Director:

Professor Fernando J. Muzzio

This dissertation aims at understanding the effects of formulation (type of excipient, APAP grade, lubricant concentration) and processing conditions (shear rate and strain) on the following properties of pharmaceutical blends and tablets:

1. Degree of Active Pharmaceutical Ingredient (API) agglomeration and homogeneity.
2. Density, flowability, and hydrophobicity of lubricated formulations.
3. Tablet hardness.

Another aim is to develop a method to assess the API de-agglomeration in blenders, when only a small fraction of the blend is sampled.

The blend properties examined are those that impact on the quality of the product: blend density determines the amount of powder that fills the tablet dies, blend

hydrophobicity determines the dissolution properties of tablets, powders, or capsules, and API agglomeration determines the probability of having out-of-specification products.

The experimental method uses a shear cell where shear rate and strain can be controlled. The different blend properties are measured using suitable analytical techniques.

For the assessment of API de-agglomeration in blenders, a numerical method is developed to design sampling protocols that detect and characterize agglomerates with a degree of statistical confidence.

The results show that:

1. The degree of API agglomeration decreases as a function of strain, and independently of shear rate. A coarser API presents a significantly smaller degree of agglomeration than a finer API. De-agglomeration proceeds at very similar rates in different excipients.
2. Blend hydrophobicity increases steadily as a function of strain and lubricant concentration. Larger shear rates increase hydrophobicity even further. Tapped density of lubricated blends increases as a function of strain until reaching a maximum value, independently of shear rate. The flowability of lubricated blends is enhanced but independently of strain and shear rate they have been exposed to.
3. The tablet crushing hardness is a function of the strain applied to lubricated blends and independent of the shear rate.

The statistical method used to detect and characterize API agglomerates in blenders yields concentration profiles that compare very well to the experimental concentration profile. This procedure validates the parameters that describe the agglomerate population (with a normal distribution of sizes) in a blend.

Acknowledgements

I am largely indebted to a number of undergraduate students in the Chemical Engineering program at Rutgers University that helped me carrying out the extensive experimentation presented here. They are Akila R. De Alwis, Ana Chavez, Martin Chen, Howard K. Eichenblatt, Robin George, Roberto Gerardi, Sheri Jones, Jenilee Julien, Muhammad M. Kizilbash, Brian T. Koo, Oleg Milberg, Marilyne Nguyen, Richard Nti-Cyabaab, Eleanor C. Okubor, Daniel Paznek, Mosidi Phaladze, Henny Salim, Bini Shah, Nikisha Shah, Abilasha Singh, Jamar Tyndale, and also to Wandilys Vargas, a student from University of Puerto Rico that collaborated during an entire summer.

Also, to Bodhi Chaudhuri, a post-doc I worked with during more than a year. At his side I learnt a great deal about Discreet Elements Methods, and he also became a true friend.

To Dr. Norma Gonzalez, the director of the Fulbright commission in Argentina, and her team, for the encouragement, advice, and support that helped me succeed in graduate school. Especial thanks to the Fulbright Foundation and the Graduate School at Rutgers University that provided the economic support during my first two years.

To Dr. Michael Levin and his amazing team at Metropolitan Computer Corporation. Most of the work in this dissertation would have not been possible without their unparalleled capability to design and manufacture equipment such as the controlled shear environment and the tableting instrumentation used here, and also without their intellectual input.

To my committee members Dr. Marianthi Ierapetritou, Dr. Bo Michniak-Kohn, and Dr. Silvina Tomassonne. Their comments have been crucial to develop this work and my education.

I am especially grateful to my advisor Fernando Muzzio because he has shaped my intellectual growth and has always set me to do my best. It has been a privilege to be exposed to his insight and to be part of his research group. The diversity of projects, ideas, and people in this group has given me a unique opportunity to learn and grow.

Finally, to my family, that from the distance in Argentina has always supported me in my endeavors, and to my friends at Rutgers with whom I have enjoyed so many good moments.

Table of Contents

LIST OF FIGURES

LIST OF TABLES

Chapter I

Introduction

Motivation

The next decade will present many opportunities for the Pharmaceutical industry to develop new business and improve the health of the population worldwide. Demography, economics, and new policies are some of the factors that generate these opportunities. However, only companies that are able to undertake fundamental transformations in current practices in R&D, development, manufacturing, commercialization, and distribution of new, safer, and less expensive products will succeed in the coming decade [1-7]. It is expected that the manufacturing processes will become much more flexible, with different manufacturing routes for different kind of products. They should also be more robust. The FDA has already issued the "GMPs for the 21st Century" initiative that calls for the design of effective and efficient manufacturing processes to assure product quality and performance, product specifications based on a mechanistic understanding of how different formulations, and processes affect product performance; and continuous real-time assurance of quality [8]. This dissertation presents several methods to understand and quantify how formulation and processing variables affect the properties of intermediates and final product in the manufacturing of pharmaceutical tablets or capsules.

1-1. Introduction and plan for this dissertation

Most pharmaceutical manufacturing activities rely on making granular solids, processing them, and assembling them into a therapeutical dosage form. The procedure to design a manufacturing process for pharmaceutical tablets or capsules involves four steps: Identification of product quality factors (functional, physical, sensorial), product formulation, design of manufacturing process (flowsheet with equipment and operating conditions), and to evaluation of the product and the processes to ensure that the product possesses the desired quality factors [9]. Manufacturing activities are classified into three broad areas; two of them are related to the making of the granular material and the third one is related to the process and assembly of a dosage [9]. The first area involves chemical and phase changes in which particles are generated, consumed, or transformed; examples include reaction, crystallization, and dissolution. The second area involves separation processes for the product of the reactor or crystallizer, which is often a slurry of solids crystals; examples include flotation, filtration, dewatering, and drying. Most of the liquid content of the original slurry is removed at this stage, leaving behind a bulk solid with moisture content below about 5%.

The third area, related to the process and assembly of a dosage (i.e. tablet, capsule, powder), deals with the crushing, agglomeration, blending, and compaction of bulk granular solids. Here, product specification such as size, shape, and composition are set and met. In order to manufacture a solid dosage, a sequence of operations must be performed (Figure 1-1 shows a typical sequence of operations, although not all of them are necessarily applied). Currently, there are many efforts to understand and quantify how formulation and processing variables affect product performance [9-17], motivated by the growing need to develop products with more complex tissue targeting and drug delivery requirements and the introduction of stronger regulatory expectation regarding quality control.

One of the major drawbacks of existing manufacturing processes (Figure 1-1) for solids products is that shear rates and stresses in most processing units are not easy to assess with current technology. At best, only the order of magnitude for shear rate is known. Based on such limited knowledge of shear rate, one selects equipment to blend cohesive drugs, which is expected to provide stresses larger than the API inter-particle forces; milling equipment, which should provide stresses larger than the crystal lattice strength; and wet granulators, where the shear rate determines the granule size distribution. The effects of strain, which is the cumulative exposure of material to shear, can not be quantitatively assessed. Due to this lack of knowledge on shear rates and strain, equipment scale-up is also difficult. Shear rate and strain affect most quality factors of tablets and capsules (i.e. active pharmaceutical ingredient (API) homogeneity and degree of agglomeration, and disintegration, dissolution, and mechanical properties of tablets), because shear rate can affect the segregation [18, 19] and the electrical charging of particles [20] and consequently the homogeneity of blends and dosages, and also the flow properties of lubricated blends and the dissolution and mechanical properties of tablets. In fact, the variables that determine the performance of solid products can be grouped under a few categories (Figure 1-2): Raw Materials, Blending, Lubrication, Dry Granulation, Compression, and Control and Sensing. It is generally the ignorance on the effects of shear rate and strain in the lubrication process and in the blending process (which are expressed here in terms of blender speed, design, operation parameters, and residence time) that lead to an unpredictable tablet CU, hardness, and dissolution and to products that fail to meet quality and performance specifications.

As a consequence of the uncertainty in shear conditions, the correlation of shear rate and strain with the properties of blends, tablets, or capsules is difficult, and process design is limited to empirical methods. This dissertation uses a new instrument (Controlled shear environment) that generates uniform shear conditions and allows studying the effect of shear rate and strain on API de-agglomeration and several other properties of lubricated blends and tablets; specifically, hydrophobicity, density, flowability, and tablet hardness are examined.

The occurrence of an agglomerate is a local event, and due to the typically limited number of samples typically taken, their detection is a rare event. Therefore, the assessment of agglomerate population characteristics is often based on scarce data. Data on a few agglomerates can only be interpreted in the context of a properly designed statistical method. In order to study the API de-agglomeration capability of blending units, a statistical method based on the typical limited number samples and the characteristics of the agglomerates must be developed. However, correlation with shear rate or strain is difficult because shear conditions in blenders are typically non-uniform.

Section 1.2 lays the objectives for this dissertation and the Sections 1.3 and 1.4 present the experimental background to study shear in granular flows and blenders.

1-2. Objectives for this dissertation

Shear rates and strain have multiple effects on the properties of blends and finished products, and have massive impact on the properties of two minor but critical components of the formulation (API and lubricant). Thus, our objectives are:

1. Study the impact of operating conditions and scale of different blending units and processes on minimization of API agglomeration (Chapter 2).
2. Develop a method to analyze the de-agglomeration in blenders using scarce data from typical sampling protocols (Chapter 3).
3. Study the impact of shear rate and strain on API de-agglomeration (Chapter 4).
4. Study the impact of shear rate and strain on the lubricant homogeneity, density, flowability, and tablet hardness of lubricated blends (Chapter 5), and more in-depth study of their effect on the hydrophobicity of lubricated blends, because it directly impacts tablet dissolution (Chapter 6).

The sequence of objectives and chapters follows the typical manufacturing outline. First, there is the mixing of API and excipients. Additionally, the sequence of chapters dealing with API de-agglomeration starts with a comparative study (based on RSD and mixing curves) of the conditions that minimize API agglomeration in blending units, followed by the development of a method to assess the extent and characteristics of agglomeration for a specific operating condition (based on concentration profiles and statistical analysis), and ends with a study of the effect of fundamental variables on API de-agglomeration. Later there is the addition of lubricant to the formulation.

In the Chapters on lubrication, we analyze the effect of shear rate and strain on the properties of blends and tablets. The properties include density, hydrophobicity, flowability, lubricant homogeneity, and tablet hardness.

In Section 1.3, some useful background that can help the reader visualize and understand the concept of shear rate and shear stress is introduced. Although this information applies mainly to free-flowing materials, it helps to interpret the effects of fill level, tumbling speed, and scale of a blender on API de-agglomeration presented in subsequent chapters. Cohesive powders have a more complex behavior, due to phenomena such as non-uniform dilation and the inability to fluidize, and the regimes described in Section 1.3 are no longer valid.

1.3 Shear in granular processes. Shear cells

In most flowing powders, there is typically a slip failure zone between coherent blocks of material. In this zone, known as the shear band, there is a velocity gradient which translates into a shear rate. Shear bands are typically between 5 to 20 particle diameters wide, and they are reported to be wider within the bulk flow of a controlled shear environment [21]. The Couette geometry is used in this dissertation because it generates a nearly uniform flow to study the effects of shear rate on blends.

Shear stresses determine the ability of a flow to micro-homogenize cohesive material in a mixing process (i.e. the stresses should be large enough to separate a cohesive API into the individual particles), or to reduce particle size in a milling process. Shear rate is a very important fundamental variable because it determines the mechanism for stress transmission in a flowing powder without interstitial fluid [22, 23]. Typically, three regimes (Figure 1-3) are identified:

1- Slow, frictional flow with extended sticking, sliding, or rolling particle contacts, that occurs under very slow shear. This flow typically has a high solids fraction. Coulomb materials at the onset of yielding constitute a good example. Stresses range from moderate to high and they are determined by forces applied at boundaries, which cause surface friction, particle interlocking, and force networks. Inertia is negligible and there is no obvious relation between stress and strain.

2- Rapid, fluid-like flows develop under fast shear, characterized by low solids fractions. Particles move independently of neighbors, resembling molecules in a gas. Their velocities consist of a mean flow component and a random fluctuating component described by the granular temperature (similar to the role of thermodynamic temperature for molecular gasses). Collisions are binary and instantaneous. Stresses range from moderate to high, but they are never high enough to cause particle compression. Stress has a quadratic dependence on shear rate. This regime presents some variations or modes: fast turbulent-like, supercritical flow and slow, laminar-like, subcritical flow. For example, the flow in inclined channels has been successfully treated as rapid for both modes [24-26]. Frictional forces play a greater role in subcritical flows.

3- Intermediate, transitional regime, where a combination of rate dependent and rate independent stress generations occur. As in rapid flows, velocity fluctuations produce density fluctuations [27]. With increasing mean density, sustained clusters of particles in rubbing contact occur, increasing local stresses and in turn allowing further densification. Campbell defines both elastic–inertial and elastic-quasi-static sub-regimes in which force chains and large stress variations occur [28]. Particle friction (or interlocking) determines the stability of the stress networks, and even small concentration changes dramatically affect shear generation.

Additionally, the shear layer determines the mixing rate of a process [29, 30]. For example, a shear band with a stick-slip behavior (slow, frictional flow), which is mainly found when particles are cohesive, leads to a chaotic process with exponential mixing rates. When particles are free flowing (i.e. cohesionless), they do not present the stick-slip behavior (rapid flow), and the area generated by the mixing process grows linearly (i.e. constant mixing rate).

The next section discusses shear in blenders and how it can be influenced by fill level, speed of tumbling, and use of internal impeller. The section also describes shear cells, which provide the uniform conditions necessary to study the effects of shear rate and strain.

1.4 Shear in different units

Blenders are perhaps the units the most extensively studied because of their many applications in industry. There is a large variety of blending equipment, and the majority falls in the categories of either tumbling or convective blenders [31], and some continuous blenders [32]. The variables that determine the shear conditions for both types of blenders are those that affect the motion of powder within the vessel. In tumbling blenders, motion is the result of gravitational forces, and the materials mix via avalanching and folding. As the blender tumbles, there is an upper flowing layer and the bulk of material that follows the movement of the body as a solid [30]. Convective blenders, on the other hand, induce mixing through the motion of a blade in a stationary vessel. The powder moves within the vessel mainly as the result of the force applied by this blade and the shear rates depend exclusively on the velocity and the design of the blade.

The shear rates in a tumbling blender are a function of several variables. For example, the speed of rotation determines both the particle velocities and the characteristics of the flowing layer [33]. As tumbling speed increases, the flowing layer shows different characteristics and is classified accordingly into avalanching, rolling, cataracting and centrifuging regimes. Centrifuging is obviously the worst regime for mixing purposes because the powder tends to just follow the motion of the vessel. Another important variable is the scale of the blender, and larger scales generate larger shear rates [34, 35]. The fill level impacts the velocities of particles in the flowing layer [36], and consequently, the shear rates and the quality of mixtures. For higher fill levels there is also a larger proportion of material resting at the bottom of the vessel not exposed to the shear rates of the flowing layer. Shear rates in tumbling blenders can always be increased using moving internals (i.e. intensifier bar or impeller).

All the blend properties mentioned in the objectives of this dissertation are critical for pharmaceutical product quality. However, blend properties derived from lubrication are relatively easier to study than API de-agglomeration because the scale at which they are tested (pharmaceutical samples) is less sensitive to the non-uniformity in blending conditions. On the other hand, API de-agglomeration is a local event, and can have a large impact on the API concentration of samples. The main problem with API agglomerates in blenders is their detection and characterization. Material properties such as flowability and density also affect the shear rates in a blending unit [34].

Blenders are not the most adequate unit to study the effect of shear rates and strain on blend properties because the material is exposed to widely non-uniform shear conditions. For example, some tumbling blenders show poor diffusive or convective mixing, which results in islands of regular, non-chaotic flow, where shear is very low, while the surrounding regions are well mixed by chaotic advection and exponentially stretched.

There are some fundamental geometries (i.e. simple shear, Couette, and gravity-driven flows) that guarantee a uniform exposure of the blend to shear. These geometries also allow studying convective effects (such as may occur in flow over blades) and diffusive mixing (such as that in a paddle blender, or horizontal drums). Although the results are not immediately applicable to specific equipment, the principles revealed can help understand a more varied range of operations and processes [36]. This approach has been successfully used for fluids processes [37], and it will be applied here to investigate two granular processes: API de-agglomeration and the lubrication of blends.

The shear cell with the Couette geometry has been extensively used and characterized, and can easily generate shear rates in the three shear regimes by operating the internal cylinder at different speeds [38-41]. The internal stresses can be determined in a granular system and are found to be a function of shear rate and also the type of deformation (i.e. elastic or inelastic). In addition, this geometry has been used to show that shear bands not only occur near a system boundary but also in the bulk of the flow, and can become arbitrarily broad. In this geometry, the bulk velocity can be described by a universal law with the form of an error function. The velocity profiles are independent of shear rate; however they are affected by the granular microstructure. Particle velocity (motion within the shear band and inter-particle slip), particle rotation, and packing density in three dimensions have been characterized with several non-intrusive experimental techniques (magnetic resonance imagining, X-ray tomography and high-speed video particle tracking).

Most of these findings about the Couette geometry have been recorded using with large particle sizes (seeds, disks, etc) [42, 43]. However, the focus of this dissertation is to study the impact of shear rate and strain on pharmaceutical powders, which have another range of particle size (microns). While the bulk of large, free-flowing particles in the traditional Couette geometry acquires kinetic momentum by the force transmitted by a rough wall (i.e. with large particles tethered to the wall), the micron-sized particles can not develop momentum by this method. On the contrary, the powder bulk of micron sized particles slips from the moving wall. The reason is that cohesive powders show a wide range of density, and the cohesive stresses in the controlled shear environment would cause centrifugal densification and no shear. Instead, the free flowing large particles dilate and compact little and they move with the rough wall. In order to generate uniform flow conditions for most pharmaceutical powders, the walls of the cylinders need more than the asperity of particles attached to the surface. The traditional Couette geometry is modified by attaching some equally spaced protruding pins that are capable of transferring momentum to the bulk of powder, even when the powder becomes denser.

Despite the non-uniform shear conditions of blenders and the lack of methods to assess them, it is important to establish the effect that operating variables and different processing protocols have on issues such as API agglomerate mitigation. The practitioner can profit from this information and make the most advantageous utilization of mixing equipment. The following chapter studies in great detail the effect of different practices on agglomerates mitigation, such as the conditioning of pure API prior to loading the blender, the effects of operation parameters for low shear equipment, and the effect of using different high shear units in the process.

REFERENCES

1- “Pharma 2020: The vision. Which path will you take?”. PricewaterhouseCoopers. http://www.pwc.com/extweb/pwcpublications.nsf/docid/91BF330647FFA402852572F2005ECC22

2- “Pharma 2005:. Marketing to the Individual”. PricewaterhouseCoopers. www.pwc.com/gx/eng/about/ind/pharma/marketing_to_individual.pdf

3- “Pharma 2005: An Industrial Revolution in R&D”. PricewaterhouseCoopers. http://www.pwc.com/gx/eng/about/ind/pharma/industrial_revolution.pdf

4- “Pharma 2010: The threshold of innovation”. IBM Institute for Business Value. http://www-03.ibm.com/industries/healthcare/doc/content/resource/insight/941673105.html

5- HealthCast 2010: Smaller World, Bigger Expectations (November 1999). PricewaterhouseCoopers. http://www.pwc.com/il/heb/about/svcs/publication/alerts/3HEALTHCAST_2010.pdf

6- “Pharma 2010: The value-creating supply chain”. IBM Institute for Business Value. http://www-935.ibm.com/services/us/index.wss/ibvstudy/imc/a1002998?cntxtId=a1000060

7- US Food and Drug Administration, “Final report on Pharmaceutical cGMPs for the 21st Century – A risk-based Approach” (Fall 2004). http://www.fda.gov/cder/gmp/gmp2004/GMP_finalreport2004.htm

8- US Food and Drug Administration, “Final report on Pharmaceutical cGMPs for the 21st Century – A risk-based Approach” (Fall 2004). http://www.fda.gov/cder/gmp/gmp2004/GMP_finalreport2004.htm

9- Fung, K.Y.; Ng, K.M. Product-centered processing: Pharmaceutical tablets and capsules. *AIChE Journal* 49 (2003), p. 1193.

10- Fung, K.Y.; Ng, K.M. Product-centered processing: Pharmaceutical tablets and capsules. *AIChE Journal* 49 (2003), p. 1193.

11- Edwards, M.F.; Instone, T. Particulate products-their manufacture and use. *Powder Technology* 119 (2001), p. 9.

12- Hardy, I.J.; Cook, W.G. Predictive and correlative techniques for the design, optimization and manufacture of solid dosage forms. *Journal Pharm Pharmacol.* 55 (2003), p. 3.

13- Wibowo, C.; Ng, K.M. Synthesis of bulk solids processing systems. *AIChE Journal* 45 (1999), p. 1629.

14- Torquato, S.; Hyun, S.; Donev, A. Optimal design of manufacturable three-dimensional composites with multifunctional characteristics. *Journal of Applied Physics* 94 (2003), p. 5748.

15- Gani, R. Chemical Product Design: Challenges & Opportunities. *Computers and Chemical Engineering* 28 (2004), p. 2441.

16- Kind, M. Product engineering. *Chemical Engineering and Processing* 38 (1999), p. 405.

17- Costa, R.; Moggridge, G.D.; Saraiva, P.M. Chemical product engineering: An emerging paradigm within chemical engineering. *AIChE Journal* 52 (2006), p. 1976.

18- Savage, S.B.; Lun, C.K.K. Particle size segregation in inclined chute flow of dry cohesionless granular solids. Journal of Fluid Mechanics 189 (1988), p. 311.

19- Stephens, D.J.; Bridgewater, J. The mixing and segregation of cohesionless particulate materials. Failure zone formation. Powder Tech. 21 (1978), p. 17.

20- Schönert, K.; Eichas, K.; Niermöller, F. Charge distribution and state of agglomeration after tribocharging fine particulate materials. Powder Technology 86 (1996), p. 41.

21- Fenistein, D.; van Hecke, M. Wide shear zones in granular bulk flow. Nature 425 (2003), p.256.

22- Tardos, G.I.; McNamara, S.; Talu, I. Slow and intermediate flow of a frictional bulk powder in the Couette geometry. Powder Technology 131 (2003), p. 23.

23- Hartley, R.R.; Behringer, R.P. Logarithmic rate dependence of force networks in sheared granular materials. Nature 421 (2003), p.928.

24- Savage, S.B. Gravity flow of cohesionless granular materials in chutes and channels. J. Fluid Mech. 92 (1979), p. 53.

25- Johnson, P.C.; Nott, P.; Jackson, R. Frictional–collisional equations of motion for participate flows and their application to chutes. J. Fluid Mech. 210 (1990), p. 501.

26- Louge, M.Y.; Keast, S.C. On dense granular flows down flat frictional inclines. Physics of Fluids 13 (2001), p. 1213.

27- Savage, S.B. The mechanisms of rapid granular flows. (in Advances in applied mechanics). 1984, Academic Press, Inc., p. 289.

28- Campbell, S.C. Granular shear flows at the elastic limit. J. Fluid Mech. 465 (2002), p. 261.

29- Shinbrot, T.; Alexander, A.; Moakher, M.; Muzzio F.J. Chaotic granular mixing. Chaos 9 (1999), p. 611.

30- Shinbrot, T.; Alexander, A.; Muzzio, F.J. Spontaneous chaotic granular mixing. Nature 397 (1999), p.675.

31- Harnby, N. An engineering view of pharmaceutical powder mixing. Pharmaceutical Science & Technology Today 3 (2000), p. 303.

32- Pernenkil, L.; Cooney, C.L. A review on the continuous blending of powders. Chemical Engineering Science 61 (2006), p. 720.

33- Sudah, O.S.; Coffin-Beach, D.; Muzzio, F.J. Effects of blender rotational speed and discharge on the homogeneity of cohesive and free-flowing mixtures. International Journal of Pharmaceutics 247 (2002), p. 57.

34- Johanson, K. Predicting cone-in-cone blender efficiencies from key material properties. Powder Technology 170 (2006), p. 109.

35- Wu, L.S.; Pang, J.; Chen, J.G.; Hussain, M.A. Dry Blending Process Scale-up for a Very Low Dose Drug Candidate. AAPS PharmSciTech, 2000.

36- Bridgwater, J. Fundamental powder mixing mechanisms. Powder Technology 15 (1976), p. 215.

37- Michaels, J.N. Toward rational design of powder processes. Powder Technology 138 (2003), p. 1.

38- Kumara, J.; Lakshmana Rao, C.; Massoudi, M. Couette flow of granular materials. International Journal of Non-Linear Mechanics 38 (2003), p. 11.

39- Mueth, D.M.; Debregeas, G.F.; Karczmar, G.S.; Eng, P.J.; Nagel, S.R.; Jaeger, H.M. Signatures of granular microstructure in dense shear flows. Nature 406 (2000), p.385.

40- Miller, B.; O'Hern, C.; Behringer, R.P. Stress Fluctuations for Continuously Sheared Granular Materials. *Physical Review Letters* 77 (1996), p. 3110.

41- Savage, S. B.; Sayed, M. Stresses developed by dry cohesionless granular materials sheared in an annular shear cell. *Journal of Fluid Mechanics* 142 (1984), p. 391.

42- Elliott, K.E.; Ahmadi, G.; Kvasnak, W. Couette flows of a granular monolayer—an experimental study. J. Non-Newtonian Fluid Mech. 74 (1998), p. 89.

43- Karion, A.; Hunt, M.L. Wall stresses in granular Couette flows of mono-sized particles and binary mixtures. Powder Technology 109 (2000), p.145.

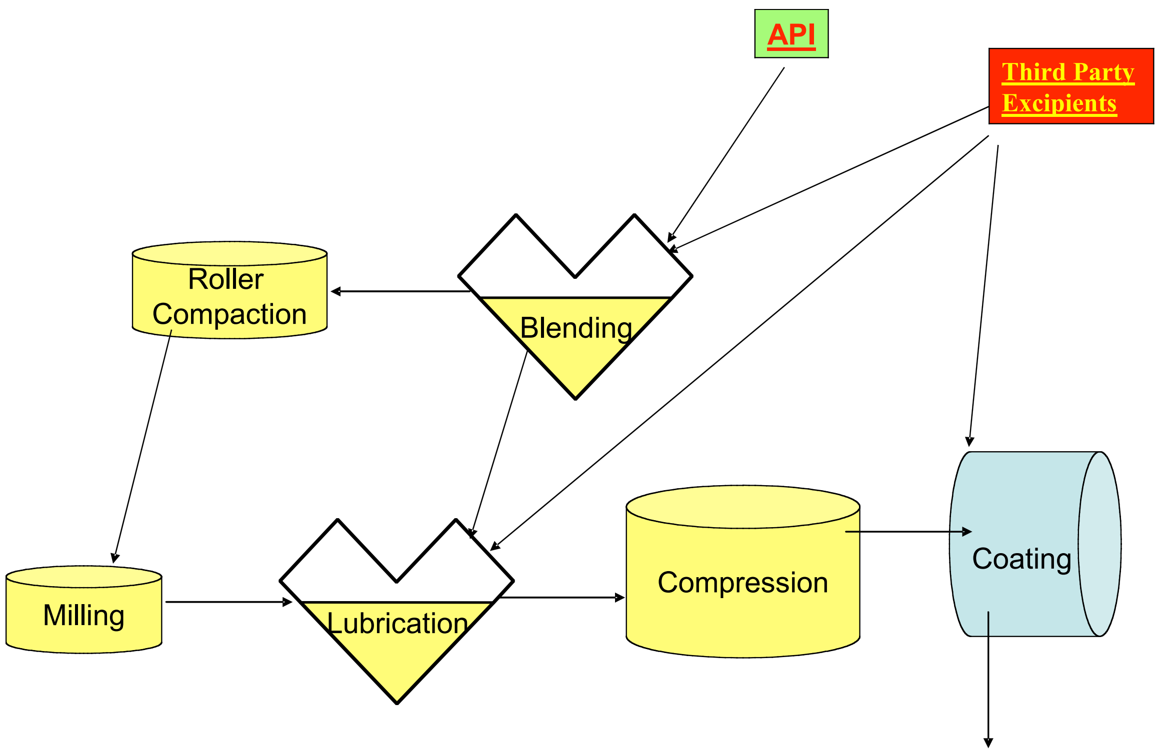

Figure 1-1: Sequence of dry solid operations to assemble a pharmaceutical dosage

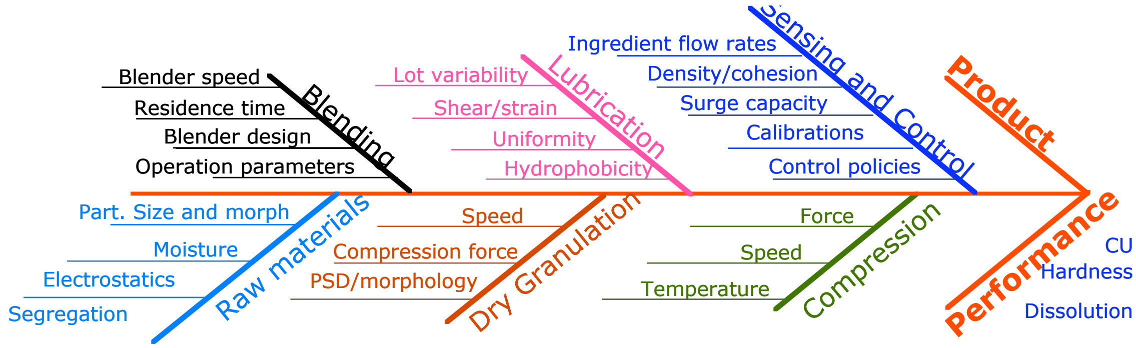

Figure 1-2: Groups of factors that contribute to the product performance

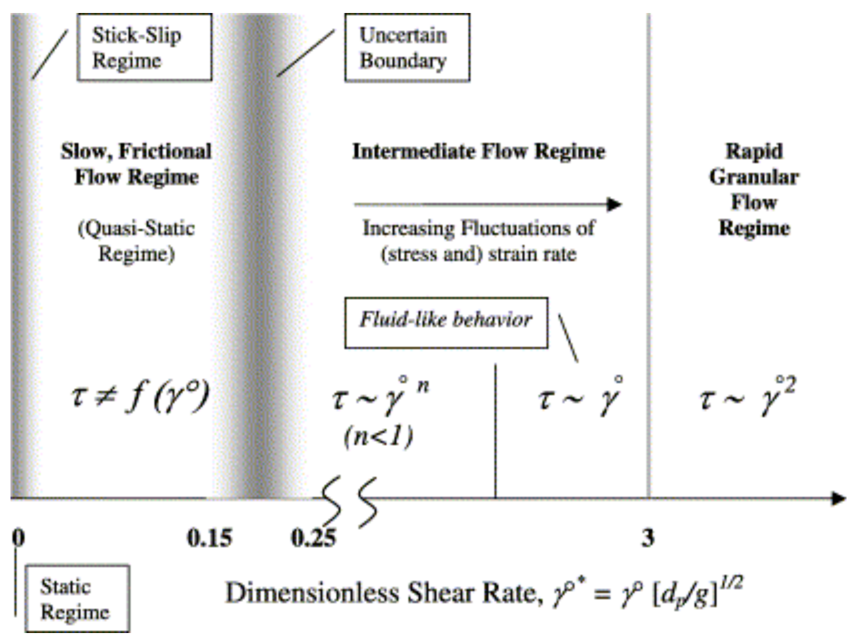

Figure 1-3: Shear regimes as determined by shear rate (diagram by Tardos [21])

CHAPTER II

MITIGATING DRUG AGGLOMERATION IN BLENDERS AND PROCESSES

Summary

This chapter[1] examines the effect of different blender parameters and the effectiveness of several processes on the mitigation of active pharmaceutical ingredients (API) agglomerates in solid formulations.

The results show that API de-agglomeration is sometimes a reversible process and agglomerates may form again. Additionally, parameters like fill level and scale affect the API de-agglomeration performance of a blender, while baffles do not affect it at all. Against common belief, the inclusion of a moving internal (i.e. impeller) in a bin blender may not always lead to an improvement in the API de-agglomeration performance. The design and the positioning of the impeller play an important role as well.

The de-agglomeration reversibility is minimized when the API is pre-blended with some excipients in a high shear unit or when the final blend is passed through a mill. The effectiveness of these two processes is compared, and the pre-blend of API and excipients in a high shear unit, followed by dilution in a larger blender (300-liters) yields similar API concentration variance and de-agglomeration than blending all API and excipients in a blender (300-liters) and then milling the final blend. The scale-up of these

---

[1] Special thanks to Osama Sudah for providing the picture of NaCl agglomerates in Figure 2-8, and Kurt Sturm for providing the data to study the effects of scale, pre-blending, and milling of blends

two types of process, in general, leads to more extensive API de-agglomeration, as larger blenders are involved.

2-1 Introduction

This chapter begins describing API agglomerates, the conditions that favor their existence, and their consequences for solid pharmaceutical products. Subsequently, it describes shear in granular processes, which is the mixing mechanism that leads to de-agglomeration. Finally, it compares different approaches (milling pure API, pre-blending API, scale of blender, etc) to minimize API agglomeration in a solid formulation.

Cohesive powders are characterized by inter-particle forces (capillary, Van der Waals, solid bridge, etc) much larger than the particle weight. These inter-particle forces, which are determined by the nature of the granular material (chemical, electric) and also by environmental conditions (humidity), cause particles to have a strong tendency to adhere to each other and form agglomerates. Agglomerates constitute an omnipresent problem in almost every type of industry, including food [1], construction [2], paints [3], and pharmaceuticals. API agglomeration, which is documented in the literature for a variety of granular materials and processes [4, 5], is the primary cause of several problems for dry solid pharmaceutical formulations [6]. API agglomerates are particularly a challenge for the preparation of potent, low-dose direct compression formulations. They increase the variability in blend and tablet API concentration [7, 8], and sometimes generate inadmissibly super potent tablets [9, 10]. Agglomerates have been identified in previous studies as a manifestation of poor micro-mixing, decreasing the homogeneity of blend and tablet uniformity [11]. Additionally, they sometimes dissolve more slowly than dispersed particles [12, 13], reducing the bioavailability of the drug. In fact, dissolution rates have been used to determine the degree of agglomeration of low solubility drugs in blends [14].

The variables that determine particle agglomeration include particle properties, and environmental and processing conditions. The first group includes particle size distribution, surface area, particle shape, characteristics of particle surface, material properties (i.e. electrical properties), etc. The second group includes relative humidity and tribo-electrification due to a high shear process (i.e. milling).

Particle size and particle surface area are closely linked. As particle size decreases, particle surface area and all the type of forces that are a function of this variable (i.e. Van der Waals), increase [15, 16]. Consequently, the behavior of small particles becomes dominated by surface forces and by neighboring particles rather than by the gravitational force. Surface characteristics also affect particle cohesion [17]. Smooth particles can develop large contact areas and therefore large interacting forces, which helps explain the decrease in cohesion via dry coating. Finally, electrical properties of materials can be extremely important for agglomeration [18-20] because electrical forces (i.e. dipoles, net charge, etc) can be several orders of magnitude larger than other surface forces (i.e. Van der Waals).

Higher environmental relative humidity leads to larger particle humidity content, which in turn, increases particle cohesion [21-24]. For large humidity content, the fluid can form bridges between particles, which is one of the key particle building mechanisms used in the wet granulation process. Processing may favor particle agglomeration. For example, when a powder is exposed to a high shear environment to produce micronization [25, 26], the outcome may be particles with a tendency to form agglomerates due to acquired electric charge and increased relative magnitude of surface forces (i.e. Van der Waals), thus failing to achieve the intended enhancement in drug homogeneity and solubility [27].

In order to separate agglomerates into single particles (or agglomerates of smaller size), the mechanical stresses externally applied to the aggregate must be larger than the adhesive forces within the agglomerate. This problem has long been studied in fluid-solid (wet) systems. The shear stresses in fluid and pastes can also be modeled using constitutive and continuity equations. Therefore, the conditions required to mix a granular solid in a fluid or a paste (i.e. a pigment in a paint, cement powder in a cement paste, etc) can be established experimentally as well as numerically [28-30]. On the other hand, the conditions to de-agglomerate a powder in a dry granular matrix are largely unknown and are usually established using empirical methods. The lack of realistic constitutive equations for granular material also limits the modeling to computational techniques such as DEM (Discrete Element Modeling).

Shear stresses are developed within a powder blend during the mixing process. Powder mixing takes place through a combination of three mechanisms; shear mixing, convection and dispersion [31]. These mechanisms, which predominate in different areas of a blender, can be easily visualized in a tumbling blender. The circulation pattern (convection mechanism) for the powder in such a blender consists of an upper layer that flows down in the direction of tumbling, and a large bulk at the bottom that moves upward as a solid body, driven by the vessel motion. Shear mixing, which is caused by velocity gradients, takes place mainly in the thin band that separates the flowing layer and the static region. Dispersion, which is driven by the random motion of individual particles, is mainly observed in the transversal direction of the flowing layer. Shear mixing also happens in any unit where powder flows (i.e. sieves, blender, feed frames, granulators, mills, etc).

Shear mixing is the only mixing mechanism capable of generating the stresses necessary for de-agglomeration [32]. The magnitude of shear stresses is a function of the shear rates [33, 34], and they vary according to the type of unit (i.e. mill [35], blender, blender with intensifier bar), its operation conditions (i.e. fill level [36], speed of rotation of the blender [37, 38] or of intensifier bar), and its scale [39].

This chapter studies the effect of blender parameters on API agglomerate mitigation and also the efficiency of different combinations of units and operating conditions that mitigate API agglomeration. Section 2-3-1 discuses the use of sieves or mills to de-agglomerate the pure API before blending it with the excipients. These experiments show that API de-agglomeration is a reversible process because API agglomerates are found in the final blends. Section 2-3-2 analyzes the effect of several operation parameters for low-shear blenders (i.e. use of baffles, fill level, scale, and use of an internal impeller) on the API de-agglomeration performance. The results show that baffles do not contribute to API de-agglomeration, while fill level and scale affect de-agglomeration performance significantly. Although an internal impeller may increase shear rates in a cylindrical blender, it does not enhance its de-agglomeration performance. This section also shows that the design and positioning of the moving internal in a blender is critical, as agglomerates may survive regardless of the increased shear rates generated by a high-speed impeller.

Section 2-3-3 studies different blending protocols that mitigate API agglomeration. They consist of either pre-blending the API and part of the excipients in a high shear unit (blender with moving internals, or milling an API pre-blend) or milling final blends. The experiments show that the preparation of API pre-blends in high shear environments reduces the risk of API agglomerates forming again because now the API particles can adhere to a different carrier. Milling final blends also mitigates API agglomeration, and the improved de-agglomeration performance of a larger blender can still be appreciated even when the final blends are passed through a mill. Finally, this section shows that pre-blending methods and the milling of final blends yield blends with equivalent API homogeneity and de-agglomeration.

Prior to the discussion of results, Section 2-2 describes materials, blends and the equipment utilized in the different situations as well as the experimental techniques (i.e. loading of the blender, sampling instruments, analytical techniques to determine sample concentration, and definition of homogeneity index RSD). Section 2-4 concludes this chapter and summarizes the recommendations to mitigate API agglomeration.

2-2. Materials, Equipment, and Experimental Techniques

2-2-1. Excipients

Two excipients are used in the experiments described in this chapter: Fast-Flo lactose (Foremost Farms), with an average particle size of ~100 µm, and Microcrystalline cellulose (Avicel PH-102, FMC, Rothschild, WI), with an average particle size of ~90 µm.

2-2-2. Minor components

Micronized NaCl (Fisher): This salt is highly cohesive, hygroscopic and with strong tendency to form agglomerates. NaCl is sieved to control the initial size of agglomerates using sieves, and the mean and maximum agglomerate sizes are 360µm and 595 µm respectively. The NaCl concentration in samples is determined using conductimetry (this technique is described in the "Analytical Techniques" section).

Acetaminophen (APAP): This API is always sieved before its addition to the blender using a 100 µm mesh. The API concentration in samples is determined via NIR spectroscopy. Two types of acetaminophen are used in our experiments:

- Micronized acetaminophen (Wuxi), average particle size ~1µm.
- Micronized acetaminophen (Mallinckrodt), average particle size ~20µm.

Magnesium stearate (Mallinckrodt): the concentration of this lubricant in samples is determined via NIR spectroscopy.

Cohesive API (not disclosed due to proprietary reasons): This API is passed through a conical mill prior to its addition to the blender. The API concentration in samples is determined using UV absorbance of a dissolved sample.

2-2-3. Other minor components

The formulation with cohesive API also contains Dibasic calcium phosphate, which is a typical filler with good flow properties, and Sodium starch glycolate, which is a common swelling compound that leads to the rapid disintegration of tablets.

2-2-4. Blends

Six blends were prepared in this study (Table 2-1). Reading the columns in Table 2-1, from top to bottom describes the blending protocol to prepare each blend.

2-2-5. Blenders

Blends were prepared in one of the following pieces of equipment:

Tote blenders (Figure 2-1-a) have a square body, a pyramidal bottom section, an upper closing lid, and they often have internal baffles. The blenders used here are equipped with an internal baffle of a rhombic cross-section. To study the effect of blender scale on the de-agglomeration of a cohesive API (Blend 1 – Table 2-1), geometrically similar 14-liter, 56-liter, and 300-liter stainless steel Tote blenders, operating at tumbling speeds of 16 RPM, 12 RPM, and 9 RPM respectively, are used. A 14-liter Tote blender, operated at 5 RPM, 10 RPM, and 15 RPM, is used to study salt de-agglomeration (Blend 2 – Table 2-1).

Cylindrical bin blenders (Figure 2-1-b) have a cylindrical body, a conical bottom, and optional baffles attached to the closing lid. Here, a 40-liter acrylic blender at 10 RPM is used to investigate the effect of baffles and fill level (20%, 60%, and 80%) on commercial acetaminophen de-agglomeration (Blend 3 – Table 2-1). Also, a 20-liter stainless steel blender, operated at 14 RPM and 60% fill level, is used to investigate the effect of increasing shear rates by adding a vertical impeller spinning at ~110 RPM on the API de-agglomeration (Blends 4 and 5). A 7-inch diameter blade is placed on a centered shaft, and it is located at the top of the blender conical bottom.

V-blenders (Figure 2-1-c) consist of two cylindrical bodies that intersect each other at an angle. There are openings at this intersection, which is used to empty the blender, and also at the top of both cylinders. V-blenders often have an intensifier bar to increase shear rates. Two acrylic V-blenders, of 4-qt. and 16-qt. volume, and operated at 9 RPM, with an intensifier bar spinning at ~400 RPM, are used to prepare pre-blends (Blend 1 – Table 2-1).

2-2-6. Conical mill

Conical mills have a conical chamber with an internal impeller, an upper opening used to feed the blend and a lower opening with a screen used to empty the mill. The impeller generates high shear rates necessary to de-agglomerate cohesive API. Mills, unlike blenders with moving internals, can guarantee that shear is applied to the entire blend and, in the absence of re-agglomeration, the screen guarantees that there will not be agglomerates larger than the mesh in the final blend [40, 41]. However, mills have some disadvantages, such as adding an extra process step, generating dust (which may increase the exposure of personnel to potent drugs) and generating higher temperatures (which can be detrimental for thermo-labile APIs). Additionally, the shear stresses achieved in a mill can be high enough to overcome not only inter-particle forces but also crystal lattice forces, leading to size reduction of primary particles. An important comment is that a mill does not provide “back-mixing”, and therefore it can not compensate for disparities in API concentration between portions of the blend that pass through the mill at different times. If portions of the blend have different drug concentrations due to segregation of one component or incomplete mixing, the mill will not correct such a situation.

The conical mill used here has an impeller operating at a speed of ~2500 RPM, and a screen with a mesh of 1 mm. Blends are passed through the mill only once and collected in a container, which is sampled to analyze the effect of high shear rates.

2-2-7. Initial distribution of component in the blenders

A key step in the set up of blending experiment is the loading of material in the blender. The initial "lay out" of API may seem a trivial step but it can have a large impact on blender performance [42]. For example, for Tote and cylindrical bin blenders, it can affect the overall mixing rate and sometimes lead to inhomogeneous blends. In these tumbling blenders, the axial mixing is dominated by a slow dispersive process [43] and an uneven initial distribution of API along the axis of rotation will be compensated only after long mixing times. Since cross-sectional mixing is driven by the faster convective process, mixing rate is significantly enhanced by loading the API (or the API pre-blend) in an even distribution along this axis of rotation. The loading method, known as "sandwiching" or "layering", first places a fraction of the excipients in the blender, then distributes the drug (or a pre-blend containing the drug) evenly over the entire surface of excipients, and finally places the remainder of excipients on top. Distributing a pre-blend of API and excipients into a layer may be simpler than forming a thin uniform layer of pure API. The larger volume of material makes it easier to form an even layer and reduces the risk of a having widely different API concentrations along the axis. Loading methods for API also affects the performance of V-blenders [44], and especially the API mixing rate.

2-2-8. Sampling instruments and sampling locations

Once the blender is loaded, the blending operation can begin. In order to analyze the evolution of the process and understand the effect of the different variables of the process (i.e. fill level, speed of tumbling, etc), the blender should be scrutinized either continuously or at pre-determined time intervals (stratified sampling). There are some non-invasive techniques (i.e. Positron Emission Tomography) that make it possible to continuously inspect flow and velocity profiles inside small blenders [45, 46], but the most widespread techniques involve stopping the blender to extract samples with an instrument. Appropriate sampling instruments cause a minimum perturbation to the powder bed (which is especially if sampling at several different times). They also cause a minimum perturbation to the samples since a key element for a successful study of powder blending is the collection of representative samples. Some of the instruments with these characteristics are the groove sampler and the core sampler, whose performance has been tested in previous studies [47, 48]. The core sampler (Figure 2-2) is a pipe of ¾ inch diameter that, when inserted in the blend, is filled up with powder. The powder is later extruded and subdivided into samples which are collected in glass vials. The groove sampler (Figure 2-3) consists of a cylinder with a slit, surrounded by a jacket. The groove sampler is inserted in the blend with the slit exposed, powder fills up this cavity and then the jacket is rotated, trapping the powder inside the slit. The powder is subdivided into samples using a set of small trays, and the samples are subsequently transferred from the trays to vials for analysis. The samples in the vials are used to estimate a homogeneity index for the blend.

In all experiments reported here, sampling positions were pre-determined and usually kept unchanged for a given process by using a Plexiglas® template. Typically, several equally spaced cores are extracted along the axis of rotation, and this sampling operation is repeated at different mixing times (i.e. number of revolutions). The number of cores depended on the size of the blender and the degree of confidence needed for the homogeneity index. For example, for the 20-liter cylindrical blender, three equally spaced cores were extracted, whereas for the 40-liter cylindrical blender five equally spaced cores were extracted.

2-2-9. Analytical techniques to determine API concentration in samples

The samples extracted with the sampling tools must be analyzed for composition. There are several analytical techniques available, both destructive (i.e. UV, conductimetry, titration, etc) and non destructive (i.e. NIR). The advantage of a non destructive technique for the study of agglomeration is that one can first determine the API concentration for each sample and later be able to inspect those samples with anomalously large API concentration for the presence of agglomerates. If agglomerates are present, one can sometimes separate them and determine its chemical composition with UV, conductimetry or titration. The selection of a technique also depends on the chemical nature of the drug and the number of samples to analyze. A brief description of the analytical techniques to determine the sample composition is presented next.

Near infrared (NIR) spectroscopy for solids

The near infrared (NIR) spectroscopy is a non destructive technique that measures the reflectance of a solid sample. A comparative advantage of NIR is that it allows a fast determination of concentration because it does not require sample dissolution (as in UV or conductimetry) or any other sample preparation (although it is best if the sample itself is homogeneous). The technique requires developing a calibration equation that correlates sample concentration and reflectance [49-53]. To develop this equation one must use standard samples with a known drug concentration. The concentration of the standards is usually verified with a secondary technique (i.e. UV for acetaminophen, titration for Magnesium stearate). The chemometric software provided by the Foss NIR 5082 system facilitates the selection of the most appropriate standards to build the calibration equation based on the spectra collected and on the concentration of each standard. The software classifies the standards into a calibration, a validation (redundant samples) and an outlier set. The first set is used to build the calibration equation, the redundant samples or alternatively a second set of standards with know concentrations is used for the validation of the calibration equation and the outlier set is not used at all.

The chemometrics software also facilitates the building of the calibration equation. It offers two methods, denominated MLR (Multi-Linear Regression) and PLS (Partial Least Squares), which are based in single wavelengths or in ranges of wavelengths values of the infrared spectra. For each component (APAP and lubricant), we choose the method that yields the equation with the best linear fit between reflectance and standard concentration. The software selects the wavelength values or range of wavelengths values based on mathematical treatment of the spectra.

Ultraviolet (UV) absorption technique

The UV absorption technique is a destructive method that correlates the absorption of ultraviolet radiation and the concentration of a chemical compound in solution. This technique requires the dissolution of samples. For experiments with a large number of samples, the analytical procedure can become laborious. A calibration curve needs to be prepared with samples of known drug concentration and excipients. Samples are dissolved in a specified solvent and the solutions filtered to remove any insoluble excipients. The wavelength utilized to measure absorbance is specific to each compound. The blank solution sample is prepared only with excipients.

Conductimetry

Conductimetry is a destructive technique used when the component of interest is the only soluble ionic compound, and correlates electrical conductivity of a solution and concentration of ions. This technique requires the dissolution of samples (or agglomerates) in a solvent. For experiments with a large number of samples, the analytical procedure can be time consuming. A calibration equation is generated measuring the electric conductivity of the solutions with known concentrations of ions in the presence of the standard amount of soluble non-ionic excipients.

2-2-10. Homogeneity analysis

The last part of the experimental procedure is the analysis of experimental data. The typical approach is to compute a single number that describes the homogeneity (or quality) of the blend at each time point using the concentration of samples. Then, a mixing curve that can be used to analyze the performance of the blender is generated plotting the homogeneity index versus mixing time (or revolutions of the blender). While many indices have been proposed [54], RSD (relative standard deviation), also known as C.O.V. (coefficient of variability), is the most commonly used. RSD is defined as:

$$RSD = \frac{s}{\overline{C}} \qquad \text{(Eq. 2-1)} \qquad\qquad s = \sqrt{\frac{n\sum_{i=1}^{n} C_i^2 - \left(\sum_{i=1}^{n} C_i\right)^2}{n(n-1)}} \qquad \text{(Eq. 2-2)}$$

In the previous equations, s is the standard deviation of all sample concentrations, $\overline{C}$ is the average concentration, C_i is the concentration of each individual sample, and n is the total number of samples.

API agglomerates have an impact on the sample concentration that is directly proportional to the mass of the agglomerate and inversely proportional to the mass of the sample. The impact of an agglomerate on sample concentration is obviously lower for pre-blends with a high API concentration. Samples with agglomerates are typically few but their high API concentration has a large impact on the standard deviation of sample concentration, rendering the RSD value meaningless beyond the observation of it being “very high”, i.e. a blend with agglomerates is highly non-homogeneous and has a large homogeneity index. In industrial practice, an acceptable blend RSD value is customarily below 0.05 (5%) for samples of size similar to the finished product unit (a tablet or a capsule).

2-3. Results

The results section is organized as follows: Section 2-3-1 discuses how agglomerates can reform in low-shear blending equipment, even when the pure API is sieved or milled before blending it with the excipients. Section 2-3-2 studies the effect of several operation parameters for low-shear blenders (i.e. use of baffles, fill level, scale, and use of an internal impeller) on the API de-agglomeration performance. Section 2-3-3 studies different blending protocols that mitigate API agglomeration. They consist of either pre-blending the API and part of the excipients in a high shear unit (blender with moving internals, or milling an API pre-blend) or milling final blends.

2-3-1. Conditioning of pure API: Reversible de-agglomeration

This section describes the two most common practices intended to reduce the presence of agglomerates in blends: to sieve or to mill a cohesive API prior to its addition to the blender. Material is certainly de-agglomerated when exposed to the shear conditions of a sieve or a mill. However, as this section shows, re-formed agglomerates of pure API can sometimes be found in the final blends. This is evidence that sometimes de-agglomeration is a reversible process and, when API particles are in contact with each other and the inter-particle forces are strong enough, agglomerates form again.

Milling the API before adding it to the blender does not guarantee absence of agglomerates in the final blend. For example, in the preparation of Blend 1 (Table 2-1), a cohesive API is milled, laid in a sandwich manner in the blender, and then blended with excipients in Tote blenders of different scales (14-liter, 56-liter and 300-liter), which are rotated for a total of 256 revolutions using tumbling speeds that decrease with blender size. Once again, agglomerates whose composition was confirmed to be 100% API using UV technique (Figure 2-4) are found after the blending process in the three blender scales.

In the preparation of Blend 2 (Table 2-1), pure NaCl is sieved, allowing that the largest possible agglomerate size is 595 μm, and then loaded in the blender in a sandwich manner and blended for 32 revolutions in a 56-liter Tote blender, operated at 10 RPM and at a 40% fill level. NaCl agglomerates or clumps of up to 2-cm in diameter (Figure 2-4) and composed almost exclusively of NaCl can be found in the discharge of the blender. Agglomerates had the chance to form again, possibly due to NaCl's ability to sequester moisture from the other components. While care was taken to work in a low RH environment, consistent with industrial practice, in these experiments, the bulk excipient was not dehumidified to the point where the salt would not reform agglomerates.

The same situation is observed in the preparation of Blends 4 and 5 (Table 2-1). Acetaminophen is sieved below 30 μm, and then loaded in the 20-liter cylindrical blender in a sandwich manner and blended for 400 revolutions, operated at 14 RPM and at a 60% fill level. Acetaminophen agglomerates of up to 100 μm in diameter (Figure 2-4) and composed almost exclusively of APAP can be found after 100 revolutions of the blender.

2-3-2. Effect of blender parameters on API de-agglomeration

The previous section shows that agglomerates can reform in a low-shear blender; however, there are several blender parameters that can affect the extent of API de-agglomeration. Shear rates in units without moving internals are moderate (or low) since the powder is driven mainly by gravitational forces and can only achieve limited velocities. Sometimes these low shear rates may not be sufficient to overcome the inter-particle forces and achieve API de-agglomeration. A moving internal may increase shear rates, however, the effect on API de-agglomeration may not be always substantial. The effects of fill level, internal baffles, blender scale, and an internal impeller in blenders are subsequently analyzed.

2-3-2-1. Effect of fill level and baffles

Blender fill level is a variable of interest for industry because it determines process throughput. Additionally, fill level affects mixing and the API de-agglomeration performance of bin blenders. Baffles are often claimed to increase the shear rates in a blender, which, if true, would help to de-agglomerate cohesive APIs. The effect of baffles and fill level on API homogeneity and de-agglomeration is studied here using a 40-liter cylindrical blender, operated at 10 RPM, at different fill levels (20%, 60% and 80%), and with and without baffles for the preparation of Blend 3.

Figure 2-5 shows three mixing curves that correspond to different fill levels of the blender with baffles. The 80% fill level (square points) yielded the poorest homogeneity (or highest RSD values), the 60% fill level (triangular points) yielded a more homogeneous blend, and the 20% fill level (diamond points) yielded the most homogeneous blend. At the highest fill level (80%), agglomerates survived for long times. In fact, many large agglomerates were found after 320 revolutions of the blender, and some were still present after 640 revolutions. Lower fill levels (60% and 20%) presented fewer and smaller agglomerates and they tended to disappear as mixing time increased. The differences among the mixing curves in Figure 2-5 reflect the influence of agglomerates on blend homogeneity for the different fill levels. The more and larger agglomerates present, the larger the homogeneity indexes are.

The effect of baffles on API de-agglomeration and homogeneity is studied for each of the fill levels. The curves in Figure 2-6 show that, for the lowest fill level (20%) of the blender, baffles (red squares) improve mixing rates (i.e. larger slope of the mixing curve at short mixing times), but they do not improve final blend homogeneity or drug de-agglomeration. Baffles only come into contact with the powder when the bin is inverted. Otherwise, when the bin is upright, they do not interact with the powder layer at all. Most likely, the baffles prevent the "slumping" flow often observed at low fill levels in vessels without baffles and deflect the flow in the axial direction. However, there is no discernible factual foundation for the often-made claim that they increase shear rates since they do not change the magnitude of velocities in any observable manner, and they do not improve final blend homogeneity and drug de-agglomeration. After a mixing time of ~150 revolutions, the RSD for the blender with baffles (red squares) coincides with the set-up without baffles (blue diamonds).

For the 60% (Figure 2-7) and 80% (Figure 2-8) fill levels, the baffles do not enhance API homogeneity or mixing rates. For these fill levels, there is not an advantage in the mixing rates of the baffle set-up, probably because slumping does not occur at higher fill levels. For the 60% fill level, the mixing curves and the homogeneity for the two set-ups becomes very similar at a mixing time of ~300 revolutions (Figure 2-7). This evidence also leads to the conclusion that baffles do not affect shear rate because there is no improvement in drug de-agglomeration or final homogeneity.

Mixing curves typically reach a plateau, with certain variations, and homogeneity does not increase further with mixing time. The RSD values in the plateau of each mixing curve (Table 2-2) are used in an ANOVA test to establish the effect of fill level and internal set-up. In this test, the null hypothesis is that all fill levels lead to equivalent blend homogeneity. Regarding the effect of baffles, the hypothesis establishes that the existence of absence of internals lead to identical blend homogeneities. Such hypothesis are typically rejected if the p-value is smaller than 0.05. The results of the ANOVA test (Table 2-3) show that baffles do not affect blend homogeneity. However, fill level affects the drug homogeneity and de-agglomeration substantially.

Possible reasons for higher fill levels to allow API agglomerates surviving longer and yielding a poorer API homogeneity are:

- Lower shear rates (i.e. the velocities are smaller and also the velocity gradients).
- The material is exposed to shear mixing less often, on a per-blender revolution basis. The amount of material in the flowing layer is proportionally smaller as the zone of non-flowing material that lies below the flowing layer increases for higher fill levels. However, increasing the mixing time for higher fill levels does not necessarily compensate blend homogeneity as shear rates are smaller.
- In the largest fill level (80%), there is a “dead zone” in the blender [31] and while the upper layer flows down and the powder at the bottom moves as a solid with the blender, the powder in the center of the blender remains unperturbed for very long times.

2-3-2-2. Effect of using an impeller in a cylindrical bin blender on API de-agglomeration

One of the main limitations of blenders is their low-shear conditions. This section investigates the feasibility of overcoming this limitation by including an impeller in a cylindrical bin blender to de-agglomerate and mix the API. A 20-liter cylindrical blender is equipped with an internal impeller (~110 RPM) to prepare blends of different grades of acetaminophen and lactose (Blends 4 and 5 – Table 2-1) and its performance is compared with that of the same blender equipped only with baffles. The pure acetaminophen is sieved before loading it in the blender.

The effect of the impeller is studied by comparing the mixing curves for each blend in the blender equipped with the impeller and in the blender equipped with baffles. Figure 2-9 shows that the mixing curves for Blend 4 are very similar for the baffle (full line) and the impeller (dash line) set-up. API agglomerates can be found after 100 revolutions of the blender in the baffle and in the impeller (which rotated ~785 revolutions) set-ups. However, after 400 revolutions of the blender, API agglomerates are neither detected in the baffle set-up nor in the impeller set-up (which rotated for ~3140 revolutions). The agglomerates were subsequently tested with UV absorbance for composition and were nearly 100% API, causing the observed super-potency of the samples.

Figure 2-10 presents the mixing curves for Blend 5 in the blender equipped with the impeller (dash line) and in the blender equipped with baffles (full line). They present some differences at short mixing times (<100 revolutions) due to the different number of agglomerates detected in each set-up. However, after 100 revolutions, agglomerates are not detected in either set-up and yet the homogeneity is still marginally better in the baffle set-up. The effect of increased shear rates provided by the impeller seems to be negligible for blend 5.

API agglomerates can survive long mixing times, regardless of the presence of the impeller, because this internal only applies shear in the central region of the blender. Since axial mixing in tumbling blender is slow, many agglomerates in other regions are seldom exposed to the shear action of the blade. Additionally, when the blender is upside down, the impeller is outside the powder bed and has no effect on API de-agglomeration. Therefore, API agglomerates disappear at the same rate regardless of the presence of the impeller.

2-3-2-3. Effect of blender scale

In order to scale-up a granular process it is important to first determine the dynamic variable that governs it. For example, mixing rate in blender is affected by fill level, which suggests that a factor such as (mass of contents in motion)/(total mass) may be an important variable for the scaling process [55]. Here, the scale-up of the Tote blender to prepare Blend 1 is performed maintaining dynamic similarity (approximately) by keeping the Froude number constant [56]. Therefore, the speed of rotation of the three geometrically similar blenders decreases as the volume of the blender increases. The speeds for the 14-liter, 56-liter and 300-liter Tote blenders are 16 RPM, 12 RPM and 9 RPM, respectively. The 14-liter blender has a higher drug concentration (3.5%) as compared to 1% for the larger blenders. Blends are sampled and homogeneity is assessed after 256 revolutions of the blender.

Because a single RSD values for each blender scale is not enough to draw statistical conclusions about their relative API de-agglomeration capability, the focus is on the sample concentration variances. Comparing population variances involves determining if sample concentration distributions belong to the same population. An essential requirement for the test is that concentration values have a normal distribution. The sample concentration variance for direct blending of API and excipients in a 300-liter blender is 1.07 E-02, for 56-liter blender is 0.763, and for the 14-liter blender is 1.23. The procedure to determine if these concentration variances belong to the same sample population consists of setting a hypothesis about the variances, which is accepted or rejected according to the value that a statistical parameter adopts. For example, the hypothesis is that the sample concentration variances for the medium and large scale blenders are the same. The alternate proposition is that the sample concentration variance for the medium-scale blender is larger than that of the large blender. The ratio between the two variances gives an F value, which is compared to a critical value, at a certain significance level. The degrees of freedom for the test is given by the number of samples in each of the distributions being compared. The hypothesis is rejected because the F value is smaller than the critical value, and the test shows that the sample population variance of the large blender is larger than that of the medium-scale blender[2]. The same test is carried out for the small and medium size blenders, with the hypothesis that the variances are the same, and an alternate proposition that the variance for the medium scale blender is larger than that of the small blender. This test shows that the sample

[2] $f = 71.3$ is larger than $F_{0.05,33,36} = 1.72$. The variance of the medium scale blender is statistically larger than that of the large blender.

population variances are actually the same[3]. However, it should be noted that the net API concentration in the final blends is different (1% for the medium scale and 3.5% for the small scale blender). The results for the effect of blender scale-up on API de-agglomeration are compiled in Figure 2-11.

2-3-3. Blending protocols that mitigate API agglomeration. Analysis of their efficiency and the scale-up possibilities on the degree of API agglomeration

In this section, two types of protocols that mitigate API agglomeration are considered. One type of protocol involves blending all API and excipients followed by the milling of the entire blend. The second type of protocol involves pre-blending API and a portion of excipients in a high shear unit, followed by dilution with more excipients in a large blender. Two protocols are considered to prepare Blend 1 and they include either pre-blending the API in V-blender with intensifier bar or pre-blending it in a tote blender followed by a milling step. The concentrated pre-blends are then diluted with more excipients in tote blenders. The effect of scaling-up these protocols on API homogeneity and degree of agglomeration is also examined. The results are for each protocol are discussed in the three subsequent sections and are compiled in Figure 2-13.

2-3-3-1. Milling of final blends

The blends prepared in blender of different scale in section 2-3-2-3 are milled afterwards, API agglomerates and highly concentrated samples are no longer detected, and sample concentration variances are therefore much lower. The sample concentration variance for the 300-liter blender is 2.26E-03, for 56-liter blender is 7.08E-03, and for the

[3] $f = 1.61$ is smaller than $F_{0.05,18,34} = 1.86$. The variances are the same.

14-liter blender is 4.22E-02. The tests to compare sample concentration variances before and after milling for each blender scale contrast the hypothesis that variances are the same against the alternate proposition that the sample concentration variance of the milled blend is smaller than that for the blend before milling. Milling the outcome of a blender significantly reduced the API sample concentration variance for the small-scale[4], for the medium-scale[5], and for the large-scale[6] blenders.

The effect of larger blender on the API homogeneity, when the process consists of a blender and a mill, may seem negligible. However, the effect of a larger scale blender on sample concentration variance is still significant. The test hypotheses are that the sample concentration variances for the small and medium scale blender, and for the medium scale and large blenders are the same. The alternate propositions are that the variance of the small blender is larger than that of the medium scale blender, and the variance of the medium scale blender is larger than that of the large blender. The sample concentration variance for the protocol with the 14-liter blender is not larger than the variance for the protocol with the 56-liter blender[7]. (Again, note that the net API concentration in the medium scale blender is 1% and in the small scale blender is 3.5%). The sample concentration variance for the protocol with the 56-liter blender is statistically larger than the variance for the protocol with the 300-liter blender[8].

In conclusion, statistical evidence suggests that larger scale blenders favor API de-agglomeration, besides the lower RSD and the fewer agglomerates detected in the 300-liter blender. The effect of blender scale on sample concentration variance becomes less

[4] $f = 29.07$ is larger than the critical value $F_{0.05,8,18} = 2.51$.
[5] $f = 107.74$ is larger than the critical value $F_{0.05,23,33} = 1.86$.
[6] $f = 4.75$ is larger than the critical value $F_{0.05,46,36} = 1.68$.
[7] $f = 5.96$ is smaller than the critical value $F_{0.05,8,23} = 2.37$
[8] $f = 3.14$ is larger than $F_{0.05,23,46} = 1.763$.

important when the final blend is milled; however the larger-scale process still produces a more homogeneous blend with a statistical significance. All the statistical comparisons are summed up in Figure 2-12.

2-3-3-2. Effect of milling pre-blends on API de-agglomeration

When API particles are in contact with each other in a low shear environment, agglomerates of pure API reform (Section 2-3-1). In this section, the processing method consists of mixing the API with some excipients in a unit with increased shear rates to de-agglomerate the API, and at the same time, minimize the probability that API particles form new agglomerates. In this approach, API particles are able to adhere to excipient carriers rather than adhering back with each other [57-59].

The protocol used here to prepare Blend 1 involves pre-blending API and excipients in a small Tote blender, then passing this pre-blend through a conical mill, and finally diluting it with the remainder of the excipients in a large Tote blender. This protocol is tested in two scales. In the 56-liter-scale version, API is pre-blended in a 14-liter Tote blender, the pre-blend is passed through the mill, and finally diluted in a 56-liter Tote blender. In a large-scale version, API is pre-blended in a 56-liter Tote blender, then the pre-blend is milled, and finally diluted in a 300-liter Tote blender.

The effect of scale for the protocol “Small Tote-blender/Mill/Large Tote-blender” is substantial, and the large-scale protocol (300-liter) produces a blend with a concentration variance (2.11E-3) statistically smaller than the medium-scale protocol (7.74E-2)[9]. (the concentration averages are different for the two scales). Also, the benefit of milling a pre-blend is that the volume of material to be handled is smaller, with the

---

[9] $f = 36.66$ is larger than the critical value $F_{0.05,56,58} = 1.541$

consequent reduction in the generation of dust and exposure of personnel to potentially dangerous drugs. However, a larger fraction of API can be lost due to its higher concentration.

2-3-3-3. Effect of pre-blending API in a V-blender with intensifier bar on API de-agglomeration

An alternative protocol to prepare Blend 1 consists of pre-blending API and excipients in a V-blender with intensifier bar, and then diluting the pre-blend to a final concentration of 1% in a Tote blender. The effect of scale is also studied for this protocol. In the small scale, a pre-blend with an 8% API (mass basis) is prepared in the 4-qt V-blender that tumbles at a speed of 16 RPM, which is later diluted in a 56-liter Tote blender. In the larger scale, a pre-blend with an 11% API (mass basis) is prepared in a 16-qt V-blender that tumbles at 13 RPM, which is later diluted in a 300-liter Tote blender. The hypothesis is that the concentration variances for both scales are the same, and the alternate proposition is that the larger scale has a lower variance.

The effect of scale for the protocol "V-blender with intensifier bar/Tote-blender" is not significant. The small scale protocol yields a concentration variance of 4.65E-07, while the large scale protocol yields one of 2.67E-07. These variances are not statistically different[10]. Pre-blending API and excipients in a high shear V-blender, and then diluting the pre-blend in a Tote blender, makes the effect of larger blender scale on API de-agglomeration negligible.

---

[10] $f = 1.73$ is smaller than $F_{0.1,38,31} = 1.571$, therefore the variance for the large-scale protocol is larger than for the small-scale protocol at a significance level of 0.1.

2-3-3-4. Comparing the de-agglomeration efficiency of previous protocols

The aim of this section is to determine the benefits of including high shear rate in an early or late process step, and also to compare the efficiency of the two pre-blending methods. The hypothesis is that the variances for the processes compared are equivalent, and the alternate proposition is that the variance of the protocol "Small Tote-blender/Mill/Large Tote-blender" is larger than any of the other two pre-blending processes.

In the medium scale (56-liter), the variance of the protocol "Small Tote-blender/Mill/Large Tote-blender" (0.077) is in fact statistically larger than the variance for the protocol "Tote-blender/Mill" (7.08 E-03)[11], and the variance of the "V-blender with intensifier bar/Tote-blender" (4.65E-3)[12] (bear in mind that the protocol "Small Tote-blender/Mill/Large Tote-blender" is carried out with an average concentration of 3.5% and the other two protocols are carried out using an average concentration of 1%). However, the variances for the "Tote-blender/Mill" (7.08 E-03) and "V-blender with intensifier bar/Tote-blender" (4.65E-3) are equivalent[13].

For the 300-liter scale, the sample concentration variances for "V-blender with intensifier bar/Tote-blender" (2.67E-03) is statistically similar to that for the "Small Tote-blender/Mill/Large Tote-blender" (2.11E-03)[14] and that for the "Tote blender/Mill" (2.26E-03)[15]. Also, "Small Tote-blender/Mill/Large Tote-blender" and "Tote-

---

[11] $f = 10.93$ is larger than the critical value $F_{0.05,56,23} = 1.86$
[12] $f = 16.66$ is larger than the critical value $F_{0.05,56,38} = 1.66$
[13] $f = 1.52$ is smaller than the critical value $F_{0.05,23,38} = 1.81$
[14] $f = 0.78$ is smaller than the critical value $F_{0.05,58,31} = 1.73$. The variance for both protocols is similar at the 300-liter scale.
[15] $f = 0.84$ is smaller than the critical value $F_{0.05,46,31} = 1.73$. The variance for both protocols is similar at the 300-liter scale.

blender/Mill" have concentration variances (2.11 E-03 and 2.26 E-03) that are not statistically different[16]. Additionally, the three protocols yield an RSD of ~0.039.

2-4. Conclusions

Powders with high inter-particle forces due to absorbed water (i.e. NaCl or any hygroscopic material) or powders with strong electrostatic properties (i.e. APAP and many other APIs) tend to form agglomerates. In order to mitigate API agglomeration in pharmaceutical formulations it is necessary that shear stresses larger that the inter-particle forces exist in the process. However, API de-agglomeration can be a reversible event, especially when previously sieved or milled pure API is blended in a low-shear equipment. In such units, there are high chances that API agglomerates are present in the final blend. For a cylindrical or a tote blender without moving internals, there are operating conditions that do not contribute to mitigate agglomeration. For example, high fill levels, which reduce the exposure of the material to shear on a revolution basis, give agglomerates the possibility to survive inadmissible long mixing times. Baffles enhance the axial mixing rates but there is no evidence that they increase shear rates or contribute to the API de-agglomeration. Larger blender scales generate larger shear rates and more favorable conditions for de-agglomeration. Finally, a moving internal can increase shear conditions in a cylindrical blender but it may not guarantee the absence of API agglomerates. As it is shown in this chapter, the design of such unit is critical.

In order to mitigate API agglomeration, high shear units such as a V-blender with intensifier bar or a mill must be included in the mixing process. The high shear rates provide the stresses necessary to de-agglomerate the API and the presence of excipients

[16] $f = 0.936$ is smaller than the critical value $F_{0.05,58,46} = 1.601$

reduces the possibility of particles coming into contact again. In general, pre-blending API and excipients in a high shear unit or milling such pre-blend is as effective mitigating API agglomeration as it is the milling of the final blend. Milling a concentrated pre-blend is easier to carry out (because of the smaller volume of material) and safer (because the dust generation by the milling is minimized) than milling a diluted blend. The benefits of scale become less important, although they are still significant, when the process involves a high shear unit (i.e. mill or V-blender with intensifier bar).

Finally, the nature of the minor components must be considered to design a mixing protocol that minimizes API agglomeration. For example, one should avoid mills for thermo labile compounds and frail crystals. A mill can change particle size distribution, affecting flow properties, and the heat generated can modify the active principle. In the mixing of lubricants, high shear units increase the risk of over-lubrication (i.e. reduced solubility and yielding weak tablets).

The knowledge on the effects of material properties, environmental conditions, and processing variables on the API degree of agglomeration accumulated in this chapter as well as in many of the references cited can help the practitioner design a process, select equipment, and choose operating conditions that minimize the presence of API agglomerates in the product. However, most of this knowledge is expressed in terms of the relative advantage of using one condition or equipment over another. For example, we compare the relative benefits of different fill levels. In order to establish in a more quantitative manner the net advantage of a particular equipment or operating condition, it is necessary to create a method to quantify and characterize the degree of agglomeration in certain blend. Such method would have the additional value of being able to monitor, on-line (such as in PAT methods) or off-line, a blending process. An off-line sampling method typically consists of a few samples and therefore there is limited information about the blend and the agglomerates. The next chapter of this dissertation focuses in developing a method that, using this limited information on sample concentration combined with a statistical model, can predict the API distribution (either dispersed or in the form of agglomerates) throughout the entire blend.

REFERENCES

1- Beckett, S. T. Conching. In S. T. Beckett (Ed.), *Industrial chocolate manufacture and use* (3rd ed). Oxford: Blackwell Science (1999).

2- Yang, M.; Jennings, H.M. Influences of mixing methods on the microstructure and rheological behavior of cement paste. *Advanced cement based materials* 2 (1994), p. 70.

3- Chen, Y.K.; Mackley, M.R.; Sayer, T.S.B. Color change and microstructure evolution of wet flowing paint when subject to shear. *Chem. Eng. Science* 58 (2003), p. 2505.

4- Swaminathan, V.; Kildsig, D. Polydisperse Powder Mixtures: Effect of Particle Size and Shape on Mixture Stability. *Drug Dev. Ind. Pharm.* 28 (2002), p. 41.

5- De Villiers, MM. Description of the kinetics of de-agglomeration of drug particle agglomerates during powder mixing. *Int. J. Pharm.* 151 (1997), p. 1.

6- DesRosiers Lachiver, E.; Abatzoglou, N.; Cartilier, L.; Simard, J.S. Agglomeration tendency in dry pharmaceutical granular systems. *European Journal of Pharmaceutics and Biopharmaceutics* 64 (2006), p. 193.

7- De Villiers, M.M.; Van der Watt, J.G. Measurement of mixture homogeneity and dissolution to predict the degree of drug agglomerate breakdown achieved through powder mixing. *Pharmaceutical Research* 11 (1994), p. 1557.

8- De Villiers, M.M.; Van der Watt, J.G. Interactive mixing between agglomerated drug particles and coarse carrier particles. *Drug Development and Industrial Pharmacy* 15 (1989), p. 2055.

9- Saunders, R. The Effect of Particle Agglomeration in Pharmaceutical Preparations. *The Statistician* 40 (1991), p. 77.

10- Thiel, W.J.; Nguyen, L.T.; Sberna, F.J. Content uniformity of microdose tablets (dosage 1 microgram--10 mg) produced by fluid bed granulation of interactive mixtures. *Journal of Pharmacy and Pharmacology* 38 (1986), p. 335.

11- Garcia, T.; Carella, A.; Pansa, V. Identification of factors decreasing the homogeneity of blend and tablet uniformity. *Pharm. Tech.* (March 2004), p. 110.

12- Stewart, P.J.; Zhao, F.Y. Understanding agglomeration of indomethacin during the dissolution of micronised indomethacin mixtures through dissolution and de-agglomeration modeling approaches. *European Journal of Pharmaceutics and Biopharmaceutics* 59 (2005), p. 315.

13- Swanepoel, E. Liebenberg, W. De Villiers, MM. Dekker, TG. Dissolution properties of piroxicam powders and capsules as a function of particle size and the agglomeration of powders. *Drug Development and Industrial Pharmacy* 26 (2000), p. 1067.

14- De Villiers, M.M.; Van der Watt, J.G. Dissolution rate as measurement of the de-aggregation of furesomide agglomerates during an interactive mixing process. *Drug Development and Industrial Pharmacy* 16 (1990), p. 1391.

15- Kurfe□, D.; Hinrichsen, H.; Zimmermann, I. Statistical model of the powder flow regulation by nanomaterials. *Powder Technology* 159 (2005), p. 63.

16- Jones, R.; Pollock, H.M.; Geldart, D.; Verlinden, A. Inter-particle forces in cohesive powders studied by AFM: effects of relative humidity, particle size and wall adhesion. *Powder Technology* 132 (2003), p. 196.

17- Buckton, G. Characterization of small changes in the physical properties of powders of significance for dry powder inhaler formulations. *Advanced Drug Delivery Reviews* 26 (1997), p. 17.

18- DesRosiers Lachiver, E.; Abatzoglou, N.; Cartilier, L.; Simard, J.S. Insights into the Role of Electrostatic Forces on the Behavior of Dry Pharmaceutical Particulate Systems. *Pharmaceutical Research* 23 (2006), p. 997.

19- Staniforth, J.N.; Rees, J.E. Electrostatic charge interactions in ordered powder mixes. *Journal of Pharmacy and Pharmacology* 34 (1982), p. 69.

20- Schönert, K.; Eichas, K.; Niermöller, F. Charge distribution and state of agglomeration after tribocharging fine particulate materials. *Powder Technology* 86 (1996), p. 41.

21- Bocquet, L.; Charlaix, E.; Restagno, F. Physics of humid granular media. *Comptes Rendus Physique* 3 (2002), p. 207.

22- Podczeck, F.; Newton, J.M.; James, M.B. Influence of relative humidity of storage air on the adhesion and autoadhesion of micronized particles to particulate and compacted powder surfaces. *Journal of Colloid and Interface Science* 187 (1997), p. 484.

23- Faqih, A.M.N.; Mehrotra, A.; Hammond, S.V.; Muzzio, F.J. Effect of moisture and magnesium stearate concentration on flow properties of cohesive granular materials. *International Journal of Pharmaceutics* 336 (2007), p. 338.

24- Gröger, T.; Tüzün, U.; Heyes, D.M. Modeling and measuring of cohesion in wet granular materials. *Powder Technology* 133 (2003), p. 203.

25- Shah, N.H.; Phuapradit, W.; Bachynsky, M.; Infeld, M.H.; Malick, A.W. et al. High energy ordered mixture for improving the dissolution rate of sparingly soluble compounds. *Drug development and industrial pharmacy* 20 (1994), p. 873.

26- Perrut, M.; Jung, J.; Leboeuf, F. Enhancement of dissolution rate of poorly-soluble active ingredients by supercritical fluid processes. Part I: Micronization of neat particles. *International Journal of Pharmaceutics* 288 (2005), p. 3.

27- Perrut, M.; Jung, J.; Leboeuf, F. Enhancement of dissolution rate of poorly-soluble active ingredients by supercritical fluid processes. Part I: Micronization of neat particles. *International Journal of Pharmaceutics* 288 (2005), p. 3.

28- Heitzmann, D.; Dodds, J.A.; Berthiaux, H. De-agglomeration of pigments: from batch to continuous. *Chem. Eng. Sci.* 49 (1994), p. 463.

29- Rwei, S.P.; Manas-Zloczower, I.; Feke, D.L. Characterization of agglomerate dispersion by erosion in simple shear flows. *Polymer Eng. Sci.* 31 (1991), p. 558.

30- Seyvet, O.; Navard, P. In situ study of the dynamics of erosion of carbon black agglomerates. *J. Applied Polymer Sci.* 80 (2001), p. 1627.

31- Cooke, M.H.; Stephens, D.J.; Bridgwater, J. Powder mixing — a literature survey. *Powder Tech.* 15 (1976), p. 1.

32- Llusa, M.; Muzzio, F.J. The Effect of Shear Mixing on the Blending of Cohesive Lubricants and Drugs. *Pharm. Tech.* (2005).

33- Aarons, L; Sundaresan, S. Shear flow of assemblies of cohesive and non-cohesive granular materials. *Powder Tech.* 169 (2006), p. 10.

34- Campbell, C.S. Granular shear flows at the elastic limit. *J. Fluid Mech.* 465 (2002), p. 261.

35- Yasmin, A.; Abot, J.L.; Daniel, I.M. Processing of clay/epoxy nanocomposites by shear mixing. *Scripta Materialia* 49 (2003), p. 81-86

36- Broadbent, C.J.; Bridgwater, J.; Parker, D.J. The effect of fill level on powder mixer performance using a positron camera. *The Chem. Eng. J. and Biochem. Eng. J.* 56 (1995), p. 119.

37- Santomaso, A.; Olivi, M.; Canu, P. Mixing kinetics of granular materials in drums operated in rolling and cataracting regime. *Powder Tech.* 152 (2005), p. 41.

38- Sudah, O.S.; Coffin-Beach, D.; Muzzio, F.J. Effects of blender rotational speed and discharge on the homogeneity of cohesive and free-flowing mixtures. *Int. J. Pharm.* 247 (2002), p. 57.

39- Alexander, A.; Shinbrot, T.; Muzzio, F.J. Scaling surface velocities in rotating cylinders as a function of vessel radius, rotation rate, and particle size. *Powder Tech.* 126 (2002), p. 174.

40- Bauer-Brandl, A.; Becker, D. Evaluation of a conical mill for screening of direct compression formulations. *Drug Dev. Ind. Pharm.* 22 (1996), p. 417.

41- Poska, R.P.; Hill, T.R.; Van Schaik, J.W. Use of statistical indices to gauge the mixing efficiency of a conical screening mill. *Pharm. Res.* 10 (1993), p. 1248.

42- Portillo, P.M.; Muzzio, F.J.; Ierapetritou, M.G. Characterizing powder mixing processes utilizing compartment models. *Int. J. Pharm.* 320 (2006), p. 14.

43- Brone, D.; Muzzio, F.J. Enhanced mixing in double-cone blenders. *Powder Tech.* 110 (2000), p. 179.

44- Lemieux, M.; Bertrand, F.; Chaouki, J.; Gosselin, P. Comparative study of the mixing of free-flowing particles in a V-blender and a bin-blender. *Chem. Eng. Sci.* 62 (2007), p. 1783.

45- Bridgewater, J.; Broadbent, C.J.; Parker, D.J. Study of the influence of blade speed on the performance of a powder mixer using positron emission particle tracking. *Trans. I. Chem. E.* 71 (1993).

46- Bridgewater, J. The dynamics of granular materials – toward grasping the fundamentals. *Granular Matter* 4 (2003), p. 175.

47- Muzzio, F.J.; Goodridge, C.L.; Alexander, A.; Arratia, P.; Yang, H.; Sudah O.; Mergen, G. Sampling and characterization of pharmaceutical powders and granular blends. *Int. J. Pharm.* 250 (2003), p. 51.

48- Muzzio, F.J.; Robinson, P.; Wightman, C.; Brone, D. Sampling practices in powder blending. *Int. J. Pharm.* 155 (1997), p. 153.

49- Duong, NH.; Arratia, P.; Muzzio, F.; Lange, A.; Reynolds, S. et al. A homogeneity study using NIR spectroscopy: Tracking magnesium stearate in Bohle bin-blender. *Drug Dev. Ind. Pharm.* 29 (2003), p. 679.

50- Luypaert, J.; Massart, D.L.; Vander Heyden, Y. Near-infrared spectroscopy applications in pharmaceutical analysis. *Talanta* (2006).

51- Blanco, M.; Romero, M.A.; Alcalà, M. Strategies for constructing the calibration set for a near infrared spectroscopic quantitation method. *Talanta* 64 (2004), p. 597.27.

52- Naicker, K.; Kilian, G.; Olivier, J. Introducing PAT, using near-infrared analysis, to a pharmaceutical blending process. *Pharmaceutical Manufacturing* 6 (2007), p. 43.

53- El-Hagrasy, A.S.; Delgado-Lopez, M.; Drennen, J.K. A process analytical technology approach to near-infrared process control of pharmaceutical powder blending: part II: qualitative near-infrared models for prediction of blend homogeneity. *J. Pharm. Sci.* 95 (2006), p. 407.

54- Poux, M.; Fayolle, P.; Bertrand, J.; Bridoux, D.; Bousquet, J. Powder mixing: Some practical rules applied to agitated systems. *Powder Tech.* 68 (1991), p. 213.

55- Alexander, A. W.; Muzzio, F.J. Batch size increase in dry blending and mixing. Pharmaceutical Process scale-up. Chapter 5. Edited by Michael Levin, M. (2002), p. 115-132.

56- Clump, C.W. Mixing of solids. Mixing. Chapter 10. Edited by Ulh, V.W.; Gray, J.G. (1967), p. 263.

57- Hersey, J.A. Ordered mixing: A new concept in powder mixing practice. *Powder Tech.* 11 (1975), p. 41.

58- Hersey, J.A; Yeung, C.C. Ordered powder mixing of coarse and fine particulate systems. *Powder Tech.* 22 (1979), p. 127.

59- Lai, F.; Hersey, J.A. The variance-sample size relationship and the effects of magnesium stearate on ordered powder mixtures. *Chemical Eng. Science* 36 (1981), p. 1133.

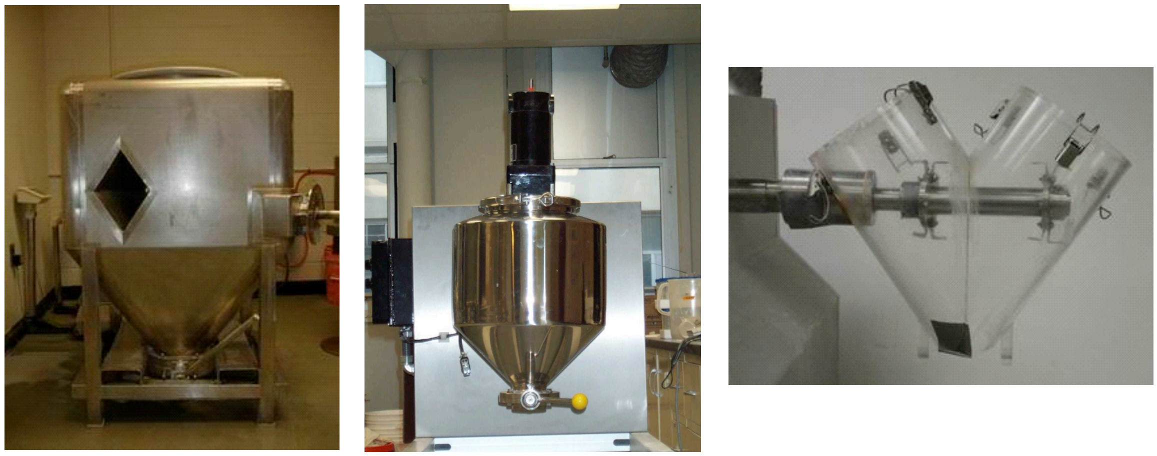

Figures 2-1: (a) 300 liter Tote blender, (b) Cylindrical bin blender with an impeller, (c) V-blender with an intensifier bar

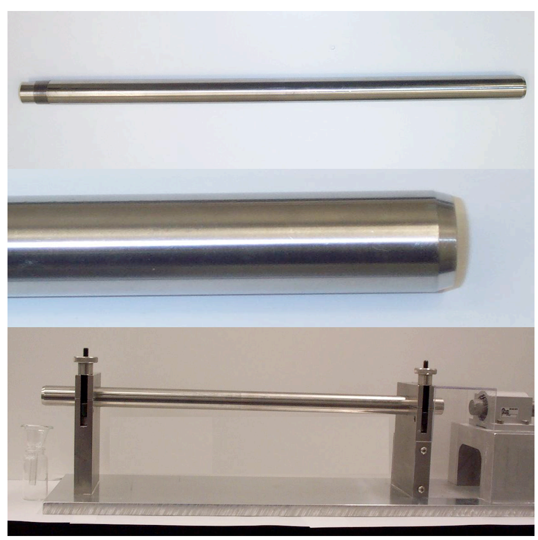

Figures 2-2: Core sampler (top), detail of chiseled tip, and extruder (bottom)

(a)

(b)

(c)

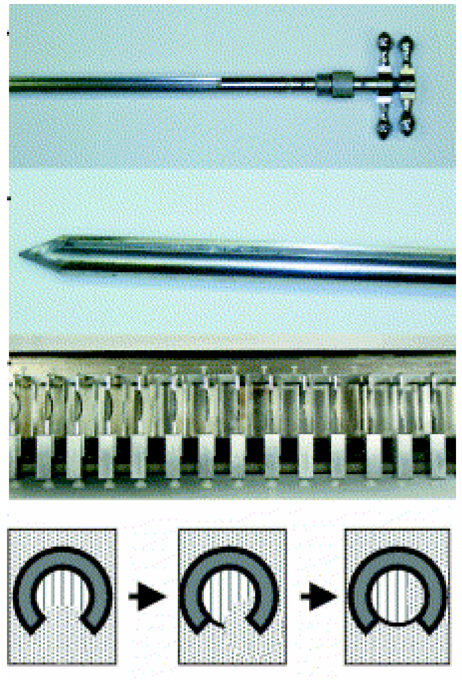

Figure 2-3:(a) Photograph of the groove sampler. The sampler enters the powder bed with minimal disturbance due to the pointed tip. The trough allows for collection of a complete column of material while the rotating outer shell isolates the sample from the bulk. (b) Photograph of the sampling trays used for collection. (c) Schematic showing the rotation of the inner to isolate the sample for removal.

Treatment Pure API	API is milled	NaCl Sieved below 500 ì	Acetaminophen Sieved below 30 ì
Blending equipment			
Outcome		 Agglomerates up to 2 cm	 Agglomerates up to 100 ì

Figure 2-4: Agglomerates in the outcome of blending operations

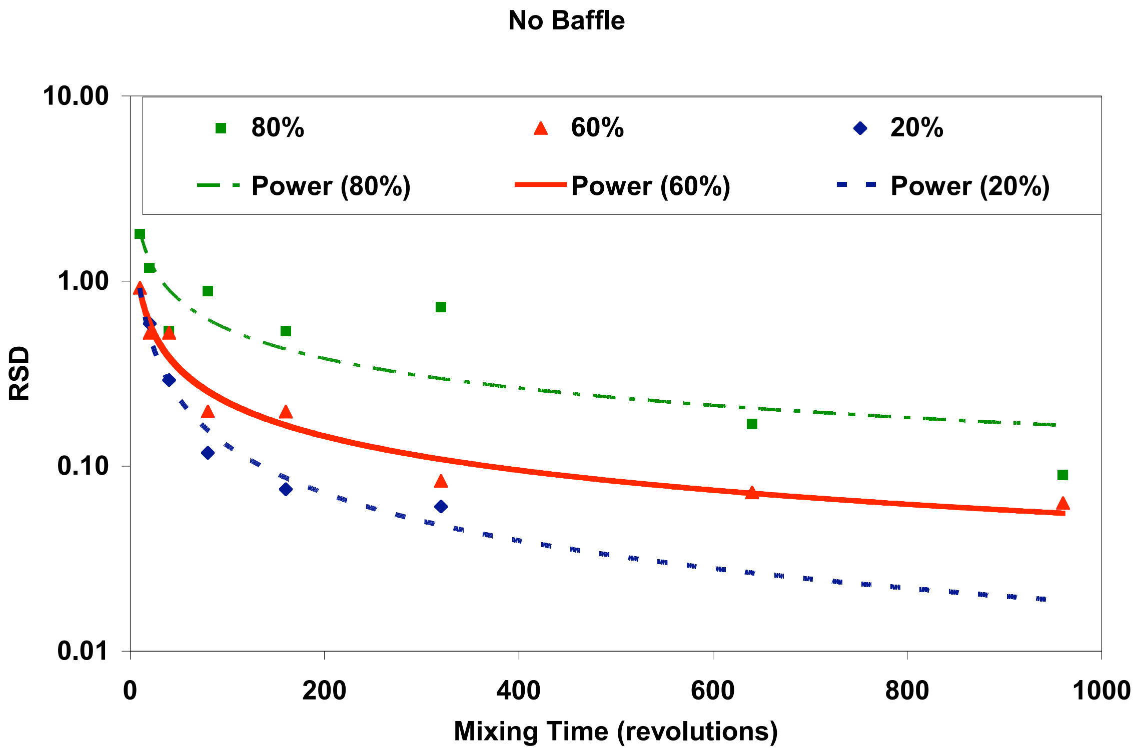

Figure 2-5: Evolution of API homogeneity in a 40-liter cylindrical blender without baffles, operated at 10 RPM, for different fill levels

.

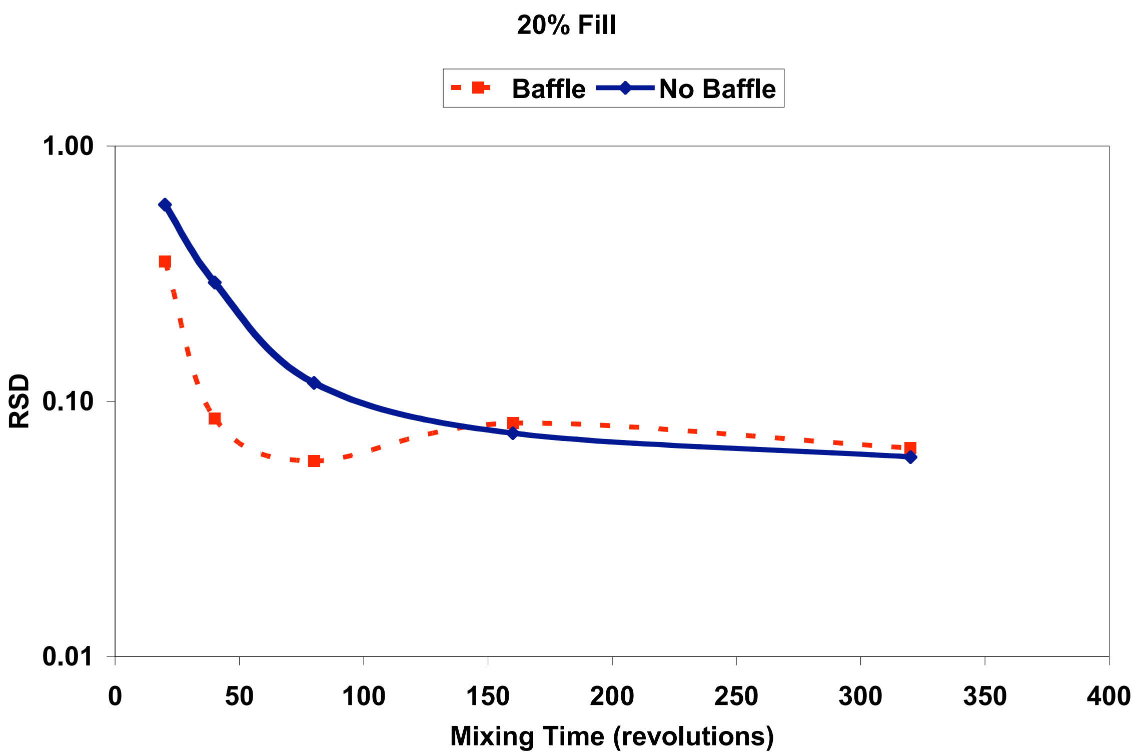

Figure 2-6: Mixing curves for Blend 3 obtained in a 40-liter cylindrical blender operated at a 20% fill level with baffles and without baffles

.

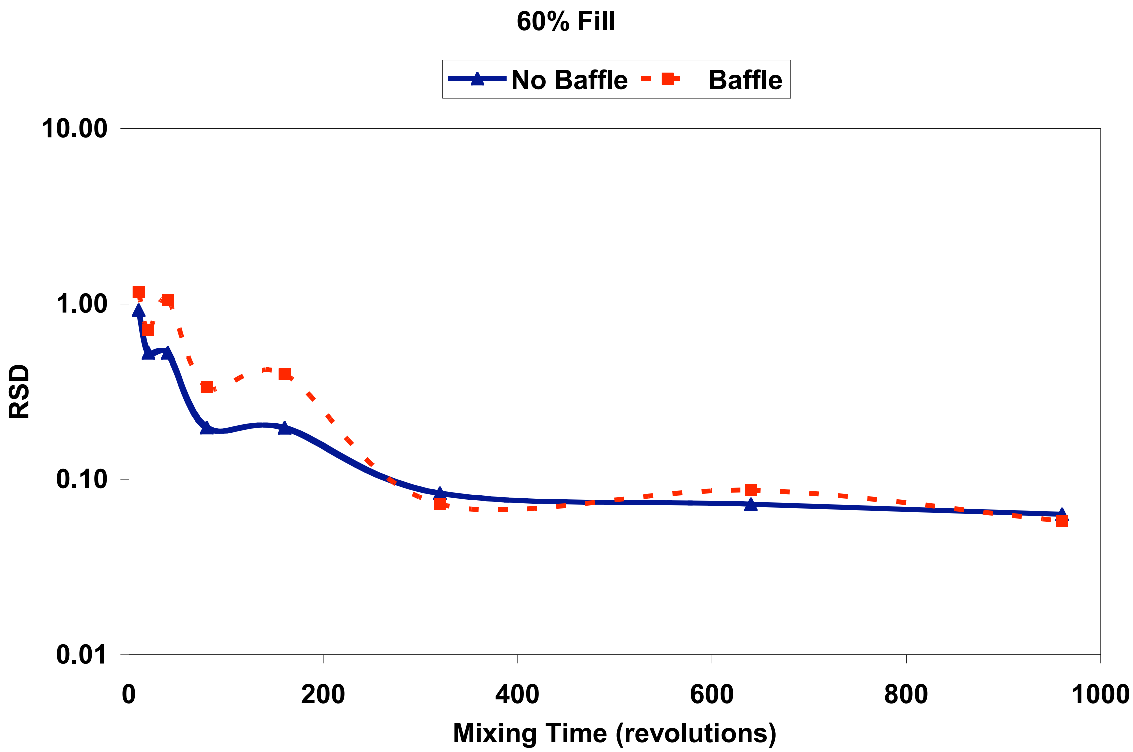

Figure 2-7: Mixing curves for Blend 3 obtained in a 40-liter cylindrical blender operated at a 60% fill level with baffles and without baffles

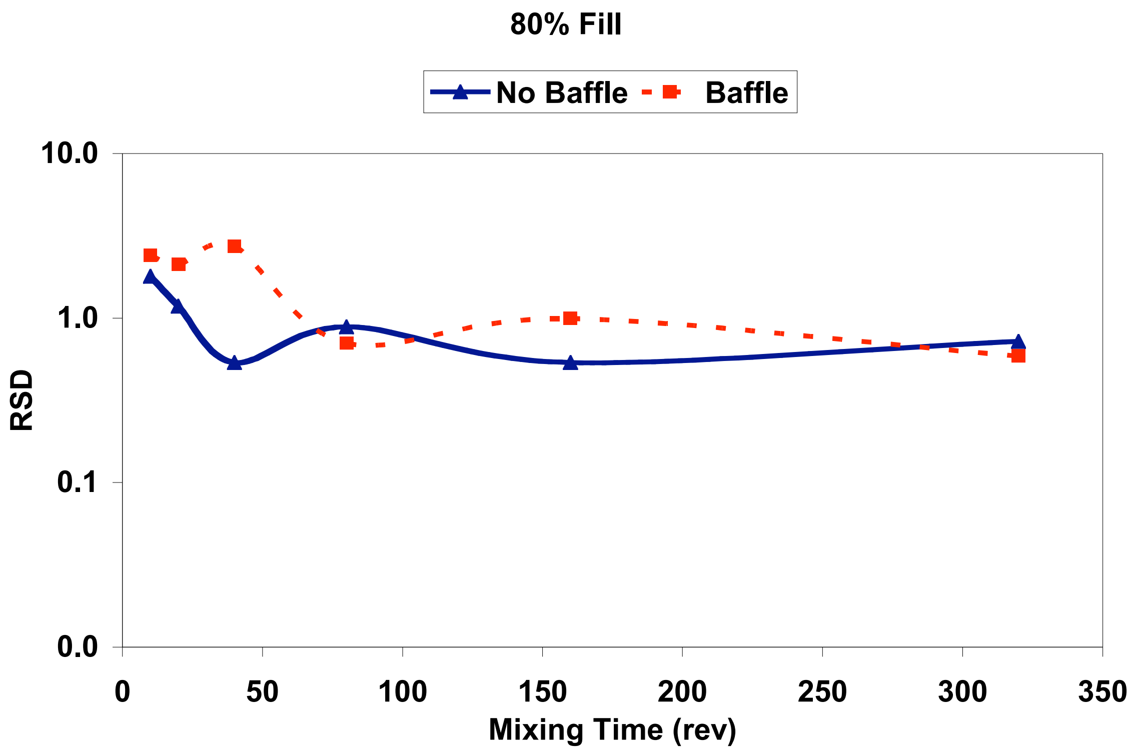

Figure 2-8: Mixing curves for Blend 3 obtained in a 40-liter cylindrical blender operated at a 80% fill level with baffles and without baffles

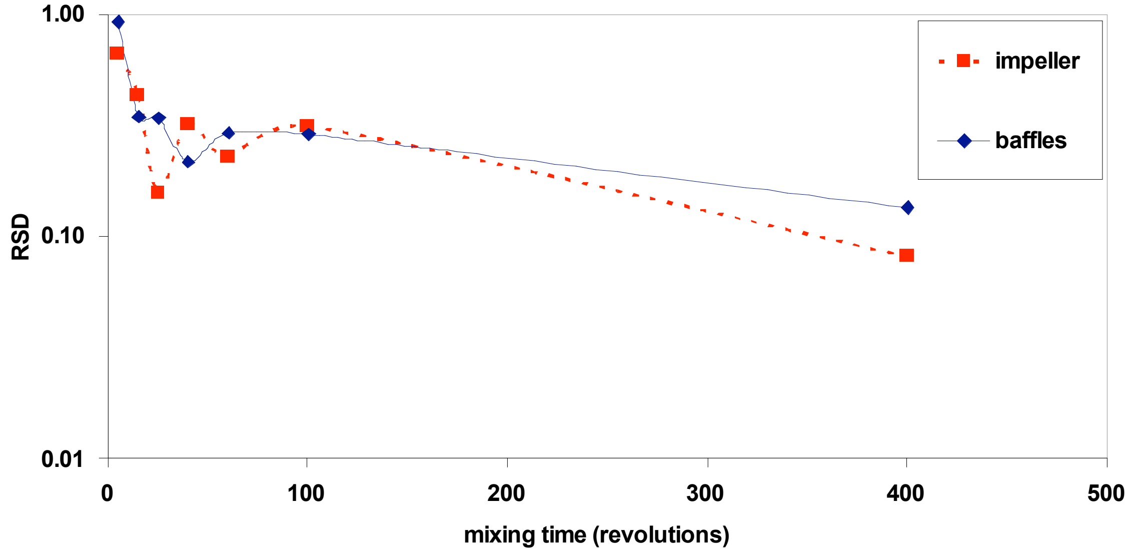

Figure 2-9: Mixing curves for Blend 4 (coarse APAP) in a 20-liter cylindrical blender with baffles or with an impeller

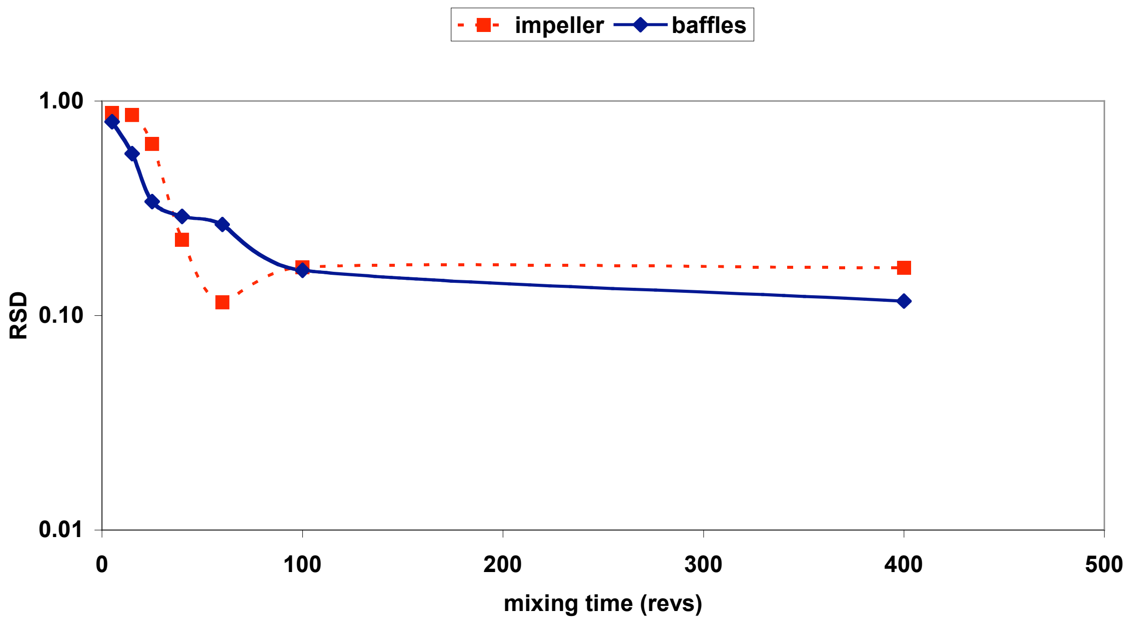

Figure 2-10: Mixing curves for Blend 5 (micronized APAP) in a 20-liter cylindrical blender with baffles or with an impeller

Scale of Tote blender	14-liter	56-liter	300-liter
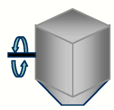	VAR = 1.23E-4 RSD = 0.304 N = 19 3%	VAR = 7.63E-5 RSD = 0.57 N = 59 1%	VAR = 1.07E-6 RSD = 0.084 N = 37 1%

Figure 2-11: Effect of scale on blend homogeneity (red arrows indicate a statistically significant improvement in homogeneity)

Scale of Tote blender	14-liter	56-liter	300-liter
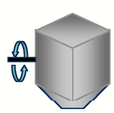	VAR = 1.23E-4 RSD = 0.304 N = 19 3%	VAR = 7.63E-5 RSD = 0.57 N = 59 1%	VAR = 1.07E-6 RSD = 0.084 N = 37 1%
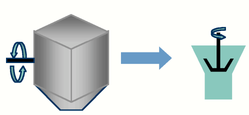	VAR = 4.22E-6 RSD = 0.064 N = 9 3%	VAR = 7.08E-7 RSD = 0.068 N = 24 1%	VAR = 2.26E-7 RSD = 0.040 N = 47 1%

Figure 2-12: Compilation of results for the effect of scale and milling on blend homogeneity (red arrows indicate a statistically significant improvement in homogeneity)

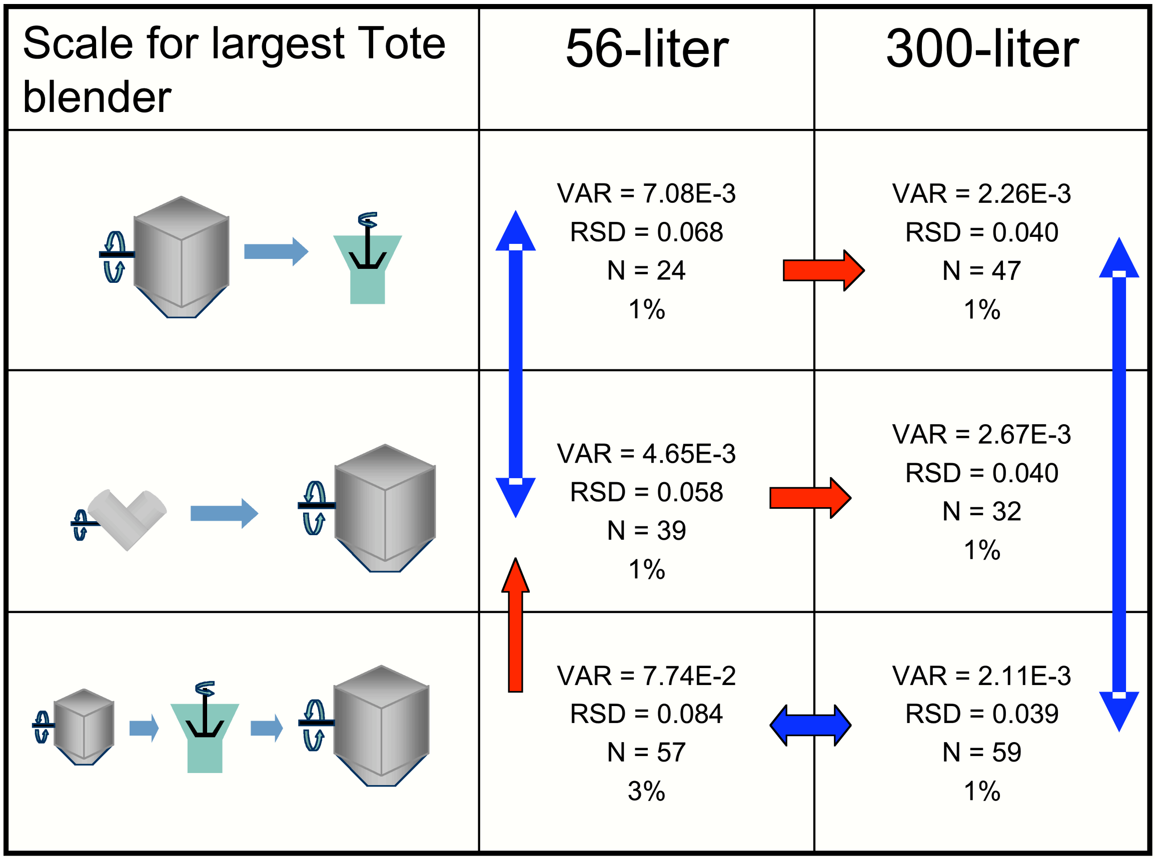

Figure 2-13: Compilation of results for the effect of different protocols (and their scale) on blend homogeneity (red arrows indicate a statistically significant improvement in homogeneity and blue arrows a statistically equivalent processes)

	Blend 1	Blend 2	Blend 3	Blend 4	Blend 5
Microcrystalline cellulose	60%-65%	96%	38.5%		
Lactose			58.5%	99%	99%
Sodium starch glycolate	2%				
Dibasic calcium phosphate	33%				
Pre-Mix excipients	Tote blender, 256 revs.		Cylindrical bin blender (400 revs)		
APAP Wuxi			3%		1%
APAP Mallinckrodt				1%	
Cohesive API	% depends on scale				
NaCl below 180 ì m					
NaCl below 595 ì m		3%			
Mix API	Tote blender (256 revs), or pre-blend and dilution		Cylindrical bin blender (980 revs)	Cylindrical bin blender (400 revs)	Cylindrical bin blender (400 revs)
Magnesium stearate		1%			
Mix API + lubricant		Tote blender (32 revs)			

Table 2-1: Blend compositions and Preparation

	20%	60%	80%
baffle	0.059, 0.082, 0.066	0.072, 0.087, 0.058	0.704, 0.994, 0.588
No baffle	0.118, 0.075, 0.061	0.083, 0.072, 0.063	0.885, 0.536, 0.722

Table 2-2: RSD values at the plateau of the mixing curves for different internal set-ups and fill levels

Source	DF	Seq SS	Adj SS	Adj MS	F	P
fill level	2	1.76056	1.76056	0.88028	69.99	0.000
baffle	1	0.00049	0.00049	0.00049	0.04	0.847
fill level*baffle	2	0.00331	0.00331	0.00166	0.13	0.878
Error	12	0.15093	0.15093	0.01258		
Total	17	1.91529				

Table 2-3: ANOVA analysis of the effect of baffles and fill level on API homogeneity and agglomeration

CHAPTER III

A QUANTITATIVE METHOD FOR MODELING BLEND COMPOSITION DISTRIBUTIONS IN THE PRESENCE OF AGGLOMERATES

Summary

This chapter communicates a methodology that uses experimental data and a new statistical method that uses a simulation to reconstruct the composition distribution of a powder blend containing drug agglomerates. The reconstructed distribution can be used subsequently to optimize sampling protocols, compute operating characteristic curves, and estimate process capability for blends containing agglomerates.

A blend containing a cohesive API and an excipient is prepared in a blender. Although the API is sieved (mesh 100μm) prior to its addition to the blender, API agglomerates are found in samples after blending. These agglomerates have either survived the mixing operation, or been created by the operation. The population of sample concentrations is used to estimate the parameters of a statistical model that combines multiple distribution functions to describe the binary mixture with the minor component partially agglomerated. The local concentration for the non-agglomerated portion of the minor component throughout the entire blend is estimated using a Gaussian distribution with parameters $\bar{x}$ (mode) and s (standard deviation) that are typically well established. The

function and the parameters that describe the population of agglomerates of the minor component are estimated using (typically sparse) experimental data. The optimization of the parameters describing the agglomerate population is performed using a simulation of the powder bed in an iterative manner. The simulated blend, built using the statistical model, is extensively examined and a distribution of RSD estimates is obtained. The iterative process for seeking the parameters that describe the agglomerate population converges when the mode of the distribution of RSD estimates matches the experimental RSD value, which is the best available estimate of the blend homogeneity.

This methodology is applied to populations of samples for different binary formulations prepared in different blenders. In all cases, after iterating to adjust the parameters of the model, there is an agreement between the experimental and the simulated population of samples with a confidence of, at least, 95%.

The methodology described here is an effective tool to create an accurate representation of agglomerated blends based on limited sampling results.

3-1. Introduction

API agglomerates exist when the blending unit does not generate adequate shear to overcome inter-particle forces, or when not all the blend is exposed to the typically localized high shear rates. A common problem for low-dose powder-based products (capsules, DC tablets, powder formulations) is that agglomerates can occur infrequently and can be difficult to detect using standard sampling procedures (with sparse data). Hence, the need to develop sampling protocols to detect and assess characteristics of agglomerated powders with acceptable confidence. In this chapter we develop a methodology that, with several assumptions, assesses the characteristics of agglomerates through the analysis of a limited number of samples. The method is also ideally suited to develop accurate representations of blends using the typically more abundant data obtained by PAT (Process and Analytical Technology) methods. It also works well when agglomerates are substantially more rare than those observed here; however, in such a case, larger data sets (i.e., more samples, or a better sampling method) are required.

In a report of the Product Quality Research Institute's (PQRI) [1], it is stated that "the limitations in current sampling technology and subsequent handling (powder segregation) might limit the effectiveness of using blend sample analysis to ensure the adequacy of mix". The assessment of blend homogeneity is usually accomplished using thief sampling tools. The most basic requirement for the sampling instrument is the ability to extract a representative portion of the blend while minimizing the disturbance of the remaining powder bed. The sampling protocol, which is defined by the number, size and position of the samples to be extracted, should be designed according to the type of blend (ordered or random, high or low potency) under analysis, the type of blender, the risks involved, etc. Establishing an adequate sampling method to validate the uniformity of a final blend has been the subject of much debate, and there are different approaches and acceptance criteria to ensure final product content uniformity [2 - 7]. Another important aspect is to identify the causes of sampling error for sampling tools and protocols, which has been the focus of several previous studies [8-11]. Recent interest in PAT notwithstanding, typical blend homogeneity data typically consists of a small number of samples extracted with the sampling tool from different positions of the blend. Across industry, the concentrations of samples extracted from blends are utilized to calculate a homogeneity index. There are many indexes available [12], but the one most commonly used is RSD (relative standard deviation).

The impact of agglomerates on the concentration of API in samples is directly proportional to the agglomerate size and inversely proportional to the total drug content of the sample. The value and statistical significance of the homogeneity index depends on the number [13] and size of samples [14] used to compute it and on the type of mixture. The confidence in the estimation of the homogeneity index increases as the number of samples increases [13]; but once again, sampling protocols typically involve less than ideal numbers of samples.

In the PQRI report [1] mentioned above, data mining is performed on a large quantity of information, provided by several industrial partners, on content uniformity for blends and finished products. The conclusion of the statistical study is that blend uniformity testing provides useful information during process development and validation and as part of investigations to identify causes of issues that may arise during commercial production. The PQRI report also determined that blend uniformity testing is not necessary during routine manufacture of solid dosage forms when stratified sampling and testing of in-process dosage units is used as an alternative [15]. If during routine production, high dosage unit RSD values are suddenly observed, then performing blend analysis on subsequent batches may be a useful diagnostic tool for trouble-shooting the problem.

Agglomeration and poor blend flow are two of the main obstacles to successful development of direct compression formulations. It is especially problematic to detect an agglomeration event during process scale-up or validation. Thus, the focus of this chapter is to provide statistical tools for the development of appropriate sampling protocols that could be used effectively to detect agglomerates and assess the characteristics of partially agglomerated blends in an early stage of product development. The method can also be used, in inverse fashion, to estimate the number of samples that are needed when facing different degrees of API agglomeration, agglomerate size, etc.

3-2. Materials and Methods

3-2-1. Preparation of blends, sampling and detection of agglomerates

Two binary formulations are prepared with the same excipient and different APIs. The excipient is free flowing lactose (average particle size: ~100 microns) and, for Mixture 1, the API is micronized acetaminophen (average particle size: ~1 micron) while for mixture 2, the API is a coarser grade of acetaminophen (average particle size: ~30 microns). The API is sieved with a 100 □m mesh prior to being loaded into the blender.

3-2-2. Blending and sampling operations

Both mixtures are prepared in a 20-liter Bohle blender, operated at 60% fill level and equipped either with internal baffles or with an impeller rotating at 110 rpm for increased shear conditions. The blender is loaded in a layered manner, first introducing half of the excipients, then covering the surface evenly with the drug and finally adding the remaining half of the excipients. The two mixtures and the two blender set-ups generate four scenarios for analysis. The blender rotates at 14 rpm and, after completing a specific number of revolutions, samples are extracted at three positions along the horizontal axis of rotation. A core sampler is utilized to extract an undisturbed column of powder spanning the entire depth of the blend. Figure 3-2 shows a representation of a blend with agglomerates and three core samplers used to extract a group of samples. The powder is gradually extruded out of the sampler and collected into vials each one containing undisturbed samples of approximately 0.4 grams, generating groups of approximately 140 samples at each sampling time [8, 9]. The API concentration is determined using NIR and the distribution of sample concentrations is presented in histograms. The histogram (Figure 3-3) presents in the y-axis the number of samples that have the API concentration indicated on the x-axis. Typically, the majority of the samples extracted from a low dosage, partially agglomerated blend do not contain agglomerates and their API concentrations fit a Gaussian distribution of values, which denotes a random mixture. The few samples that contain agglomerates form an upper tail in the otherwise Gaussian distribution of concentrations, altering its basic symmetric shape. In these experiments there are between 5 and 10 samples with very high drug concentration in a group of ~140 samples. Those samples are visually examined and the agglomerates are separated and analyzed with UV for chemical composition. The agglomerates consist in all cases of pure API. This distribution of concentrations can be modeled as the contribution of two basic distribution functions and a first estimate of the parameters will be obtained from the very same data set.

3-2-3. Numerical simulation of a blend with agglomerates

The blend is represented using a custom-developed computer model where a cubic matrix is used to represent a blend with spatially distributed concentration values. Each position in the cubic matrix corresponds to a physical region of a blend large enough to represents a sample. The number of positions in the simulated matrix is on the order of 10^6, a number large enough to allow the study of the statistical properties of a blend.

Each position in the matrix has associated values for the mass of the sample, the concentration of non-agglomerated API and, if an agglomerate is present, its diameter (Figure 3-4).

The concentration of non-agglomerated API that is part of a Gaussian distribution of values with parameters $\overline{x_1}$ and s_1 is randomly assigned throughout the matrix. A number of agglomerates N, proportional to the agglomerated mass fraction q of the drug, with a normal distribution of sizes and parameters d_{mean} and s_d (the first estimated values for this distribution), are distributed randomly throughout the matrix. Agglomerates are assigned to a sufficiently large number of contiguous cells in the matrix to represent the agglomerate volume. Under most conditions, all agglomerates are smaller than a single cell.[17]

While very simple, this numerical simulation allows the user to simulate large data sets having the same statistical properties as blends with a wide range of agglomerating conditions. Such large data sets can be used for multiple purposes, such as optimizing sampling protocols, predicting the probability of Type I and Type II errors, and developing specifications and control limits appropriate for the specific type of agglomeration behavior displayed by the system

[17] While the custom-developed software used to perform the simulations is not published here in the interest of brevity, it is available to other researchers who can request copies via email

3-2-4. Statistical model of a blend with agglomerates

For a random mixture in the absence of segregation, if we could exclude the agglomerates from the blend, then all sample concentrations would display a Gaussian distribution. Hence we propose to represent the concentration of all samples in an agglomerated blend as the contribution of two distribution functions: One distribution function $n(x)$ is used to describe the concentration of non-agglomerated active and a second distribution function $a(x)$ describes the additional contribution of agglomerates. If we assume that the presence of agglomerates is statistically independent of the local concentration of the remaining blend (i.e., if agglomerates can be assumed to occur anywhere with equal probability), then the concentration for any sample is expressed by:

$$c(x) = n(x) + \frac{a(x).\rho}{W} \qquad \text{(Eq. 3-1)}$$

where,

$c(x)$ = distribution function for the concentration of drug in all samples

$n(x)$ = normal distribution function that describes the contribution to the sample concentration due to the non-agglomerated drug

$a(x)$ = distribution function for the size of agglomerates, assumed to be a normal distribution. For samples that do not contain agglomerates $a(x) = 0$

ρ = drug density in the agglomerates

W = sample weight

3-2-5. Estimation of parameters for n(x), the normal distribution of concentrations of samples with non-agglomerated drug

We refer the reader to Figure 3-3 to observe the mode $\overline{x_1}$ for the normal central mode n(x). A mode $\overline{x_1}$ lower than the mass fraction of drug initially added to the blend suggests that part of the drug is in the form of agglomerates. Samples without agglomerates are slightly sub-potent because some amount of the total drug is concentrated in agglomerates that are not included in those samples. If the distribution of drug excluding agglomerates is Gaussian, the mean concentration and the mode of the distribution coincide, and the mass fraction q of drug in the agglomerates comes from the difference between $\overline{x_1}$ and the total mass fraction of drug initially added to the blend.

In an agglomerated blend, the active ingredient is in two mass fractions:

$$p + q = \frac{M}{M_{Blend}} \qquad \text{(Eq. 3-2)}$$

where,

p = mass fraction of non-agglomerated drug

q = mass fraction of drug in form of agglomerates

M = total mass of drug

M_{Blend} = total mass of blend.

In order to estimate the standard deviation s_1 for n(x), the normal distribution of sample concentrations without the agglomerates, we use only the samples with concentrations smaller than the mode $\overline{x_1}$ (Figure 3-5). We assume that superimposing the agglomerates on the sub-potent samples does not affect the mode $\overline{x_1}$. The reason to use only those samples is to minimize the impact of the partial overlap of the two distributions. Agglomerates generate high concentration samples which are located on the right side of the mode of the normal distribution of concentrations for a low dosage formulation. It is uncertain at which concentration agglomerates start to appear, but a safe assumption for low dosage formulations is that they are present only in samples with concentrations higher than $\overline{x_1}$. This assumption is especially valid for low dosage formulations where hard-to-detect infrequent agglomerates cause marked super-potency[18] (i.e., the worst case scenario). Mistakenly retaining samples with agglomerates as part of n(x) would cause large errors in the estimate of s_1. Thus, using the data to the left of the mode, we calculate the standard deviation s_1 using equation 2-2, assuming that the mean $\overline{C}$ is given by the mode. Since a minimum of 30 samples is usually required to estimate the parameter with confidence, and we only use about half of the samples that are to the left of the mode, a data set of at least 60 samples is needed for our method. Approximately 140 samples were analyzed per batch, providing ample power for the evaluation of statistical properties.

3-2-6. Estimation of parameters for a(x), the distribution of agglomerate sizes

Describing the population of agglomerates requires determining both the type of distribution function and the values for its parameters. Typically, only a small number of samples is available, which might be inadequate to infer with sufficient confidence the statistical characteristics of agglomerated blends using normal procedures.

A combination of numerical and statistical tools is used here to overcome this problem. First, we assume that agglomerate sizes follow a normal distribution (different

[18]Blends with high drug content present agglomerates in the entire range of sample concentrations, but for such a blend the impact of agglomerates on the concentration of samples is usually negligible and the generation of super-potent tablets is rarely a concern; for such systems, the main problem is segregation, which requires a different statistical toolbox.

than that of the central mode). Other candidates considered were the log normal and the exponential distributions. For the data sets available, several test-of-fit approaches failed to distinguish these distributions from the normal distribution. Moreover, the normal distribution is the most convenient to assume because, among other qualities, we can use the additive properties of variance (Equation 8) within a framework that allows us to estimate the confidence of this assumption.

Samples with agglomerates also contain dispersed drug, therefore the mean or expected value E for this group of samples is:

$$E(n(x) + \frac{a(x).\rho}{W}) = \overline{x_1} + \overline{x_2} \qquad \text{(Eq. 3-3)}$$

Where,

$\overline{x_1}$ = mode of n(x), the normal distribution of concentrations due to non-agglomerated drug, and

$\overline{x_2}$ = sample concentration if the only API is that of an agglomerate of average size.

In the case of Figure 3-6 the obvious estimate for E is the second mode that appears in the plot. However, this second mode may not always be present if there is not an agglomerate size that shows up with more frequency; it is also subjected to high uncertainty due to the small size of the data set. Thus, the first estimate of E is only tentative and it is subject to adjustments in the iterative method described later. With E available, then $\overline{x_2}$ is directly obtained from equation 3-3 and the first estimate for the average diameter d_{mean} of agglomerates is calculated as:

$$d_{mean} = \sqrt[3]{\frac{6.W.\overline{x_2}}{\rho\pi}} \qquad \text{(Eq. 3-4)}$$

where,

W: sample weight

ρ: API agglomerate density

Then the total number of agglomerates N that there will be in the distribution is:

$$N = \frac{\left(\frac{q}{p+q}\right).M}{\frac{\pi.d_{mean}^3}{6}\cdot\rho} \qquad \text{(Eq. 3-5)}$$

In order to estimate the standard deviation for agglomerate sizes s_2 from the experimental data, we must remember that the samples that contain agglomerates also contain non-agglomerated API. Using the additive property for the variances of two normal distributions, the variance in the concentration for the samples with agglomerates has a contribution from both sources of API:

$$V[n(x)+\frac{a(x).\rho}{W}] = V[n(x)] + V[\frac{a(x).\rho}{W}] + 2.Cov[n(x),\frac{a(x).\rho}{W}] \qquad \text{(Eq. 3-6)}$$

where,

$$\text{V(n(x))} = s_1^2 \qquad \text{(Eq. 3-7)}$$

$$\text{V(a(x))} = s_2^2 \qquad \text{(Eq. 3-8)}$$

In order to obtain an estimation of s_2 using Equation 3-6, we assume that the covariance term is zero, i.e., we assume that agglomerates can appear in any sample regardless of its concentration of non-agglomerated drug. However, typically we do not know which samples have agglomerates and therefore we cannot estimate the term on the left of Equation 3-6. We use the experimental RSD (i.e. the index value estimated using all the samples) as the best available estimate of this value. This is a low estimate for the left side of equation 3-6 because the computation of the RSD involves a large number of samples that do not contain agglomerates; thus, the variance for the group is reduced. Consequently Equation 3-6 yields a low initial estimate of s_2 and needs to be fine-tuned using the iterative method described in the next section. We remark that the parameters $\overline{x_2}$ and s_2 are the mode and standard deviation of a distribution of sample concentrations due only to agglomerates and they are directly proportional to the mean diameter d_{mean} and standard deviation s_d for the diameters of agglomerates.

3-2-7. Validation of the parameters for the model

Once all the parameters for the distribution functions are available, it is necessary to verify that the simulation reproduces a blend that, when extensively sampled, generates concentration profiles that yield the experimental RSD value as the most probable of a distribution of RSD values, and that simulated concentration profiles are statistically comparable to the experimental sample concentration profile. The computer simulation relies on the following observations:

(1) For the case study examined here, there is no statistical evidence suggesting that they segregate in any manner. Highly problematic scenarios where API both agglomerates and segregates are typically detected early during development; such systems rarely proceed through scale up, and usually lead to process changes (such as incorporation of a granulation step) to mitigate them.

(2) Since agglomerates are relatively rare, and typically much smaller than samples, agglomerates occupy at most a single cell in the simulated

blend; some positions will have a single agglomerate whereas most positions will not have any. It is important to assign the correct mass for each position because the impact of the agglomerate on the concentration of the sample is inversely proportional to the mass of the sample. Finally, the net drug concentration of each position is given by the combination of the two contributions (equation 3-1).

In the context of the simulation, a “sampling event” consists of reading all the matrix values in one or more adjacent columns of the matrix (Figure 3-3). The computer model makes it possible to sample the entire “blend”, using as many sampling events as necessary. If the number of “samples” in a simulated sampling event is on the order of 10^2, then the total number of simulated sampling events (without replacement) is in the order of 10^4. Each event yields a homogeneity value (RSD) and all the RSD values form the population of possible RSD values for the blend. Additional validation of the computer simulation is provided by the fact that the homogeneity index correlates with the inverse square root of the sample size. When groups of samples for a simulated blend are combined to form larger samples (i.e. the mass of the smaller samples is added and their concentrations are averaged) the expected correlation between homogeneity index and sample size is observed.

If one could physically sample the real blend repeatedly without causing perturbation of the powder bed, one would obtain a distribution of RSD values. Some of these RSD values would correspond to experiments that do not capture any agglomerates and others would correspond to experiments that capture agglomerates more often than the proportion in the entire mixture. Nonetheless, the most frequent result would be experiments that capture a group of samples that is representative of the whole mixture. We assume that the experimental RSD value is the best available estimate of actual RSD (Figure 3-7). The in-silico results that share the experimental RSD value (~2400) capture different sub-populations of agglomerates (i.e. agglomerates of different sizes).

Since the requirement that the extensive sampling process does not alter the powder bed is physically impossible and the time necessary to perform such operation would be enormous, this distribution of RSD values is obtained here using the computer simulation. In the case that the most probable RSD coincides with the experimental RSD, one proceeds to statistically compare the experimental and simulated distributions of values.

A test-of-fit for a normal distribution, where actual compositions are plotted against standardized Z scores corresponding to each observed value, is shown in Figure 3-8 and subsequent.

If the distribution is indeed Normal (Gaussian), the test would render a straight line. As shown in Figure 3-8, the test of fit for normality with the experimental samples and for the simulated sampling events with the most probable RSD yields profiles where the slope of the straight line is equal to the standard deviation for the distribution function of samples with non-agglomerated drug. The intersection of the line with the ordinate is equal to the mode for this function. Figure 3-8 shows that the simulated concentration profiles have similar slopes and intersection with the ordinate when compared to the experimental profile. More significantly, the simulations accurately capture the deviations from normality due to the agglomerates (upward bend on the right hand side of the curve). In order to asses the accuracy of the parameters that describe the population of agglomerates, a chi square test of the composition values that are larger than the mode is performed. The test is performed for this group of samples because the agglomerates are distributed only among them.

3-2-9. Iterative method to adjust the parameters for the sub-population of agglomerates

In the case where the distribution of RSD values does not have the experimentally observed RSD as the most probable value, the parameters for the distribution functions will need adjustment. Typically, the parameters for the non-agglomerated drug are statistically sound because they are obtained with a large number of samples and do not need corrections. Instead, the parameters estimated for the distribution function for agglomerated drug are subject to higher uncertainty.

In order to get a distribution of RSD values with the experimentally observed RSD as the most probable value (the mode), different values for the parameters of the distribution of agglomerates are tested. Sometimes, using the first estimates for d_{mean} and s_d, one obtains a distribution of RSD values where the most probable RSD is smaller than the one observed experimentally. One reason is that the variance for the distribution of agglomerates sizes, s_d, is underestimated by using the experimental RSD for all samples in the left side of equation 3-6. As mentioned before, one is “diluting” the effect of agglomerates with the high number of samples that do not have any agglomerates. The options for increasing the value for the most probable RSD until matching the experimental value are as follows:

- First, the variance for the distribution of agglomerates sizes is increased.

- Second, if the increase in variance for the size distribution goes beyond the physically possible, the average agglomerate diameter is increased.
- And in both cases, the mass of drug in the agglomerates is maintained constant and equal to the estimate from the physical samples.

Once there is a match between the RSDs, the experimental concentration profile is contrasted with the simulated concentration profiles of most probable RSD. If both concentration profiles are in agreement within a pre-established statistical significance, the parameters are considered valid to describe the agglomerate population. Otherwise, by comparing these two profiles one can obtain a lead regarding the type of modification in the parameters for the agglomerate distribution and start the next iteration.

Once appropriate parameters for the simulation have been identified and the correct (most probable) distribution is predicted, the simulation can easily and rapidly generate extensive results, which can be used, as mentioned before, to estimate the probability of different types of failures for specific sampling protocols. As an illustration, in the results section, this method is successfully applied to a variety of blends and a discussion of situations that lead to an initial incorrect estimation of parameters is presented.

3-3. Results and Discussions

The aim of this section is to apply the procedure explained in detail in the methods section to several experimental data sets (or concentration profiles) and successfully characterize the population of API agglomerates and the concentration of dispersed API. The two mixtures analyzed are mixture 1, which contains lactose and micronized acetaminophen, and mixture 2, which contains lactose and a coarser acetaminophen. Both mixtures are prepared in a 20-liter Bohle blender equipped either with internal baffles or with an impeller rotating at 110 rpm for increased shear conditions. These conditions were selected to reflect the settings of a process of interest to one of our industrial sponsors. Although the API is sieved (mesh 100□m) prior to its addition to the blender, some API agglomerates are found in samples from both mixtures and set-ups. While agglomerates were likely present in the starting materials prior to mixing, these agglomerates have obviously survived the mixing operation[19]. Furthermore, the size of API agglomerates (Figure 3-1) is slightly larger than the mesh of the sieves, indicating that mixing has caused agglomerate growth [16]. The concentration of samples extracted after a given number of revolutions (approximately 140 samples) is plotted in the form of histograms to carry out the assessment of parameters for the distribution functions (Figure 3-9-a to 6-9-f).

The labeling of the histograms indicates the mixture, the type of intensifier in the blender (baffle or impeller) used to prepare the mixture and the number of revolutions at which the samples are extracted. The histograms present in the y-axis the number of samples that have an API concentration in the range indicated in the x-axis.

The first three histograms (Figure 3-9-a to 6-9-c) correspond to mixture 1 and the last three histograms (Figure 3-9-d to 6-9-f) correspond to mixture 2. These histograms corroborate the Gaussian mode for the distribution of concentrations with a deviation from normality for samples that contain agglomerates. The histograms facilitate the

[19] Presence of agglomerates in the raw materials prior to mixing was not examined because methods currently available for determining particle size distribution lead to significant attrition of the “soft agglomerates” of interest here.

estimation of parameters such as $\overline{x_1}$ and provide the first estimate for E (the second mode in the histogram), which allows the calculation of d_{mean} (mean diameter of agglomerates). Figure 3-9-a and 6-9-b are the samples extracted from a blender with the impeller after 40 and 100 revolutions respectively. It is noteworthy that agglomerates of micronized acetaminophen survive the increased shear mixing generated by the impeller even after 100 revolutions. Figure 3-9-c is the histogram for the samples extracted from a blender with baffles after 40 revolutions. In this baffle set-up, which has lower shear rates, there are samples containing multiple agglomerates of micronized acetaminophen and concentrations over 2.5%.

Figure 3-9-d is the histogram for the samples of mixture 2, extracted from the blender with the impeller after 60 revolutions. Figure 3-9-e and 6-9-f are the histograms for the samples of mixture 2 extracted from a blender with baffles after 40 and 100 revolutions respectively. Even though the acetaminophen is less cohesive than in mixture 1, large agglomerates that produce super-potent samples (150% super-potency) are found in samples after 100 revolutions (Figure 3-9-f).

After using these histograms to obtain a first estimation of the parameters for the distribution functions of agglomerated and non agglomerated API, blends and sampling operations are simulated. For the cases where the most probable RSD does not coincide with the experimental RSD, the parameters for the agglomerate distribution are modified accordingly. The iterations converge when the mode of the simulated RSD distribution coincides with the experimental RSD. The next step is the validation of the parameters for the distribution functions. The experimental samples and one of the in-silico experiments that yield the experimental RSD are plotted using normal probability coordinates. Figures 6-10-a to 6-10-f compare the experimental and the simulated concentration profiles for the cases already presented in Figures 6-9-a to 6-9-f.

To validate the parameters for the distribution size of agglomerates, one applies a chi square test to the concentrations larger than the mode for the experimental and the simulated profiles (that is, the samples where the agglomerates are to be found). The samples with concentrations larger than the mode $\overline{x_1}$ are grouped into 4 cells (k=4) and, with two parameters m to be estimated for the distribution of agglomerates (mean and standard deviation), the degree of freedom is 1 and the critical value is $\square_{.05,\ k-1-m} = \square_{.05,\ 1}$ = 3.843. The values first obtained for the test are presented in the following table:

Mixture 1	Mixture 1	Mixture 1	Mixture 2	Mixture 2	Mixture 2
40 revs, Imp	100 revs, Imp	40 revs, Baf	60 revs, Imp	40 revs, Baf	100 revs, Baf
3.76	3.65	9.33	1.40	1.14	9.12

Values in the chart that are larger than or equal to 3.843 indicate that the simulated data do not provide a good fit with the experimental data. For such cases, the simulation is used to find a new combination of mean and standard deviation of agglomerate sizes until acceptable values of chi square are reached.

One reason for an inadequate first estimation of the parameters for the agglomerate population is the existence of multiple agglomerates in a single sample. For example, the sample for mixture 1 with concentration >3.5 % found in the blender with baffles, after 40 revolutions (Figure 3-9-c), actually contains several agglomerates. This sample leads to over-estimation of the range of possible agglomerate sizes (i.e. larger average size and standard deviation) and the parameters for the agglomerate distribution function. As a consequence, in the normal plots, the profile for the experimental super-potent samples is located below the concentration profiles for the simulated blend (Figure 3-10-c). Excluding this sample, a new set of parameters for the agglomerate distribution function is estimated and a better fit between simulated and experimental concentration profiles is obtained. To avoid this problem, samples that present a very high concentration of drug should be inspected for multiple agglomerates.

Another case of discrepancy between simulated and experimental profiles is due to an over-estimation of s_1, the standard deviation for the normal distribution function for the non-agglomerated drug. This is caused by a group of sub-potent samples (Figure 3-10-d) that do not belong to the normal distribution of samples with dispersed drug. The fact that these samples are outliers of the normal distribution is not obvious in the histogram, unlike the few sub-potent samples observed in Figure 3-9-a. The current computational model does not currently include a distribution function to represent sub-potent samples typically caused by incomplete mixing. For such cases, a new and better adjusted value of s_1 is estimated with the help of the normal plot (i.e. use the slope of the straight line).

After the pertinent corrections, the results of the chi square test always show a very good match between the simulation and the experimental profile.

3-4. Conclusions

Agglomeration is a common event in processes that involve powdered materials. However, sampling sets that fail to detect agglomerates are common in practice. The consequences of uncontrolled agglomeration, which is a common event in direct compression systems, are almost always adverse for the quality of the final product; especially for low-dose products that are becoming increasingly common. Therefore, there is a substantial need to have sampling tools and protocols to detect and assess the extent and characteristics of agglomerates in a blend.

Blend assessment is normally done with small groups of samples. For such cases, the telling symptom of agglomeration is a slight subpotency of the blend, detected batch after batch, interrupted by the occasional detection of a few, strongly super-potent values. Such a pattern in the historical data indicates that a small fraction of the drug is in the form of agglomerates and that more extensive sampling is needed in order to get a first estimation of the parameters for the agglomerate size distribution. Alternatively, data analysis combining data from many batches can be used to perform a retrospective analysis of the size and prevalence of agglomerates, using methods very similar to the one outlined here.

The statistical model presented here is a new tool to describe random mixtures with partially agglomerated drug and is capable of reproducing experimental data with high accuracy. It must be emphasized that an advantage of the simulation is that the statistical blend characteristics, assessed using a limited number of samples, can be used for design and diagnostics purposes. This fact is particularly interesting for industrial practitioners, who can use the method as an approach to design sampling protocols, which could be tailored to different degrees of agglomeration. The simulation can be used, for example, to predict the probability that a specific sampling protocol (number and size of samples) would lead to batch failure under a specific quality requirement for a specific blend homogeneity. Perhaps most interestingly, the statistical analysis presented here provides a framework that can be used as part of a PAT strategy for on-line characterization of a blend.

The present and the previous chapters have offered a practical approach to design a process, select equipment, and choose operation conditions that minimize API agglomeration as well as providing tools to control and monitor, once the process is being performed, the degree and the characteristics of the agglomerates in the blend. However, there is a lack of fundamental understanding of the role of material and processing variables on the API de-agglomeration. The next chapter will use a method to expose API materials with specific characteristics (i.e. particle size distribution) to uniform shear conditions. Therefore, one will be able to discriminate the effect of material properties and processing variables on the degree of agglomeration in a blend. This type of information could be used as a feedback for future design of blending units and processes and minimize agglomeration.

REFERENCES

1- Boehm, G. et al. Results of Statistical Analysis of Blend and Dosage Unit Content Uniformity Data Obtained from the Product Quality Research Institute Blend Uniformity Working Group Data-Mining Effort. *PDA Journal of Pharmaceutical Science and Technology* (March/April 2004), p. 62.

2- Geoffroy, J.M.; LeBlond, D.; Poska, R.; Brinker, D.; Hsu, A. Unit Dose Sampling and final product performance: An alternative approach. *Drug Dev. and Ind. Pharm.* 27 (2001), p.731.

3- Orr, N.A.; Shotton, E. The mixing of cohesive powder. Chem. Eng. (Jan. 1973), p. 12.

4- Carstensen, J.T.; Dali, M.V. Blending validation and content uniformity of low content, non cohesive powder blends. *Drug Dev. and Ind. Pharm.* 22 (1996), p. 285.

5- Carstensen, J.T.; Rhodes, C.T. Sampling in blending validation. *Drug Dev. Ind. Pharm.* 21 (1995), p. 1257.

6- PDA Technical Report No. 25. Blend uniformity analysis: validation and in-process testing. *PDA Journal of Pharmaceutical Science and Technology* 51 (1997), Suppl.

7- Boehm, G. Report on the Industry Blend Uniformity Practices Survey. *Pharmaceutical Technology* (August 2001), p. 20.

8- Muzzio, F.J.; Robinson, P.; Wightman, C.; Brone, D. Sampling practices in powder blending. *Int. J. Pharm.* 155 (1997), p. 153.

9- Muzzio, F.J.; Goodridge, C.L.; Alexander, A.; Arratia, P.; Yang, H.; Sudah, O.; Mergen, G. Sampling and characterization of pharmaceutical powders and granular blends. *Int. J. Pharm.* 250 (2003), p. 51.

10- Garcia, T.P.; Wilkinson, S.J.; Scott, J.F. The development of a blend sampling technique to assess the uniformity of a powder mixture. *Drug Dev. Ind. Pharm.* 27 (2001), p. 297.

11- Harwood, C.F.; Ripley, T. Errors associated with the thief probe for bulk powder sampling. *J. Powder Bulk Solids Tech.* 11 (1977), p.20.

12- Poux, M.; Fayolle, P.; Bertrand, J.; Bridoux, D.; Bousquet, J. Powder mixing: Some practical rules applied to agitated systems. *Powder Tech.* 68 (1991), p. 213.

13- Lloyd, P. J. Inst. Chem. Eng. Symp. Ser. 65 (1981) S3/K/1.

14- Cooke, M.H.; Bridgwater, J. The relationship between variance and sample size for mixtures. *Chem. Eng. Science* 32 (1977), p. 1353.

15- Boehm, G., et al. The Use of Stratified Sampling of Blend and Dosage Units to Demonstrate Adequacy of Mix for Powder Blends. *PDA Journal of Pharmaceutical Science and Technology* 57 (March/April 2003), p. 64.

16- Garcia, T.; Carella, A.; Pansa, V. Identification of factors decreasing the homogeneity of blend and tablet uniformity. *Pharm. Tech.* (March 2004), p. 110.

Figure 3-1: Picture of a large agglomerate of acetaminophen found in a sample of a blend of APAP and fast flow lactose powder (length of slide 7.5 cm, scale picture: 1:1.08).

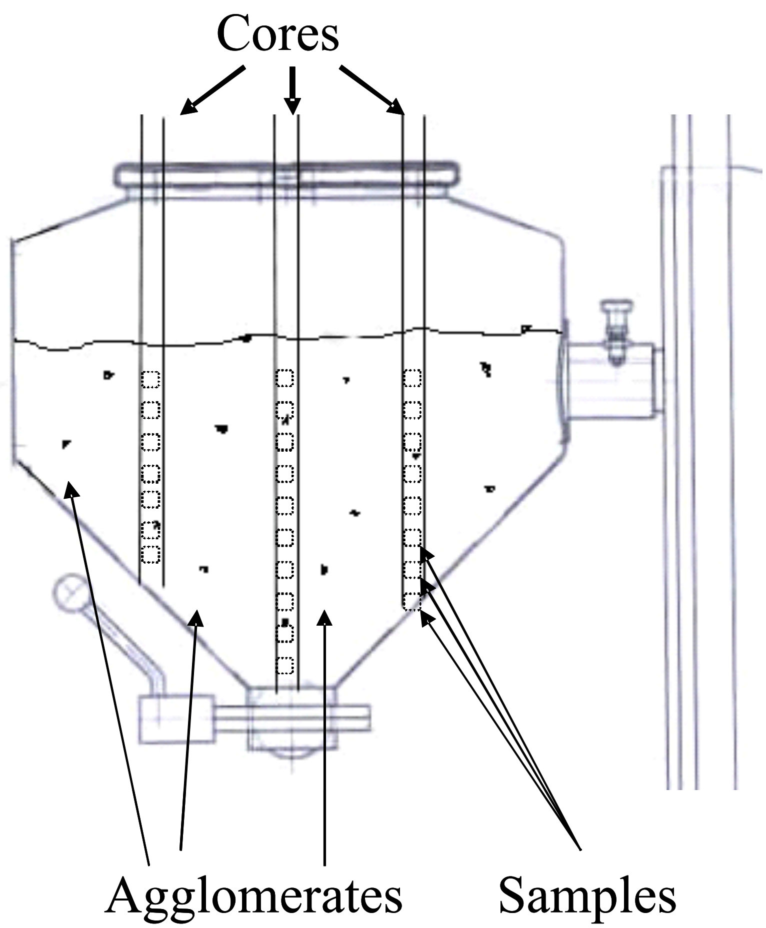

Figure 3-2: Representation of a blend with agglomerates. The three cores (or columns) extracted constitute an experiment.

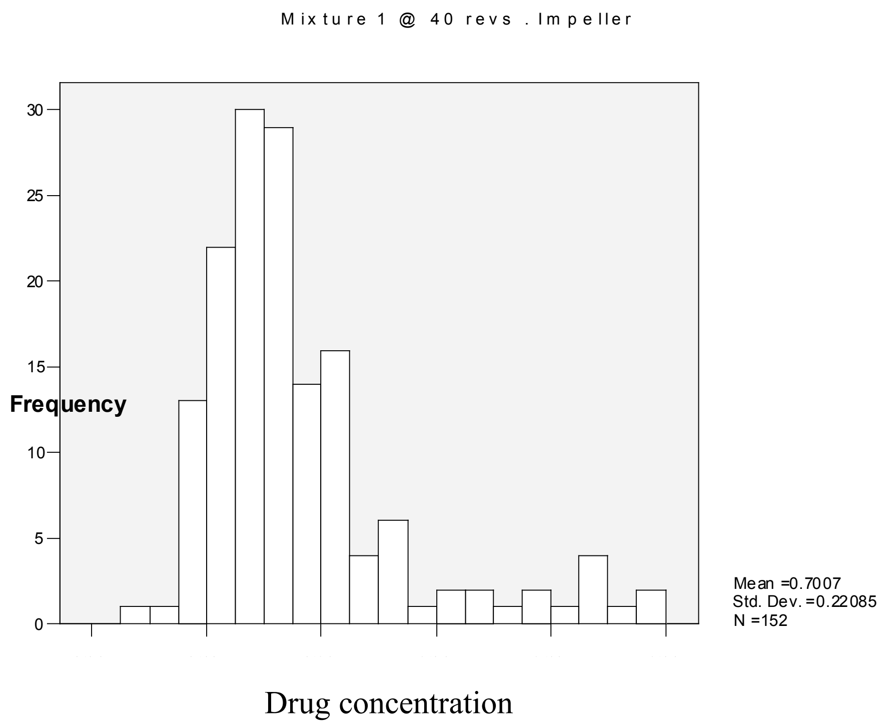

Figure 3-3: Typical histogram of a sampling event for a blend with agglomerates. Note the “normal-looking” distribution of sample concentrations and also the tail of high concentrations originated by agglomerates.

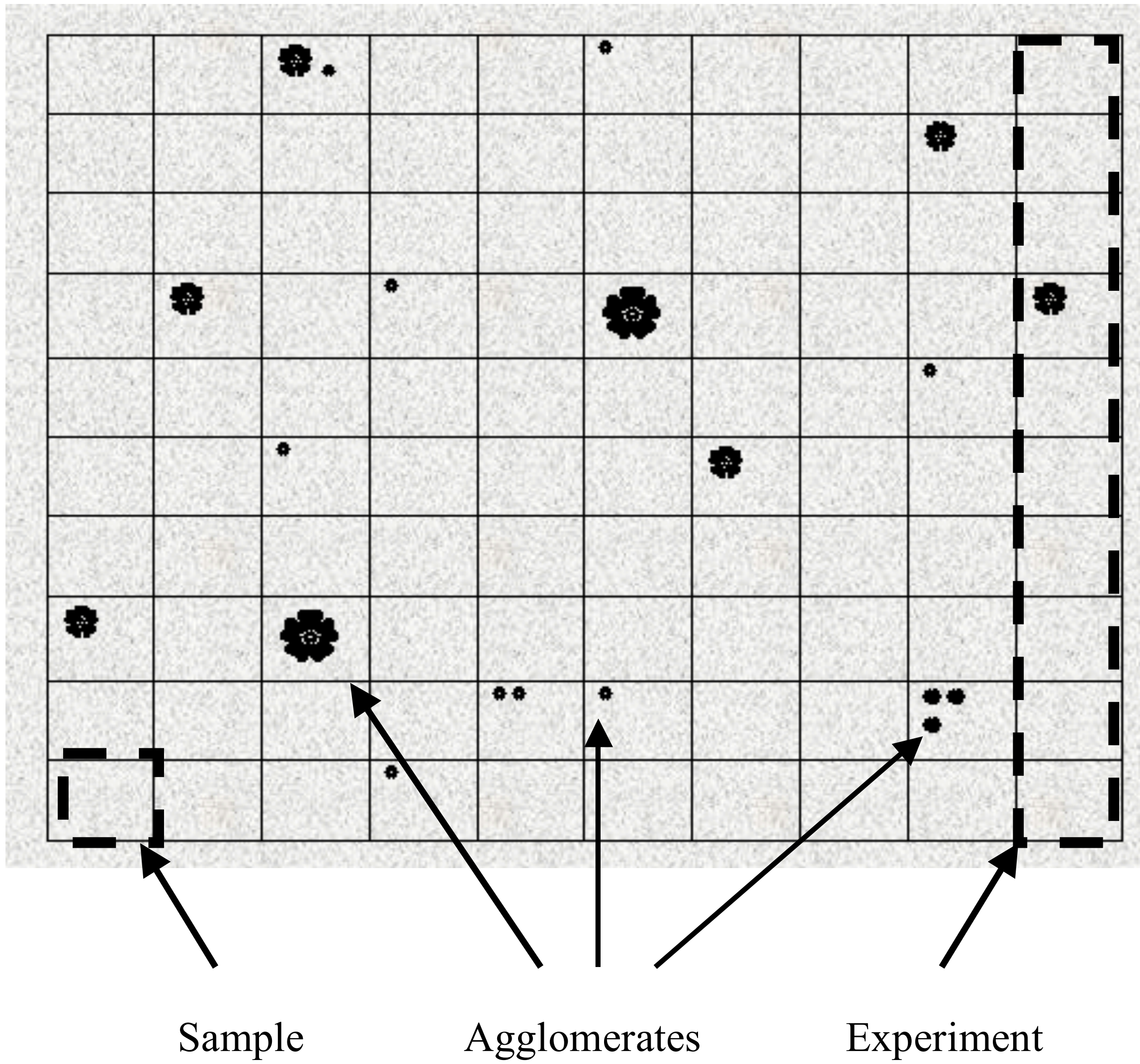

Figure 3-4: Representation of a blend with agglomerates subdivided into samples. The collection of samples in one or more columns constitute a sampling event.

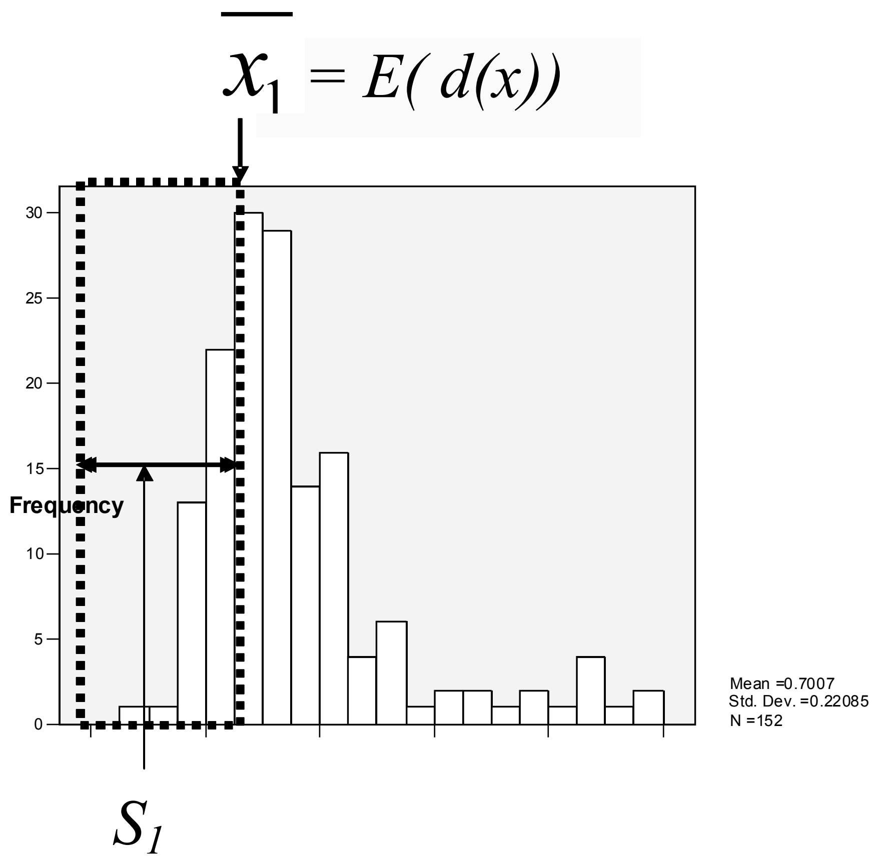

Figure 3-5: First estimation of parameters for the normal distribution of samples with non-agglomerated drug (mean)

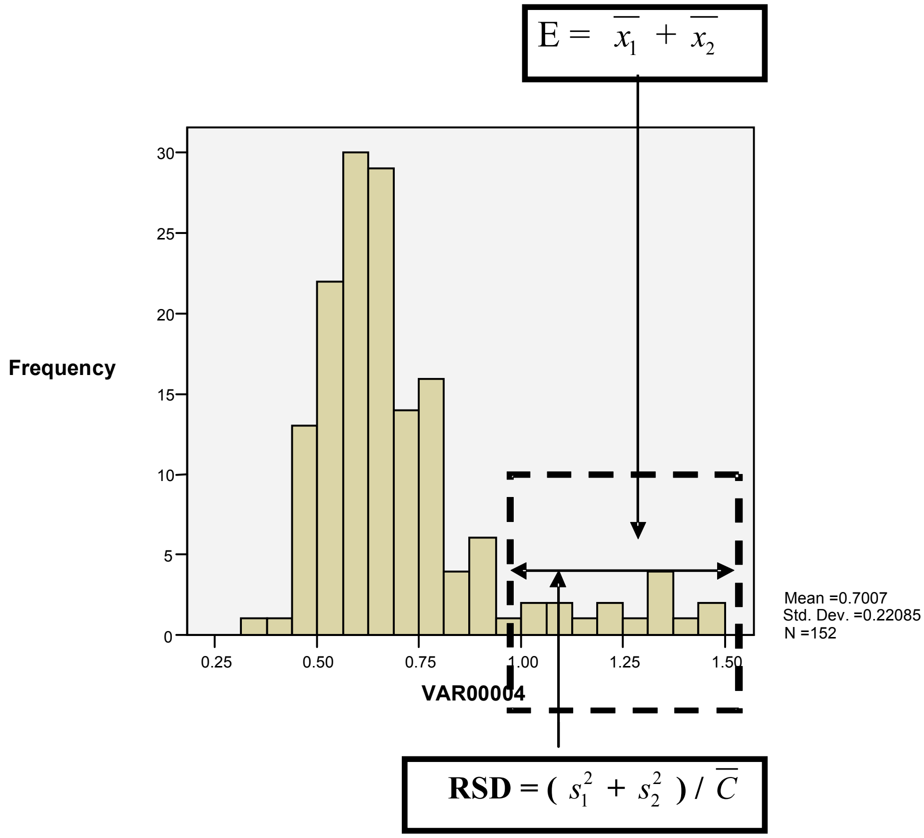

Figure 3-6: First estimation of parameters for the normal distribution of agglomerate sizes (variance)

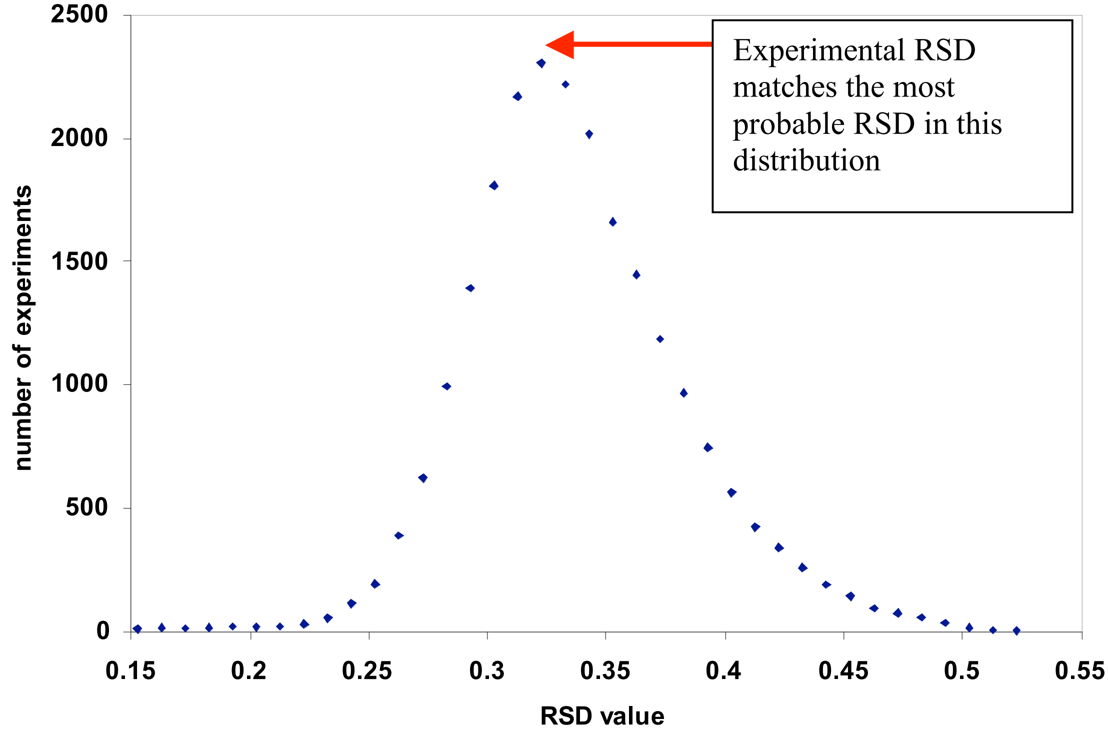

Figure 3-7: Distribution of RSD values that result from repeatedly sampling simulated blend with a number of identical experiments (in terms of number and size of samples)

Mixture 2 – 40 revolutions - Impeller

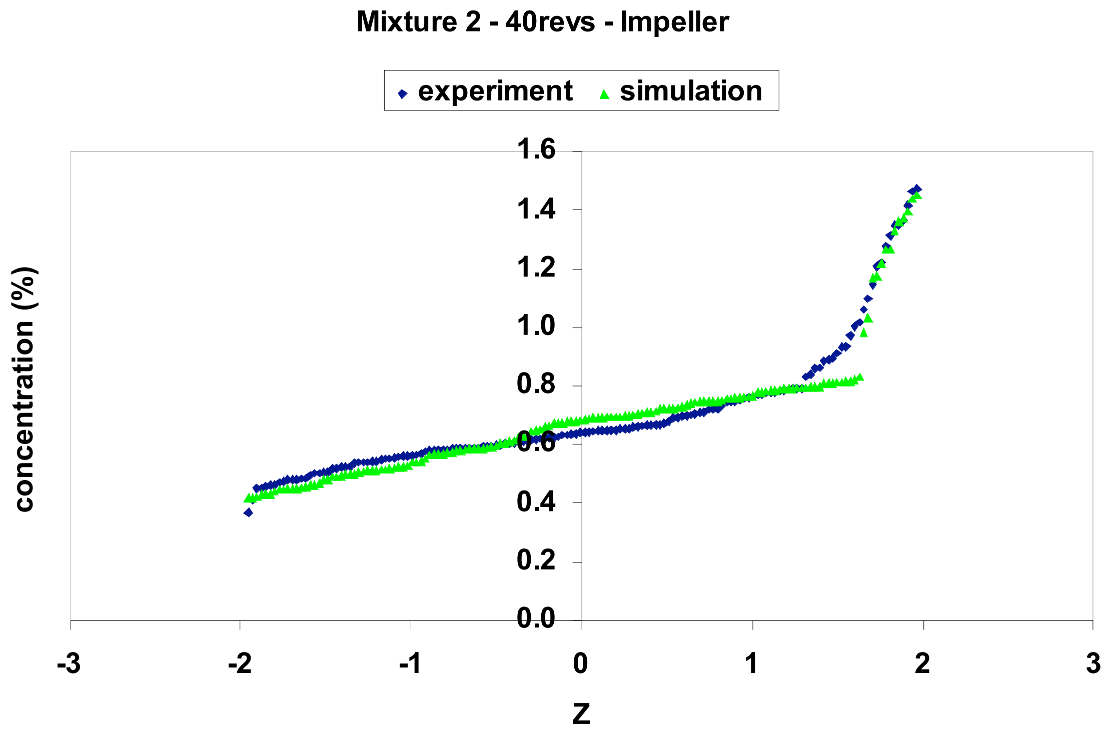

Figure 3-8: the normal test profile for the experimental sample concentrations is included among the "silico" concentration profiles. This test validates the simulation of the blend

Figure 3- 9-a: Mixture 1 – 40 revolutions - Impeller

Figure 3- 9-b: Mixture 1 – 100 revolutions - Impeller

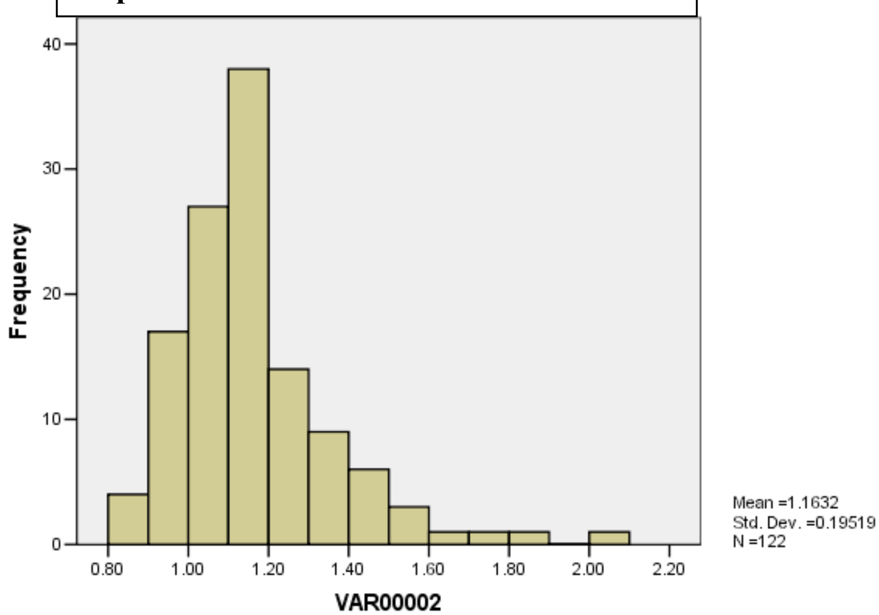

Figures 3-9-a and 3-9-b: Histograms for concentration profiles obtained in the impeller set-up for mixture 1.

Figure 3- 9-c: Mixture 1 – 40 revolutions - Baffles

Figure 3-9-c: Histogram for the concentration profile obtained in the baffle set-up for mixture 1.

Figure 3- 9-d: Mixture 2 – 60 revolutions - Impeller

Figure 3-9-d: Histograms for concentration profiles obtained in the impeller set-up for mixture 2.

Figure 3- 9-e: Mixture 2 – 40 revolutions - Baffles

Figure 3- 9-f: Mixture 2 – 100 revolutions - Baffles

Figures 3-9-e and 3-9-f: Histograms for concentration profiles obtained in the baffle set-up for mixture 2.

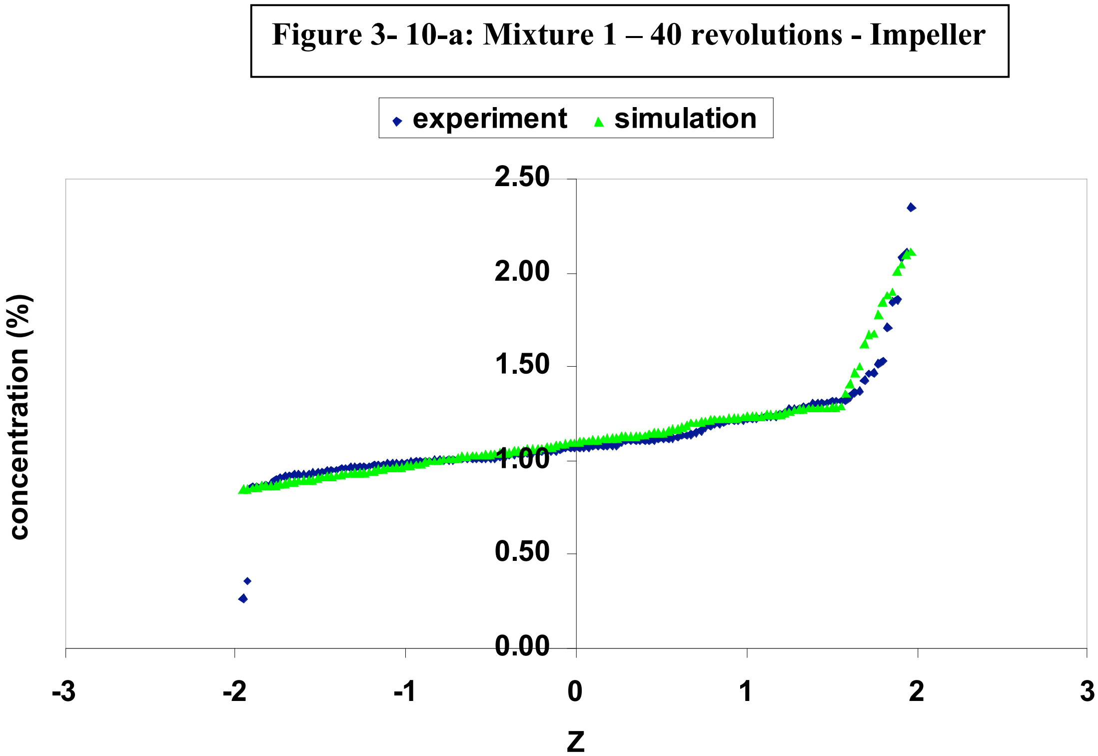

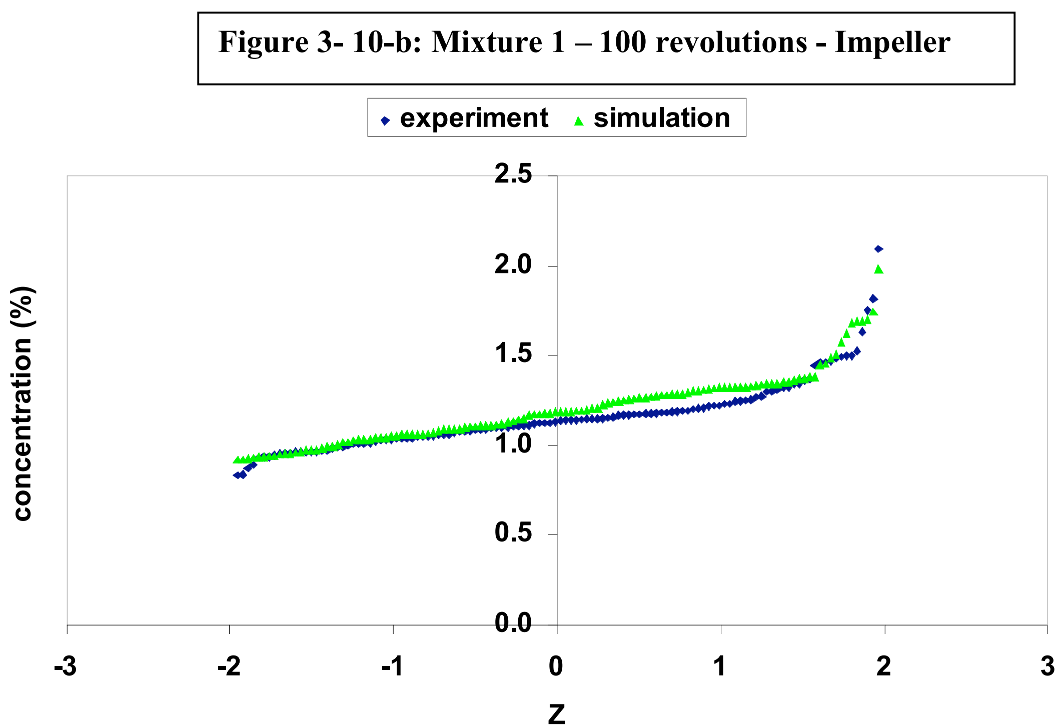

Figures 3-10-a and 3-10-b: Normality test for the experimental profile and profiles obtained in the modeling of mixture 2 in the impeller set-up.

Figure 3- 10-c: Mixture 1 – 40 revolutions - Baffles

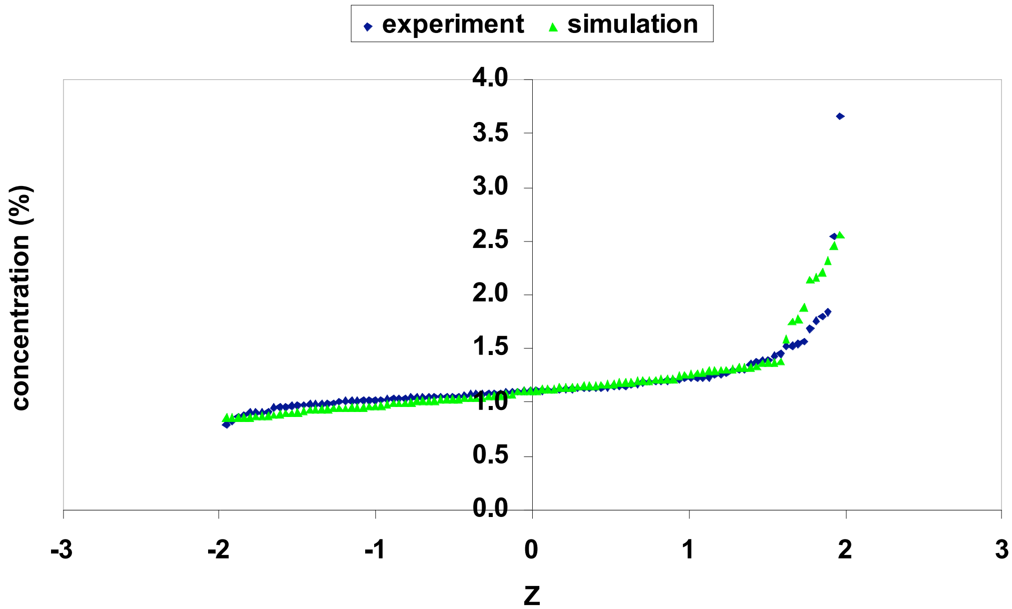

Figure 3-10-c: Normality test for the experimental profile and profiles obtained in the modeling of mixture 2 in the baffle set-up.

Figure 3- 10-d: Mixture 2 – 60 revolutions - Impeller

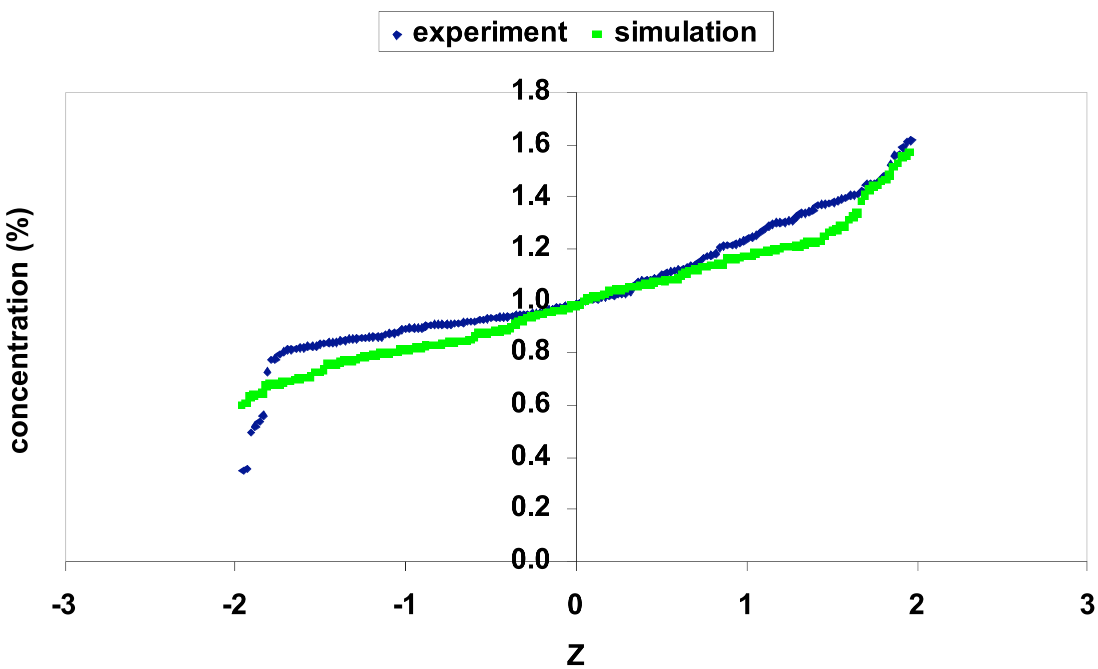

Figure 3-10-d: Normality test for the experimental profile and profiles obtained in the modeling of mixture 1 in the impeller set-up.

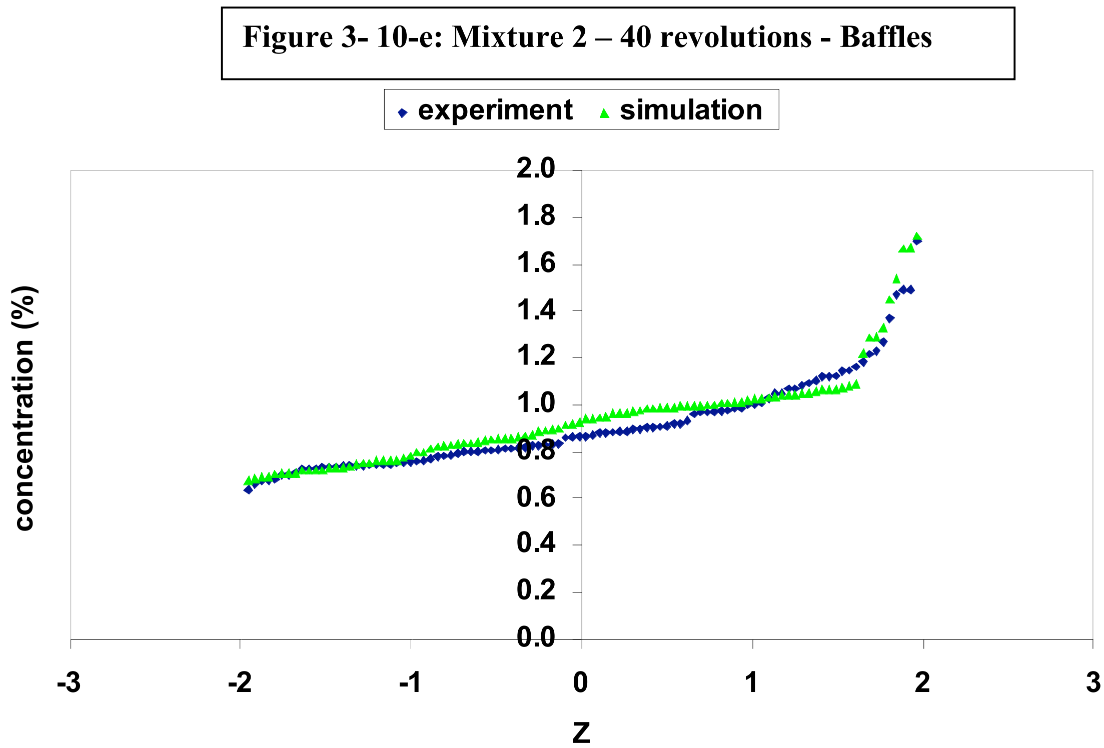

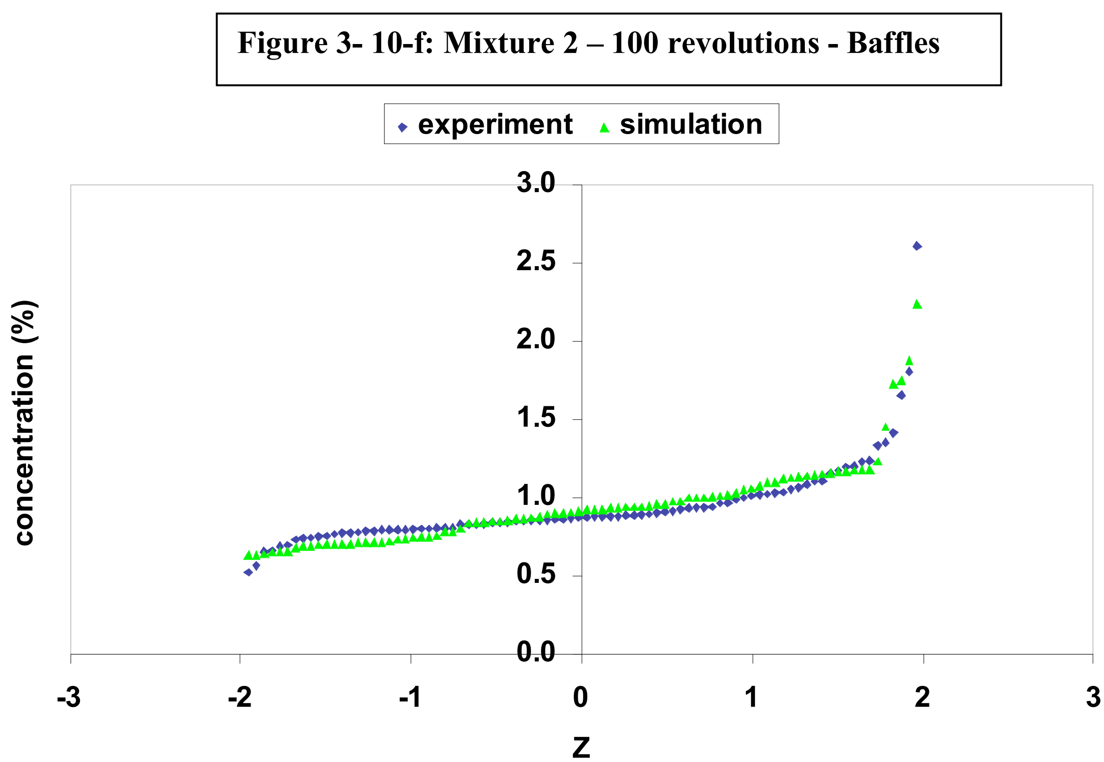

Figures 3-10-e and 3-10-f: Normality test for the experimental profile and profiles obtained in the modeling of mixture 1 in the baffle set-up.

CHAPTER IV

EFFECT OF SHEAR RATE, STRAIN, TYPE OF EXCIPIENT, AND ACETAMINOPHEN (APAP) GRADE ON APAP DE-AGGLOMERATION

Summary

This chapter studies the effects of shear rate, strain, type of excipient, and grade of acetaminophen (APAP), on the process of APAP de-agglomeration. Ten different combinations of shear rate and strain are tested using six different formulations that consist of one of three APAP grades and one of two possible types of excipient. Graphical and statistical analysis of the results shows that the finer APAP grades lead to blends with more agglomerates. They also show that the type of excipient (Fast flo lactose and Avicel 102) only affects the de-agglomeration process of the finest APAP grade. Finally, de-agglomeration occurs as a function of strain and shear rate.

4-1 Introduction

Shear rates in blenders are typically non-uniform and often unknown. Therefore, the methods that minimize API agglomeration have not correlated shear rate and strain with degree of API de-agglomeration. The controlled shear environment introduced here exposes the blend to uniform shear rates and controlled amounts of strain. In this chapter, we examine the effects of these two variables on the API de-agglomeration, as well as the effect of two material properties; type of excipient and API grade.

The Materials and Methods section describes the operation of the controlled shear environment, the blend preparation, and the sifting technique used to separate and quantify agglomerates. The Results section discusses the effects of excipient formulation, API grade, shear rates and strain on API de-agglomeration. The Conclusion summarizes the results and provides guidelines to apply this technique to practical situations.

4-2. Materials and Methods

4-2-1. Formulations

The formulations used throughout all experiments reported in this chapter (Table 4-1) are a mix of lactose (Fast flo lactose, ~100□, spherical particles, Foremost Farm, Newark, NJ) or cellulose (Microcrystalline cellulose, Avicel PH 102, ~90□, needle-like particles, FMC, Rothschild, WI), and any of three grades of acetaminophen (Fine, Semi-Fine, and Micronized, Mallinckrodt, St Louis, MO). Figure 4-1 shows the particle size distributions for APAP. The formulations contain either 300 grams of lactose and 15 grams of APAP, or 230 grams of cellulose and 15 grams of APAP. The difference in excipient mass is due to their different densities. Conditions are selected in order to have the same fill level in the controlled shear environment in all experiments. This condition arises from the fact that, in order to impart similar stresses to the blends, the area of contact between cell and blend must be the same.

The API mass was kept constant to be able to facilitate ulterior analysis in terms of the absolute mass in the agglomerated form and also in the terms of the API percentage in agglomerated form.

4-2-2. Instrument: Controlled shear environment

The geometry of the controlled shear environment is based on an annular Couette rheometer used for liquids. The device consists of two concentric aluminum cylinders 4.3 inches tall (11 cm), with a gap of 0.75 inch (1.9 cm) between them, which allows a powder volume of approximately 0.6 liters. The internal cylinder (Figure 4-1-a) has a diameter of 6.5 inches (16.51 cm). Top views of the external cylinder and the assembled controlled shear environment are shown in Figures 4-1-b and 4-1-c.

The internal cylinder can rotate at any speed in the range of 1 to 245 rpm whereas the external cylinder is stationary. Both cylinders are made of aluminum. Other Couette shear cells have been used for powders [1]. The instrument used here was designed to expose the entire powder sample to a flow and shear environment as uniform as possible. As shown in Figure 4-1, both cylinders are supplemented with equally spaced interlocking pins that create a homogeneous shear field in the flow region. The shear rates range from .45 s^{-1} (at 1 rpm) to 109 s^{-1} (at 245 rpm). The number of revolutions (N.t) determines the strain imposed (dimensionless shear units). The controlled shear environment has a lid and a seal that permits to work with an unconfined or a confined powder bed under a known amount of applied normal stress.

4-2-3. Procedure to prepare formulations under controlled shear conditions

The controlled shear environment provides the controlled and uniform shear conditions necessary to study the effect of shear rate and strain on APAP de-agglomeration (and other properties of lubricated blends). However, prior to using this cell, a pre-blend of all ingredients must be prepared. The practice of using a pre-blend is adopted because the controlled shear environment is not a good axial mixer. Dispersion is the main axial macro-mixing mechanism in the device; convection along the axis of rotation is very slow. When the controlled shear environment is loaded with the excipients and the APAP in a stratified manner, it takes a long time to achieve APAP homogeneity throughout the cell. APAP particles can form agglomerates again, if they are in contact with like-particles. Thus, a pre-blend is prepared in a small V-blender (Figure 4-3). In order to minimize uncontrolled exposure to shear, the mixing time is short (50 revolutions), the rotational speed of the blender is moderate (10 rpm), the blender scale is small (4 qt), and the loading pattern for lubricant and excipients is top-bottom.

The shear controlled environment is loaded to full capacity (~0.6 liters) with pre-blend and one of the shear conditions indicated in Table 4-2 is applied. Table 4-2 displays the shear rates in rows (with the corresponding rotational speeds of the cylinder in rpm), the strain (expressed also as number of revolutions) in columns, and a sparse diagonal design (marked with 'X') that allows examining the effect of shear rate for similar amounts of strain, and the effect of strain at a constant shear rate. In the experiments reported here, strain varies over two orders of magnitude from ~270 to ~53,000, while shear rate varies from .9 s^{-1} (at 2 rpm) to 109 s^{-1} (at 245 rpm). The duration of the process (shear time) can be used to estimate the strain imposed (dimensionless shear units). This range comprises typical values for most industrial units, including tumblers with and without intensifier bars, and “high shear” mixer-granulators.

4-2-4. Separation of agglomerates: Sieving

The physical detection and characterization of API agglomerates in blends can be done with sieves [2], LIBS, NIR scanning spectroscopy, or scanning electron microscopy (SEM). The occurrence of an agglomerate is a local event, and their detection using a thief sampler is a rare event. Therefore, the method to separate agglomerates followed in this study consists of sifting the entire blend using the following sequence of sieves (classified according to their mesh and opening diameters): 10 (2 mm), 12 (1.85 mm), 14 (1.55 mm), 18 (1.2 mm), 20 (0.925 mm), and 40 (0.6375 mm). The mass of agglomerates retained in each sieve is weighed, and then the total proportion of agglomerated APAP is calculated. The finest mesh used in the experiments is determined by the well known fact that sieves apply shear, which might further destroy agglomerates. The main reason to choose a 40 mesh as the lower limit is to have a sieves system where the blend flows through easily, without having to use vibration. In order for the blends used here to flow through a mesh finer than 40, the trays must be subject to the vibration, and this energy input can further destroy agglomerates. Obviously, the current procedure, ignores the mass of smaller agglomerates. However, the experiment allows for studying the effect of shear rate and strain on the agglomerate population larger than 40 mesh.

4-3. Results

4-3-1. Experimental design

The current experiment is designed to determine the effect of shear rate, strain, APAP grade, and type of excipient on APAP de-agglomeration. The ranges of shear rate and strain analyzed here (Table 4-2) correspond to those found in the majority of industrial equipment, and they form an incomplete factorial model. Therefore, they are grouped into ten different “shear treatments” to facilitate the graphical and statistical analysis. Then, the factorial experiment consists of ten “shear treatments”, which are tested for six different formulations, consisting of one of two types of excipients and one of three APAP grades. That generates a total of sixty experimental conditions and each of them is tested twice. The experiments are randomized, which means the conditions are not tested in any pre-determined order, and the repetitions are not performed in a sequence. Table 4-2 compiles the agglomerate mass fraction for all the combinations of shear treatment, APAP grade, and type of excipient examined (120 values).

These number of measurements (120 values) gives enough degrees of freedom to run a three-factor ANOVA and determine the effects of shear treatment (df=9), APAP grade (df=2), type of excipient (df=1), and also their possible second (df=18, 2) and third order interactions (df=18). The results of this ANOVA test (Table 4-3) show that, for a significance p level of 0.05, shear treatment (p=0), APAP grade (p=0), and type of excipient (p=0.014) affect APAP de-agglomeration. Additionally, there is significant interaction between shear treatment and APAP grade (p=0.004). In subsequent sections, the effects of API grade, type of excipient, shear rate, and strain on the API de-agglomeration are analyzed.

4-3-2. Effect of type of excipient on APAP de-agglomeration

The three grades of APAP are processed using two different granular "media". The effect of type of excipient is illustrated in Figures 4-4, 4-5, and 4-6, which plot the APAP mass fraction in the form of agglomerates for micronized, fine, and semifine APAP versus the number of revolutions (strain) of the internal cylinder of the controlled shear environment. The different colors for curves in each these Figures correspond to different speeds of rotation (shear rate) of the cylinder, while the curves for the experiments performed in lactose are full lines, and the curves for the experiments performed in Avicel 102 are broken lines. The first letter in the notation to identify the curves indicates the grade of APAP, the second letter indicates the type of excipient, followed by the speed of the internal cylinder of the controlled shear environment. For example, the curve "ml - 2 rpm" is for a blend of micronized (m) APAP in lactose (l), and the controlled shear environment operating at 2 RPM. Figure 4-4 compares the de-agglomeration data, in lactose and in Avicel 102, for micronized APAP. Figures 4-5 and 4-6 do the same for fine and semi-fine acetaminophen. The effect of type of excipient is not so evident in the curves because they have similar values, however, the following statistical analysis establishes that the differences are relevant for micronized APAP.

Three two-factor ANOVA tests, one for each type of APAP grade, examine the effect of type of excipient (df=1) on APAP de-agglomeration. These tests also consider the effect shear treatment (df=9) and the second order interaction between treatment and type of excipient (df=9). The number of data in each data set (40 values) allows estimating the effect of each variable and their second order interaction. The results for each of the APAP grades (Table 4-5 for semi-fine APAP, table 4-6 for fine APAP, and Table 4-7 for micronized APAP) show that the type of excipient only has an effect for the de-agglomeration of micronized API ($p=0.04$) (the significance p value chosen is 0.05). The effect of type of excipient on APAP de-agglomeration is less important for the coarser fine ($p=.148$) and semifine ($p=0.733$) APAP grades. Additionally, shear treatment is significant on the de-agglomeration of all grades, and there is no interaction between shear treatment and type of excipient.

4-3-3. Effect of APAP grade on APAP de-agglomeration

The effect of APAP grade is illustrated in Figures 4-7 and 4-8. They present the drug mass fraction in the form of agglomerates versus the number of revolutions of the internal cylinder of the controlled shear environment (strain) and the different colors for curves correspond to different speeds of rotation of the cylinder (shear rate). Figure 4-7 compares the de-agglomeration of micronized (full lines) and fine APAP (broken lines), which are the two finest APAP grades, and shows that they proceed in a similar manner. Figure 4-8 compares the APAP de-agglomeration for fine (full lines) and semifine APAP (broken lines); the latter is the coarsest APAP grade. The curves for these two grades are visually and statistically different, especially at low strain values (below 80 revolutions)[20]. Semi-fine APAP, which is the coarser grade, presents a smaller number of agglomerates.

Two three-factor ANOVA tests were carried out to compare the effect of APAP grade on the de-agglomeration process of semi-fine versus fine APAP (Table 4-8), and fine versus micronized APAP (Table 4-9). The number of data to perform each

[20] Since excipient plays a minor role in the de-agglomeration of semi-fine and fine APAP, the values in the curves for each shear treatment (Figures 4-7 and 4-8) are a contribution of the agglomerate fraction values, whether they are mixed with lactose or with Avicel. The excipient plays a role in the de-agglomeration of micronized APAP, however, the agglomerate fraction values were combined to facilitate the comparison among APAP grades.

comparison (80 values) allows estimating the effect of APAP grade (df=1), type of excipient (df=1), shear treatment (df=9), and their second order (df=9, 1) and third order (df=9) interactions. The results show that de-agglomeration process is very different for fine and semi-fine APAP grade and APAP grade has a strong effect (p=0). On the other hand, this process is very similar for micronized and fine APAP grades, and APAP grade does not have an effect (p=0.440).

4-3-4. Effect of shear rate and strain

The ANOVA test (Table 4-4) indicates a strong effect of the shear treatment on the APAP de-agglomeration. However, it does not provide information about whether the shear rate, the strain, or both are relevant to this process. The curves in Figures 4-4 to 4-8 suggest that APAP de-agglomeration occurs mainly as a function of strain (revolutions of the cylinder) and it is difficult to assess the effect of shear rate. The mass of API agglomerates decreases with the number of revolutions of the controlled shear environment, while the mass values obtained using different shear rates (or speeds of rotation of the cell) and same number of revolutions seems similar.

Three-factor ANOVA tests were carried out for the mass agglomerate fractions obtained using different shear rates, for the same number of total revolutions of the controlled shear environment. Table 4-10 shows that after 10 revolutions, the effect of shear rates corresponding to 2rpm and 40rpm on the de-agglomeration of three APAP grades using two types of excipients, is not significant (p=0.673). Table 4-11 shows that after 2000 revolutions, the effect of shear rates corresponding to 160rpm and 245rpm on the de-agglomeration of three APAP grades using two types of excipients, is not significant ($p=0.657$). The number of measurements available (24 values) gives enough degrees of freedom to run a three-factor ANOVA and determine the effects of shear rate (df=1), APAP grade (df=2), type of excipient (df=1), and also their second order (df=2, 1) and third order (df=2) interactions.

Table 4-12 shows that after 80 revolutions, the effect of shear rates corresponding to 2rpm, 40rpm, and 160 rpm on the de-agglomeration of three APAP grades using two types of excipients, is significant ($p=0.007$). Table 4-13 shows that after 320 revolutions, the effect of shear rates corresponding to 40rpm, 160 rpm, and 245 rpm on the de-agglomeration of three APAP grades using two types of excipients, can be considered significant ($p=0.088$). The number of measurements available in the 80 revolutions and 320 revolution analysis (36 values) gives many degrees of freedom to run a three-factor ANOVA and determine the effects of shear rate (df=1), APAP grade (df=2), type of excipient (df=1), and also their second order (df=2, 1) and third order (df=2) interactions.

Tables 4-10, 4-11, 4-12 and 4-13 show that the effect of shear rate becomes significant (or evident) at intermediate strain values (80 and 320 revolutions). For higher strain values (2000 revolutions), most of the agglomerates tend to disappear and make the distinction between shear rates more difficult, and at low strain values (10 revolutions) because the variance of the initial conditions also makes the distinction difficult. One does not know the mass of agglomerates in the APAP mass originally added to the formulation, which can obviously present some variations. One measures the decrease in agglomerate mass relative to the total mass of APAP.

4-4. Conclusions

The statistical and graphical results show that APAP de-agglomeration proceeds influenced by the shear rate, strain, the APAP grade, and in less extent by the type of excipient. The coarsest APAP presents an initial lower fraction of material in an agglomerated state. However, at larger strain values (2000 revolutions), the agglomeration degree becomes similar to blends with finer APAP grades, and the de-agglomeration curves for fine and coarse grades become similar. The type of excipient only affected the de-agglomeration of micronized APAP. The excipients used differ mainly in particle shape (Avicel has needle-shape particles and lactose has more spherical particles) rather than in the average particle size. The selection of excipients was based on the fact that the both flow very well, and facilitate the agglomerate separation in sieves. However, if other method to analyze agglomerates were available, one could use more cohesive excipients, and intuition indicates that the effect of type of excipient would be even larger.

Finally, shear rate and strain, the two processing variables, affect the de-agglomeration process. The effect of shear rate is more noticeable at intermediate mixing times (80 and 320 revolutions). This information can be used to characterize, design, and select blending units that minimize API agglomeration.

Due to the evident ability of the controlled shear environment to study the effect of processing variables (shear rate and strain), it will be used throughout the rest of this dissertation to study the effect of these variables on the lubrication process. The effects of shear rate and strain, combined with the presence of a lubricant, are perhaps the most critical step for the quality of solid products because they impact many aspects of the product performance (dissolution, tablet hardness). Therefore, the next chapter will use the controlled shear environment to study the effects of shear rate and strain on many blend properties, and in Chapter VI, we will focus on blend hydrophobicity, which is the blend property that will directly impact tablet or capsule dissolution.

REFERENCES

1- Harnby, N., Hawkins, A.E., Vandame, D. Chemical Engineering Science 42 (1987), p. 879.

2- Malmqvist, K.; Nystrom, C. Studies on direct compression of tablets. Part 8. Sieve classification method for the determination of agglomerates and the distribution of fine particles in ordered mixing. *Acta pharmaceutica suecica* 21 (1984), p. 9.

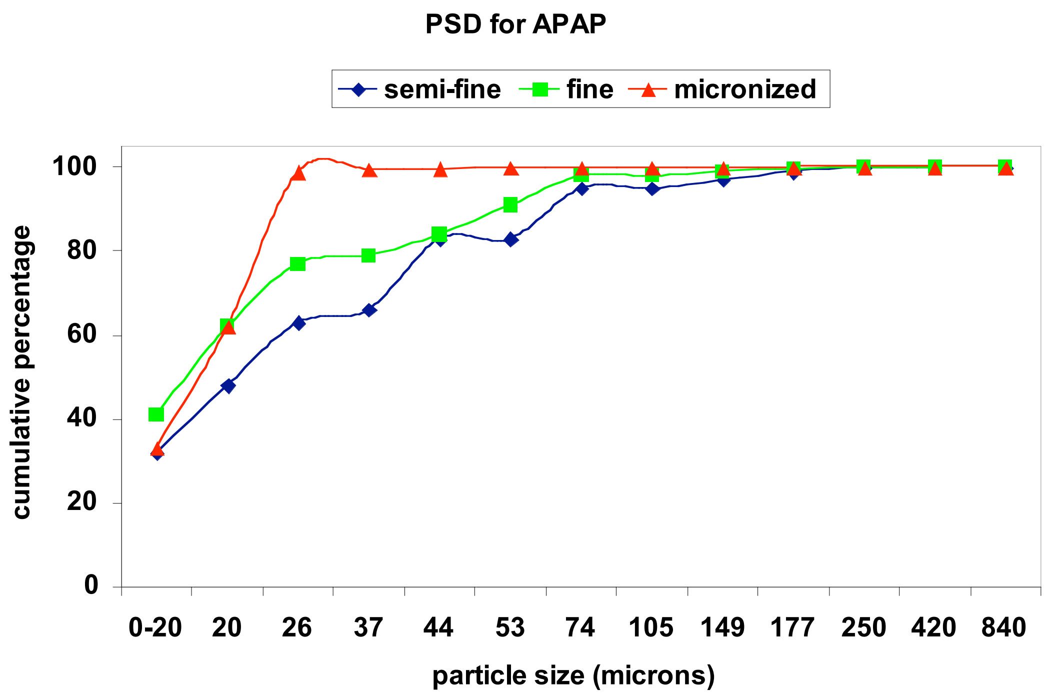

Figure 4-1: Particle size distributions for the three types of APAP.

Internal cylinder with pins
Fig 4-2-a

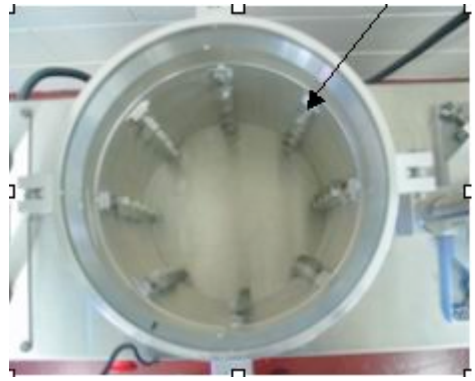

External cylinder with pins
Fig 4-2-b

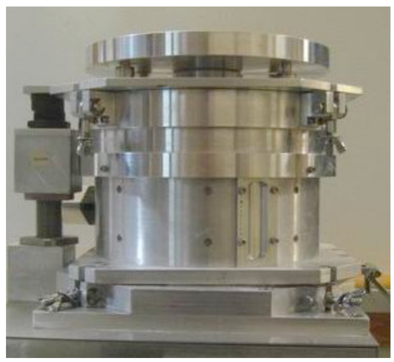

Gap between cylinders
Fig 4-2-c

Figure 4-2: Controlled shear environment

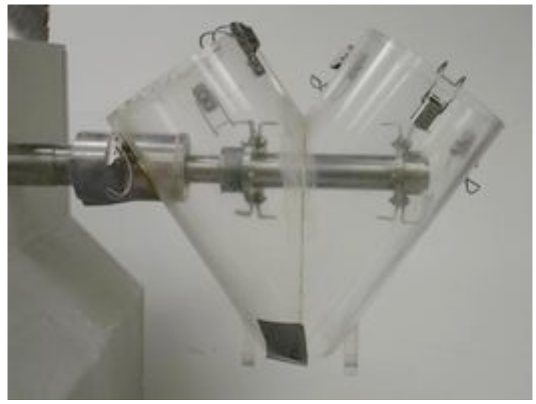

Figure 4-3: V-blender

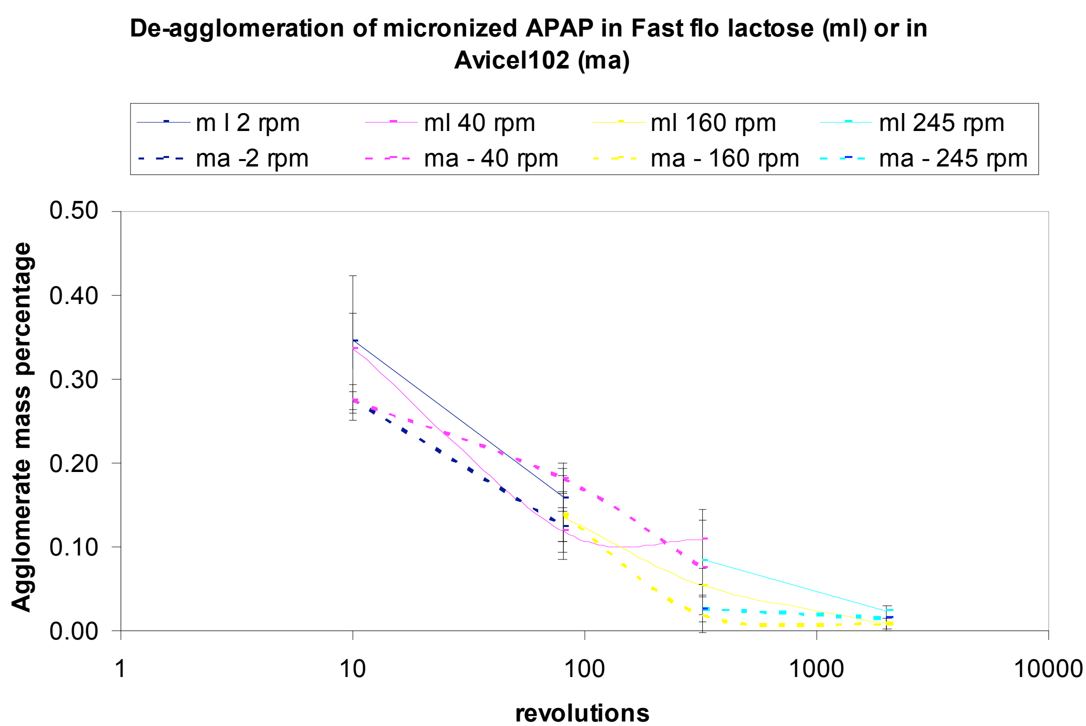

Figure 4-4: Micronized APAP de-agglomeration in lactose (ml) and in Avicel 102 (ma)

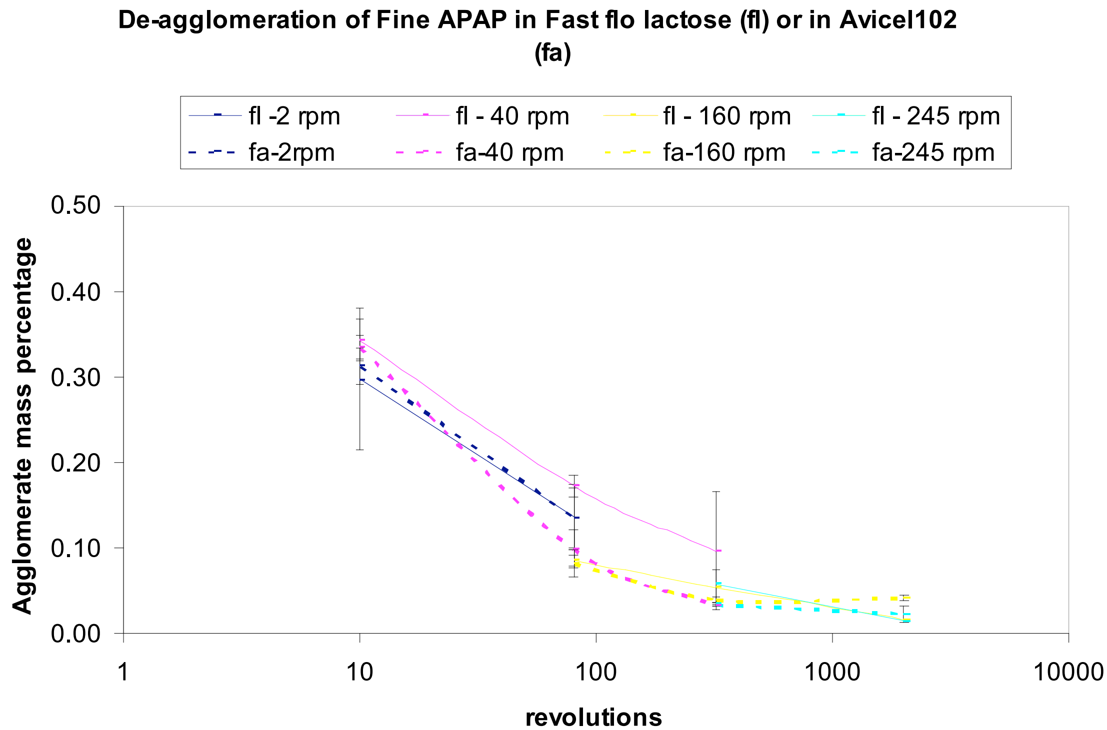

Figure 4-5: Fine APAP de-agglomeration in lactose (ml) and in Avicel 102 (ma)

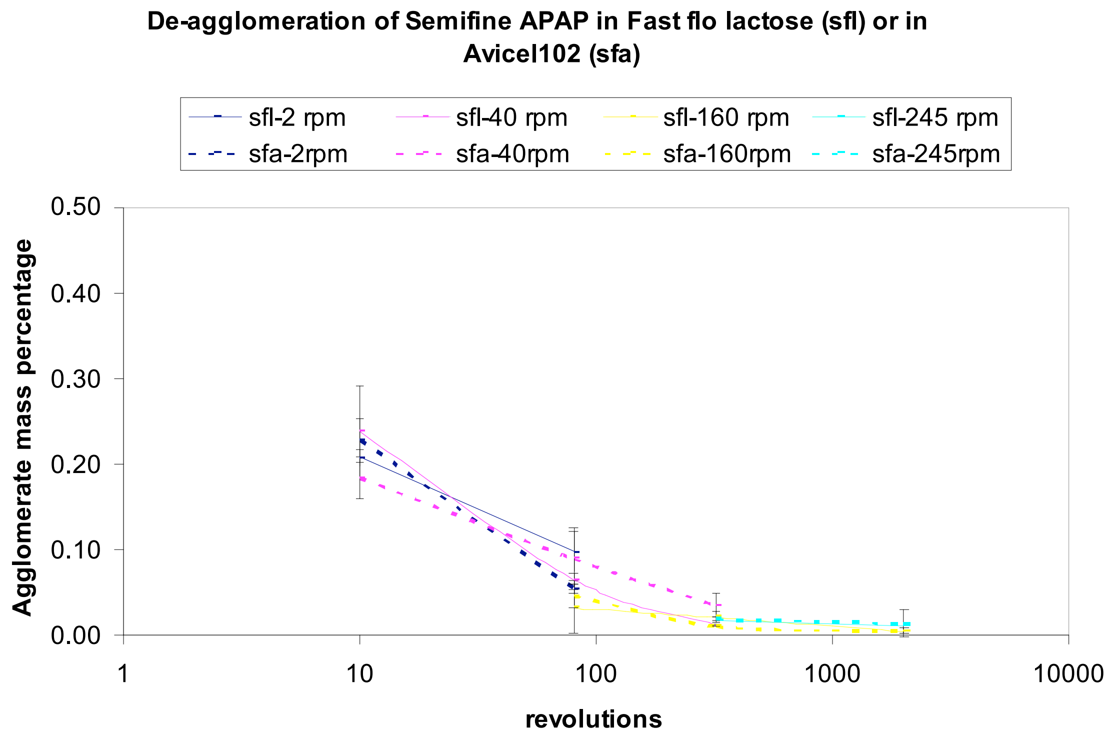

Figure 4-6: Semi-fine APAP de-agglomeration in lactose (ml) and in Avicel 102 (ma)

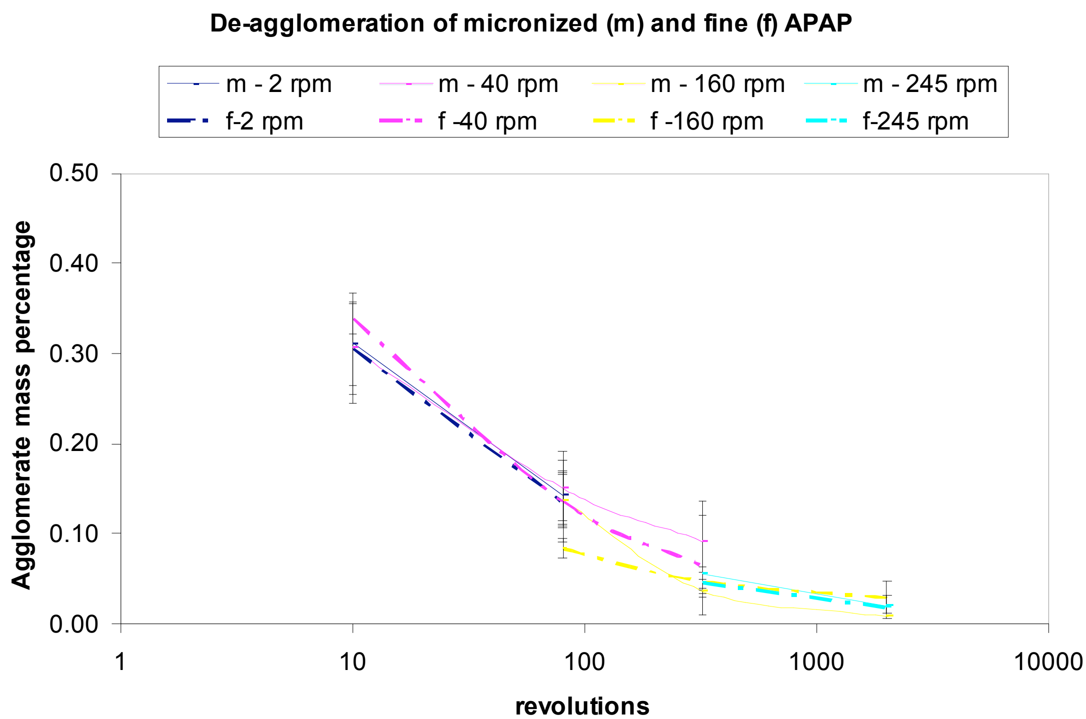

Figure 4-7: De-agglomeration of micronized (m) and fine (f) APAP (the two finest grades).

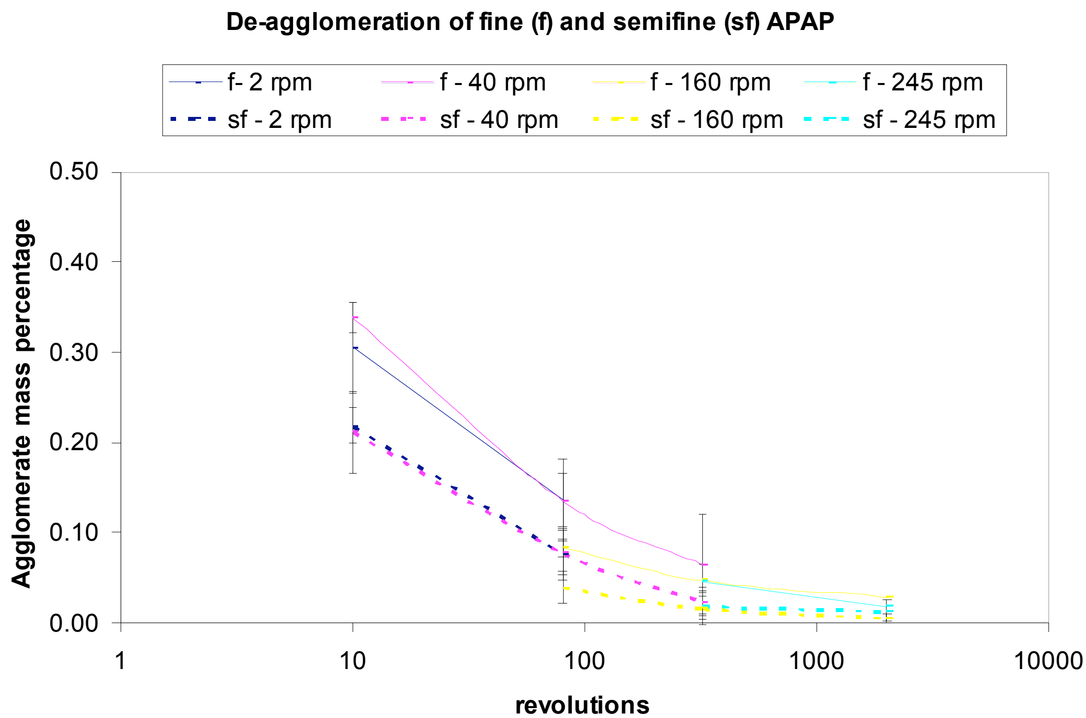

Figure 4-8: De-agglomeration of fine (f) and semifine (sf) APAP.

	Micro APAP	Fine APAP	Semi-fine APAP	Lactose	Avicel 102
Formulation 1	X			X	
Formulation 2		X		X	
Formulation 3			X	X	
Formulation 4	X				X
Formulation 5		X			X
Formulation 6			X		X

Table 4-1: Composition of the formulations

	10 revs (267)	80 revs (2,136)	320 revs (8,544)	2000 revs (53,400)
2 rpm (0.9 s^{-1})	X	X		
40 rpm (17.8 s^{-1})	X	X	X	
160 rpm (71.2 s^{-1})		X	X	X
245 rpm (109 s^{-1})			X	X

Table 4-2: Grid showing the shear environments under which the experiments were performed

Excipient	Avicel 102	Lactose	Avicel 102	Lactose	Avicel 102	Lactose
APAP	Micronized	Micronized	Fine	Fine	Semi-fine	Semi-fine
2 rpm -10 revs	0.264, 0.288	0.369, 0.322	0.328, 0.298	0.356, 0.239	0.211, 0.247	0.201, 0.215
40 rpm -10 revs	0.282, 0.267	0.398, 0.277	0.325, 0.345	0.326, 0.361	0.168, 0.201	0.276, 0.201
2 rpm - 80 revs	0.113, 0.139	0.178, 0.141	0.109, 0.163	0.111, 0.160	0.051, 0.059	0.081, 0.115
40 rpm - 80 revs	0.169, 0.195	0.139, 0.101	0.083, 0.115	0.164, 0.182	0.115, 0.065	0.071, 0.061
160 rpm - 80 revs	0.101, 0.178	0.148, 0.125	0.071, 0.093	0.092, 0.080	0.037, 0.057	0.051, 0.015
40 rpm - 320 revs	0.037, 0.115	0.135, 0.085	0.033, 0.032	0.147, 0.049	0.025, 0.045	0.011, 0.014
160 rpm -320 revs	0.034, 0.005	0.035, 0.076	0.043, 0.038	0.060, 0.051	0.011, 0.011	0.001, 0.043
245 rpm -320 revs	0.038, 0.016	0.120, 0.051	0.033, 0.036	0.069, 0.049	0.018, 0.021	0.001, 0.036
160 rpm - 2000 revs	0.013, 0.004	0.010, 0.009	0.045, 0.040	0.004, 0.031	0.004, 0.008	0.010, 0.002
245 rpm - 2000 revs	0.027, 0.005	0.045, 0.004	0.017, 0.030	0.003, 0.026	0.025, 0.003	0.023, 0.001

Table 4-3: Percentage of APAP agglomerated in the experimental conditions tested

```
Source                              DF    Seq SS    Adj SS    Adj MS       F
shear treatment                      9  1.084146  1.084146  0.120461  144.55
APAP grade                           2  0.076631  0.076631  0.038315   45.98
excipient                            1  0.005376  0.005376  0.005376    6.45
shear treatment*APAP grade          18  0.037955  0.037955  0.002109    2.53
shear treatment*excipient            9  0.007916  0.007916  0.000880    1.06
APAP grade*excipient                 2  0.002300  0.002300  0.001150    1.38
shear treatment*APAP grade*excipient  18  0.022236  0.022236  0.001235    1.48
Error                               60  0.050003  0.050003  0.000833
Total                              119  1.286562

Source                                  P
shear treatment                     0.000
APAP grade                          0.000
excipient                           0.014
shear treatment*APAP grade          0.004
shear treatment*excipient           0.408
APAP grade*excipient                0.259
shear treatment*APAP grade*excipient  0.129
Error
Total
```

Table 4-4: Results of a three-factor ANOVA analysis on APAP de-agglomeration

Source	DF	Seq SS	Adj SS	Adj MS	F	P
treat	9	0.232286	0.232286	0.025810	56.86	0.000
Ex	1	0.000054	0.000054	0.000054	0.12	0.733
treat*Ex	9	0.006522	0.006522	0.000725	1.60	0.183
Error	20	0.009078	0.009078	0.000454		
Total	39	0.247940				

Table 4-5: Results of a two-factor ANOVA analysis for Semi-fine APAP de-agglomeration

Source	DF	Seq SS	Adj SS	Adj MS	F	P
treat	9	0.464138	0.464138	0.051571	58.78	0.000
Ex	1	0.001987	0.001987	0.001987	2.26	0.148
treat*Ex	9	0.009539	0.009539	0.001060	1.21	0.343
Error	20	0.017547	0.017547	0.000877		
Total	39	0.493211				

Table 4-6: Results of a two-factor ANOVA analysis for fine APAP de-agglomeration

Source	DF	Seq SS	Adj SS	Adj MS	F	P
treat	9	0.425677	0.425677	0.047297	40.46	0.000
Ex	1	0.005636	0.005636	0.005636	4.82	0.040
treat*Ex	9	0.014090	0.014090	0.001566	1.34	0.279
Error	20	0.023378	0.023378	0.001169		
Total	39	0.468781				

Table 4-7: Results of a two-factor ANOVA analysis for micronized APAP de-agglomeration

Source	DF	Seq SS	Adj SS	Adj MS	F	P
treatm	9	0.674277	0.674277	0.074920	112.56	0.000
grade	1	0.051199	0.051199	0.051199	76.92	0.000
Ex	1	0.001348	0.001348	0.001348	2.03	0.162
treatm*grade	9	0.022147	0.022147	0.002461	3.70	0.002
treatm*Ex	9	0.005355	0.005355	0.000595	0.89	0.539
grade*Ex	1	0.000692	0.000692	0.000692	1.04	0.314
treatm*grade*Ex	9	0.010706	0.010706	0.001190	1.79	0.101
Error	40	0.026625	0.026625	0.000666		
Total	79	0.792349				

Table 4-8: Three-factor ANOVA to compare the de-agglomeration process of semi-fine versus fine APAP de-agglomeration

Source	DF	Seq SS	Adj SS	Adj MS	F	P
treatm	9	0.878926	0.878926	0.097658	95.45	0.000
grade	1	0.000624	0.000624	0.000624	0.61	0.440
Ex	1	0.007157	0.007157	0.007157	7.00	0.012
treatm*grade	9	0.010889	0.010889	0.001210	1.18	0.332
treatm*Ex	9	0.007364	0.007364	0.000818	0.80	0.619
grade*Ex	1	0.000465	0.000465	0.000465	0.45	0.504
treatm*grade*Ex	9	0.016266	0.016266	0.001807	1.77	0.106
Error	40	0.040924	0.040924	0.001023		
Total	79	0.962615				

Table 4-9: Three-factor ANOVA to compare the de-agglomeration process of fine versus micronized APAP de-agglomeration

Source	DF	Seq SS	Adj SS	Adj MS	F	P
10 rev	1	0.000327	0.000327	0.000327	0.19	0.673
grade	2	0.054375	0.054375	0.027187	15.54	0.000
Ex	1	0.004227	0.004227	0.004227	2.42	0.146
10 rev*grade	2	0.002108	0.002108	0.001054	0.60	0.563
10 rev*Ex	1	0.001412	0.001412	0.001412	0.81	0.387
grade*Ex	2	0.005097	0.005097	0.002549	1.46	0.271
10 rev*grade*Ex	2	0.001699	0.001699	0.000849	0.49	0.627
Error	12	0.020999	0.020999	0.001750		
Total	23	0.090244				

Table 4-10: Effect of shear rate on APAP de-agglomeration after 10 revolutions of the controlled shear environment

Source	DF	Seq SS	Adj SS	Adj MS	F	P
2000 rev	1	0.0000405	0.0000405	0.0000405	0.21	0.657
grade	2	0.0009253	0.0009253	0.0004627	2.37	0.136
Ex	1	0.0001255	0.0001255	0.0001255	0.64	0.438
2000 rev*grade	2	0.0005611	0.0005611	0.0002805	1.44	0.276
2000 rev*Ex	1	0.0000789	0.0000789	0.0000789	0.40	0.537
grade*Ex	2	0.0004991	0.0004991	0.0002495	1.28	0.314
2000 rev*grade*Ex	2	0.0000834	0.0000834	0.0000417	0.21	0.811
Error	12	0.0023425	0.0023425	0.0001952		
Total	23	0.0046563				

Table 4-11: Effect of shear rate on APAP de-agglomeration after 2000 revolutions of the controlled shear environment

Source	DF	Seq SS	Adj SS	Adj MS	F	P
80 rev	2	0.0086228	0.0086228	0.0043114	6.69	0.007
grade	2	0.0392783	0.0392783	0.0196391	30.45	0.000
Ex	1	0.0002831	0.0002831	0.0002831	0.44	0.516
80 rev*grade	4	0.0027057	0.0027057	0.0006764	1.05	0.410
80 rev*Ex	2	0.0017579	0.0017579	0.0008789	1.36	0.281
grade*Ex	2	0.0020560	0.0020560	0.0010280	1.59	0.230
80 rev*grade*Ex	4	0.0090250	0.0090250	0.0022562	3.50	0.028
Error	18	0.0116087	0.0116087	0.0006449		
Total	35	0.0753375				

Table 4-12: Effect of shear rate on APAP de-agglomeration after 80 revolutions of the controlled shear environment

Source	DF	Seq SS	Adj SS	Adj MS	F	P
320rev	2	0.0046582	0.0046582	0.0023291	2.79	0.088
grade	2	0.0119644	0.0119644	0.0059822	7.15	0.005
Ex	1	0.0053446	0.0053446	0.0053446	6.39	0.021
320rev*grade	4	0.0026675	0.0026675	0.0006669	0.80	0.542
320rev*Ex	2	0.0000625	0.0000625	0.0000312	0.04	0.963
grade*Ex	2	0.0037993	0.0037993	0.0018997	2.27	0.132
320rev*grade*Ex	4	0.0022772	0.0022772	0.0005693	0.68	0.614
Error	18	0.0150528	0.0150528	0.0008363		
Total	35	0.0458265				

Table 4-13: Effect of shear rate on APAP de-agglomeration after 320 revolutions of the controlled shear environment

CHAPTER V

INFLUENCE OF SHEAR RATE AND STRAIN ON THE HOMOGENEITY, FLOWABILITY, AND BULK DENSITY OF LUBRICATED PHARMACEUTICAL BLENDS AND ON TABLET HARDNESS

Summary[21]

The controlled shear environment is used to quantify the effects of shear rate and strain on the homogeneity, flowability and bulk density of a lubricated free-flowing pharmaceutical blend and on properties of resulting tablets. The range of lubricant concentrations explored is 0-2% (on a mass basis). Sheared blends are used to produce tablets in the Presster ™ (a simulator of an actual tablet press), allowing us to correlate the shear history of the blend (shear rate and strain) with the crushing hardness of tablets. Crushing hardness decreases as concentration of lubricant and strain increase. Interestingly, and unexpectedly, under constant strain, shear rate affects the crushing hardness of tablets only slightly. The results show that the larger the strain, the more homogeneous the lubricated blend. Bulk density of lubricated blends increases with strain until reaching a distinctive plateau. Results also indicate that strain affects the blend flow properties (for lubricated and un-lubricated blends).

[21] Work done in collaboration with Amit Mehrotra.

5-1. <u>Introduction</u>

Lubrication is a process of high importance in the pharmaceutical industry. Lubricants are added to tablet formulations for two reasons: (a) to prevent of sticking of granules to the tooling—anti-adherent; and (b) to improve granule flow properties—glidant [1]. As anti-adherents, they reduce the friction between the die wall and granules as the tablet is formed and ejected [1]. As glidants, they can enhance the blending of an active and decrease processing problems and weight variability during compaction [2]. There are numerous examples of the effects of lubrication on densification and compactability of mixtures [3, 4, 5] and also on tablet properties such as tensile strength, friability and disintegration time [6, 7]. Capsule filling performance of powders can also be modified by adding a lubricant such as magnesium stearate [8]. It is also reported that filling properties are better at lower MgSt concentrations, whereas the machine performance improves with an increase in MgSt. It is widely known that blend flowability and tablet properties will depend on the extent the blend has been exposed to shear. Typically, dissolution [9] and hardness [10] are adversely affected by excessive shear. This phenomenon is known as over-lubrication.

Two variables are important to the lubrication process: concentration of lubricant and exposure to shear. Some studies have correlated the performance of a lubrication process with mixing time [11] and with the scale and operating conditions of the blender [12] rather than with shear itself, presumably due to a lack of quantitative knowledge about the shear conditions existent in blenders. The controlled shear environment described here provides an excellent environment of nearly uniform shear conditions, facilitating the correlation of exposure to shear to observed blend properties. There have been multiple geometries considered for dense granular flows, but the most common ones have been parallel plates [13, 14, 15, 16], rough inclined planes [17, 18, 19], flow on a pile [20, 21] and coaxial cylinders [22, 23, 24, 25]. We consider granular Couette flow in this study as it is suitable for fundamental research because of its simplicity.

Section II in the chapter describes the materials used in the study and the geometry and working of the instrument. It also presents the experimental grid, and the methodology used for preparing and analyzing samples. Subsequently, in section III, results are described for content uniformity, bulk density, flowability and tablet hardness respectively. Finally, section IV is devoted to summary and conclusions.

5-2. Materials and Methods

5-2-1. Materials and procedure to prepare sheared blends

The materials used in our experiments are presented in Table 5-1. Magnesium stearate is used as a lubricant. Three preblends with different levels of MgSt (Table 5-2) are studied comprehensively to investigate the effect of shear rates and total shear on bulk density, flow behavior and mixing properties of lubricated pharmaceutical blends. These materials are some of the most common pharmaceutical excipients and in the interest of brevity their SEM images are not included in this paper but can be found in “Handbook of Pharmaceutical excipients” [26].

Prior to using the modified Couette shear cell, a pre-blend of all ingredients must be prepared. The practice of using a pre-blend is adopted because the Couette cell is not a good axial mixer. Dispersion is the main axial macro-mixing mechanism in the device; convection along the axis of rotation is very slow. When the cell is loaded with the excipients and lubricant in a stratified manner, it takes a long time to achieve lubricant homogeneity throughout the cell. For lubrication studies, gross homogeneity is critical because if ingredients are not pre-blended, some parts of the blend will have a high concentration of lubricant and others will have a low concentration of lubricant while being sheared, making the lubrication process uneven; unless this is avoided results could be misleading. Thus, a grossly homogeneous pre-blend of the lubricant or API and the excipients is prepared as explained in previous section. To minimize uncontrolled exposure to shear prior to the shear cell experiment, the mixing time used for preblending is short (50 revolutions), the rotational speed moderate (10 rpm) and the mixer is small (4 qt). The shear cell is loaded to full capacity (1.8 liters) with pre-blend and one of the experimental conditions indicated in Table 5-3 is used.

Samples are prepared by first mixing fast-flo lactose and Avicel 102 in a 4-quart V-blender. Powders are loaded in the V-blender from the bottom to make sure that equal amounts are added on both shells for faster mixing. The loading pattern is top-bottom as shown in Figure 5-1 and is mixed at 10 rpm for 50 revolutions only in order to minimize shear. Mixing is characterized using NIR spectroscopy and it is found that the mixture is well mixed with RSD of the order of 2%. MgSt is then added from the top and it is further mixed for 50 additional revolutions at 10 rpm. The magnesium stearate is sifted with a 20 mesh screen before addition to the powder mixture.

5-2-2. Instrument: Controlled shear environment

The controlled shear environment used in this section has the characteristics described in Chapter 4, except that the height of the controlled shear environment is 7.5 inches, and allows a volume of powder of about 1.8 liters. Figure 5-2 shows the actual picture of the controlled shear environment with schematics. The internal geometry of cylinder with pins and top view of the controlled shear environment showing the gap between the cylinders is shown in Figure 5-3. The reason for using a taller controlled shear environment is that larger volumes of blends are needed to perform the flowability experiments in the GDR.

5-2-3. Near Infrared spectroscopy

Magnesium stearate homogeneity was quantified using near infrared spectroscopy. It has been reported in literature that near infrared can be used as useful tool to characterize magnesium stearate [27, 28]. The Rapid Content Analyzer instrument (Silver Spring, MD) manufactured by FOSS NIR Systems and Vision software (version 2.1) is used for the analysis. The samples are prepared by weighing 1 g of mixture into separate optical scintillation vials; (Kimble Glass Inc. Vineland, NJ) using a balance with an accuracy of $\pm$ 0.01 mg. Near-IR spectra are collected by scanning in the range 1116-2482 nm in the reflectance mode. Partial least square (PLS) regression is used in calibration model development using the second derivative mathematical pretreatment to minimize the particle size effects. Excellent agreement is achieved between the calibrated and predicted values. The standard error of calibration (SEC) is 0.0315 and the multiple correlation coefficient (R^2) 0.9963, indicating the spectral data fits well the constituent values.

5-2-4. Experimental conditions: Shear rates and strain

As already mentioned, the main variables that are expected to affect the outcome of a lubrication process are concentration of lubricant, shear rates, and strain. In previous studies, because of the lack of means to assess shear rates in a blender and therefore estimate the exposure to strain, mixing time has been the only variable correlated in the literature with blend and tablet properties. The main advantage of the controlled shear environment presented here is that it provides a nearly uniform shear field and known shear rates in the range .45 s^{-1} (at 1 rpm) to 109.03 s^{-1} (at 245 rpm). In the experiments reported here, strain units vary over two orders of magnitude from ~270 to ~53,000.

Table 5-3 presents the experimental grid used here, displaying the shear rates in rows (with the corresponding rotational speeds of the cylinder in rpm) and strain units (or shear time expressed as number of revolutions) in columns. The combination of values used in our experiments is marked with ‘X’. In the lubricant homogeneity and blend density studies, more conditions have been tested than in the hydrophobicity studies.

5-3. Results

After conducting the experiments, the rheometer is emptied through the discharge port. The blend is collected in a beaker and it is analyzed for homogeneity, flowability and bulk density. Tablets are subsequently made out of these lubricated blends using a Presster™ to simulate the effects of tablet press brand and model, speed, and force/displacement settings. Tablet crushing hardness is then measured. Herein we discuss the results.

5-3-1. Lubricant Homogeneity

As mentioned earlier, the homogeneity of the blend is assessed by collecting a group of 20 samples of 1 gram each. The homogeneity index used is the RSD (Chapter 2.3). The results show a general trend to improved homogeneity index (lower RSD) with increased shear imparted to the system. Homogeneity is tested for both 1% and 2% MgSt concentration for blends sheared under the conditions stated in Table 5-3. Figures 3-4, and 3-5 show the resulting MgSt RSD as a function of total number of revolutions and rotation rate in the device for the two different lubricant concentrations respectively.

For 1% MgSt, as the strain increases, MgSt RSD decreases and then reaches a distinctive plateau, suggesting the existence of two separate regimes, one where MgSt homogeneity depends on strain, and another where a maximum degree of lubrication (or over-lubrication) has been achieved. Contrary to intuition, shear rate appears to have a much smaller effect than strain. For 2% MgSt, RSD decreases with strain for all shear rates. Again, strain appears to have a larger effect then shear rate. No clean plateau is observed within the range of shear values examined, but no values smaller than 1% RSD are observed either.

The homogeneity values, by themselves, do not indicate over-lubrication. There are some minimum homogeneity values that can be associated with over-lubrication but they are not sufficient evidence to indicate this usually qualitative phenomenon since some blends present equally low RSD values for multiple conditions, and RSD values are sample size dependent. To establish whether over-lubrication has occurred, the samples must be analyzed in conjunction with the results of flowability tests and resulting tablet hardness.

5-3-2. Bulk Density

The bulk density of a powder is an important parameter which is deeply affected by strain. Since processing equipment has fixed volume, density directly affects batch size and capacity (and productivity). For cohesive powders, density also affects effective flow properties [29]. Harnby et al. [30] mentioned that relative changes in bulk density can be very sensitive indicators of changes in the structural strength of a loosely compacted powder and hence of its flow characteristics in many process operations.

Finally, and most critically, density and flowability directly impact weight and dosage reproducibility of tablets and filled capsules, and affects the compression force applied in tablet presses, having an impact on hardness, porosity, dissolution and frequent problems such as sticking and capping.

Density is calculated here by accurately weighing a known volume of powder. Multiple samples discharged directly from the rheometer are collected in two different beakers of volume 155ml and 285 ml and the mass is accurately is measured. Results show that the presence of magnesium stearate strongly affects the bulk density of the sheared powders. Figure 5-6 shows the effect of strain (i.e. revolutions) on the density of unlubricated sample (mixture 1). It can be observed that even at high shear rates and high strain, the bulk density remains nearly unchanged. The bulk density at extreme shear conditions fluctuates only by a maximum of about 3% from that of the pre-blend.

However, blends with a small amount of magnesium stearate exhibit a substantial change in the bulk density of the material when exposed to shear. Figures 3-7, and 3-8 show a large increase in bulk density of mixture 2 and mixture 3 respectively. The initial density for mixture 2 (1% MgSt pre-blend) is 480 g/l and that of mixture 3 (2% MgSt pre-blend) is 490 g/l. Results show that the bulk density increases by about ~13% and then reaches a plateau, suggesting the existence of two regimes, one where density depends on shear, and another where a maximum degree of lubrication-driven densification has been achieved. The limit between these regimes corresponds closely to what was observed for MgSt RSD in Figure 5-4, once again suggesting the existence of two regimes controlled by MgSt micro homogenization.

5-3-3. Flowability

A lubricant often also works as a glidant, directly affecting the flow properties of the blend. Exposing the lubricant to extensive shear is known to strongly affect powder flow properties. The purpose of this section is to determine the shear-rate and the strain effects on flow properties.

The flowability of blends is measured using a technique denominated GDR (Gravitational Displacement Rheometer). In this novel instrument developed at Rutgers, the mixture flow properties are characterized in terms of the size of the avalanches. The GDR is based on a simple concept: Powder is loaded on a rotating drum mounted on a hinged table that is supported by a load cell. As the drum rotates, the load cell measures the change in moment of inertia of the powder bed caused by powder avalanches. The RSD measurement of the GDR which has been shown to be proportional to cohesive inter-particle forces is an easy and convenient method for characterizing the flow behavior.

Flow properties of prepared samples were strongly affected by strain. It was observed that flow properties of unlubricated blends become worse when exposed to large amounts of shear, possibly indicating electrostatic effects. Figure 5-9-a shows that flow properties of the pre-blend lies between those of fast flo lactose and Avicel 102. However, when the pre-blend is exposed to increasing amounts of strain, it is observed that the standard deviation of the GDR signal increases substantially indicating worsening of flow properties that can could be caused by the electrostatic charging of the pre-blend when subjected to high shear environments for a long period of time. Even though the controlled shear environment is made of metal, the tested materials are poor conductors, and electrostatic charging of the powder under high shear conditions could be visually observed (increase in asperity).

Flow properties of lubricated blends were also measured as a function of strain applied. As shown in Figure 5-9-b, it was observed that flow for blends lubricated with 1% MgSt under different shear environments is better than the pre-blend, which is contrary to un-lubricated blends. However, there is no marked difference in flow properties for different levels of strain (high, medium and low). It is important to notice that the improvement in flow properties occurs simultaneously with an increasing density, indicating a decrease in the cohesion of the blend.

5-3-4. Tablet Hardness

Perhaps most importantly, it is quantitatively shown that tablet hardness is consistently and reproducibly affected by the strain imposed on the blend. Figures 3-10, 3-11-a, and 3-11-b demonstrate how the hardness of tablets made by MCC's Presster^{TM} (MCC, East Hanover, NJ), strongly depends not only on the MgSt concentration (as expected) but also on strain. The Presster is operated simulating Fette PT 3090 61 station press at 60 rpm

Table 5-4 shows the treatment conditions under which pre-blend is sheared and then tablets are made and tested for crushing hardness. For each blend, five tablets are compressed under low, medium and high compaction forces. Tablet crushing hardness is measured for each individual tablet in a standard tablet tester (Dr. Schleuniger, Pharmatron, model 6D). The software that comes with the Presster^{TM} records the values of compaction pressure and tablet hardness and estimates a 95% confidence interval for these two variables. Figures 3-10, and 3-11 which consist of tablet hardness versus compaction forces, represent the CI intervals with error bars. These plots are utilized to analyze the effects of concentration of lubricant, shear rate and strain on tablet hardness.

Figure 5-10 shows the effect of lubricant concentration on the crushing hardness of tablets. Three blends with varying amounts of MgSt (0%-2%) are sheared under the same conditions and subsequently, tablets are made and tested for hardness. It was observed that as MgSt concentration increases, tablet hardness decreases.

Figures 5-11-a, and 5-11-b demonstrate the effect of shear rate and strain on tablet hardness. Tablets from three blends sheared under rates varying from 4.45 s^{-1} to 71.2 s^{-1} are tested for hardness. Against expectation, in Figure 5-11-a, it can be observed that shear rate has no effect on tablet hardness.

However, when tablet hardness is plotted as a function of strain and is found that as the strain imparted to the system increases, the corresponding tablet hardness decreases subsequently. As shown in Figure 5-11-b as the strain is increased from 2,670 to 170,890 shear units, the corresponding crushing hardness decreases by 50%.

5-4. Conclusions

This last chapter shows that other important blend properties are affected mainly by strain, and not by shear rate. For example, the larger the strain, the more homogeneous the lubricant in a blend is. Surprisingly, shear rate appears to have a much smaller effect than strain. Results show that density of lubricated blend is also affected by strain. Bulk density increases by about ~13% and then reaches a plateau, suggesting the existence of two regimes, one where density depends on shear and another where a maximum degree of lubrication-driven densification has been achieved. On the other hand, the density of unlubricated blend remains unaffected by strain.

Unlike lubricated blends, flowability of unlubricated pre-blends become worse when exposed to increasing amounts of strain. Finally, as the strain imparted to the system was increased, the corresponding tablet hardness decreased. However, again there was no effect of shear rate on tablet hardness. Results obtained in the controlled shear environment can be correlated with additional results obtained in commercial blenders and feed frames in order to determine optimum process parameters in commercial equipment.

The next chapter will continue with the current study of the effects of shear rate and strain on the lubrication process however, it will concentrate in a single property of the blend. Blend hydrophobicity is the focus because it is obviously the property that affects tablet dissolution the most.

REFERENCES

1- Moodya, G.; Rubinstein, M.H.; FitzSimmons, R.A. Tablet lubricants I. Theory and modes of action. International Journal of Pharmaceutics 9 (1984), p. 75.

2- Mackin, L.; Sartnurak, S.; Thomas, I.; Moore, S. The impact of low levels of amorphous material (<5%) on the blending characteristics of a direct compression formulation. International Journal of Pharmaceutics 231 (2002), p. 213.

3- Vromans, H.; Lerk, C.F. Densification properties and compactibility of mixtures of pharmaceutical excipients with and without magnesium stearate. International Journal of Pharmaceutics 46 (1988), p. 183.

4- Van Veen, B.; Bolhuis, G.K.; Wu, Y.S.; Zuurman, K.; Frijlink, H.W. Compaction mechanism and tablet strength of unlubricated and lubricated (silicified) microcrystalline cellulose. European Journal of Pharmaceutics and Biopharmaceutics 59 (2005), p. 133.

5- Ebba, F.; Piccerelle, P.; Prinderre, P.; Opota, D.; Joachim, J. Stress relaxation studies of granules as a function of different lubricants. European Journal of Pharmaceutics and Biopharmaceutics 52 (2001), p. 211.

6- Johansson, M.E. Granular magnesium stearate as a lubricant in tablet formulations. International Journal of Pharmaceutics 21 (1984), p. 307.

7- De Lourdes Garzón Serra, M.; Robles, L.V. Compactibility of agglomerated mixtures of calcium carbonate and microcrystalline cellulose. International Journal of Pharmaceutics 258 (2003), p. 153.

8- Podczeck, F.; Newton, J.M. Powder and capsule filling properties of lubricated granulated cellulose powder. European Journal of Pharmaceutics and Biopharmaceutics 50 (2000), p. 373.

9- Fukui, E.; Miyamura, N.; Kobayashi, M. Effect of magnesium stearate or calcium stearate as additives on dissolution profiles of diltiazem hydrochloride from press-coated tablets with hydroxypropylmethylcellulose acetate succinate in the outer shell. International Journal of Pharmaceutics 216 (2001), p. 137.

10- Aoshima, H.; Miyagisnima, A.; Nozawa, Y.; Sadzuka, Y.; Sonobe, T. Glycerin fatty acid esters as a new lubricant of tablets. International Journal of Pharmaceutics 293 (2005), p. 25.

11- Ragnarsson, G.; Hölzer, A.W.; Sjögren, J. The influence of mixing time and colloidal silica on the lubricating properties of magnesium stearate. International Journal of Pharmaceutics 3 (1979), p. 127.

12- Van der Watt, J.G.; de Villiers, M.M. The effect of V-mixer scale-up on the mixing of magnesium stearate with direct compression microcrystalline cellulose. European Journal of Pharmaceutics and Biopharmaceutics 43 (1997), p. 91.

13- Babic, M.; Shen, H.H.; Shen, H.T. The stress tensor in granular shear flows of uniform, deformable discs at high solid concentrations. J. Fluid Mech. 219 (1990), p. 81.

14- Thompson, P.A.; Grest, G.S. Granular flow and the dilatancy transition. Phys. Rev. Lett. 67 (1991), p. 1751.

15- Zhang, Y.; Campbell, C.S. The interface between fluid-like and solid-like behavior in two-dimensional granular flows. J. Fluid Mech. 237 (1992), p. 541.

16- Aharonov, E.; Sparks, D. On phase transition and self-organized critical state in granular packings. Phys. Rev. E. 60 (1999), p. 6890.

17- Drake, T.G. Structural features in granular flows. J. Geophys. Res. 95 (1990), p. 8681.

18- Ancey, C.; Coussot, P.; Evesque, P. Examination of the possibility of a fluid-mechanics treatment of dense granular flows. Mech. Coh. Frict. Mater. 1 (1996), p. 385.

19- Pouliquen, O.; Renaut, N. Onset of granular flows on an inclined rough surface: dilatancy effects. J. Phys. II 6 (1996), p. 923.

20- Khakhar, D.V.; Orpe, A.V.; Andersen, P.; Ottino, J.M. Surface flow of granular materials: model and experiments in heap formation. J. Fluid Mech. 441 (2001), p. 255.

21- Andreotti, B.; Douady, S.S. Selection of velocity profile and flow depth in granular flow. Phys. Rev. E 63 (2001), p. 1.

22- Veje, C.T.; Howell, D.W.; Behringer, R.P. Kinematics of a two-dimensional granular couette experiment at the transition to shearing. Phys. Rev. E 59 (1999), p. 739.

23- Mueth, D.M. Measurements of particle dynamics in slow, dense granular couette flow. Phys. Rev. E 67 (2003), p. 011304.

24- Mueth, D.M.; Debregeas, G.F.; Karczmar, G.S.; Eng, P.J.; Nagel, S.R.; Jaeger, H.M. Signatures of granular microstructure in dense shear flows. Nature 406 (2000), p. 385.

25- Miller, B.; O'Hern, C.; Behringer, R.P. Stress fluctuations for continuously sheared granular materials. Phys. Rev. Lett. 77 (1996), p. 3110.

26- Rowe, R.; Sheskey, P.; Weller, P. Handbook of Pharmaceutical excipients (4th edition). New York, APhA Publications (2003).

27- Roggo, Y.; Jent, N.; Edmond, A.; Chalus, P.; Ulmschneider, M. Characterizing process effects on pharmaceutical solid forms using near-infrared spectroscopy and infrared imaging. European Journal of Pharmaceutics and Biopharmaceutics 61 (2005), p. 100.

28- Ebube, N.K.; Thosar, S.S.; Roberts, R.A.; Kemper, M.S.; Rubinovitz, R.; Martin, D.L.; Reier, G.E.; Wheatley, T.A.; Shukla, A.J. Application of Near-Infrared Spectroscopy for Nondestructive Analysis of Avicel Powders and Tablets. Pharmaceutical Development and Technology 4 (1999), p. 19.

29- Abdullah, E.C.; Geldart, D. The use of bulk density measurements as flowability indicators. Powder Technology 102 (1999), p. 151.

30- Harnby, N.; Hawkins, A.E.; Vandame, D. The use of bulk density determination as a means of typifying the flow characteristics of loosely compacted powders under conditions of variable relative humidity. Chemical Engineering Science 42 (1987), p. 879.

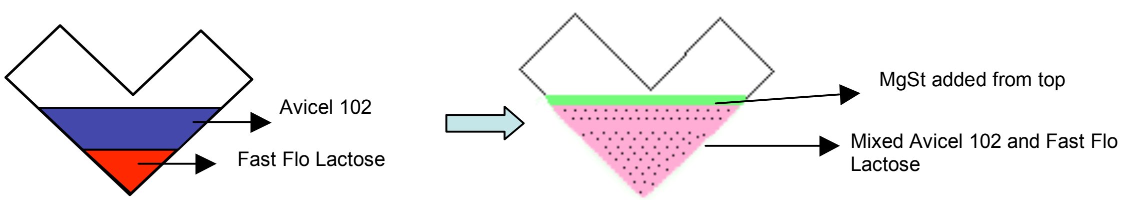

Figure 5-1: Illustration of the preblending process for the high shear experiments

Figure 5-2: The Figure shows the schematic and actual picture of the new instrument. The inner cylinder rotates at a constant speed transmitting shear to the blend in a controlled and uniform fashion. The panel displays the total torque, rotation speed and can be attached to a computer to get continuous data.

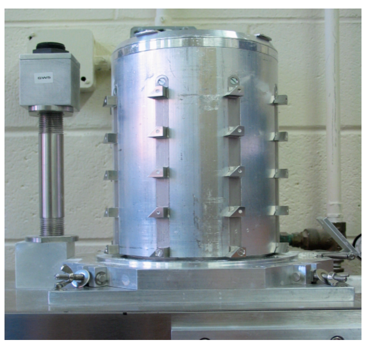

Internal cylinder with pins
Figure a

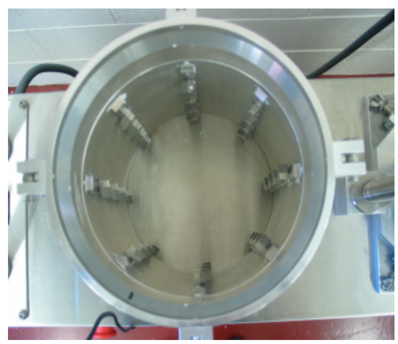

External cylinder with pins
Figure b

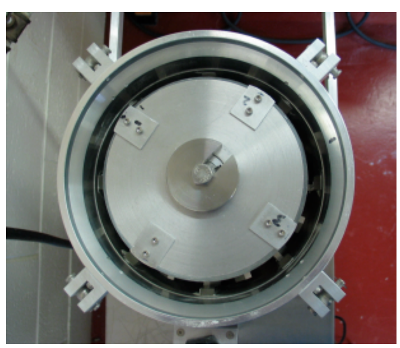

Gap between cylinders
Figure c

Figures 5-3: The Figures shows the controlled shear environment. Figure a shows the pins on the inner cylinder, Figure b shows the pins on the outer cylinder and Figure c shows the top view of the assembly

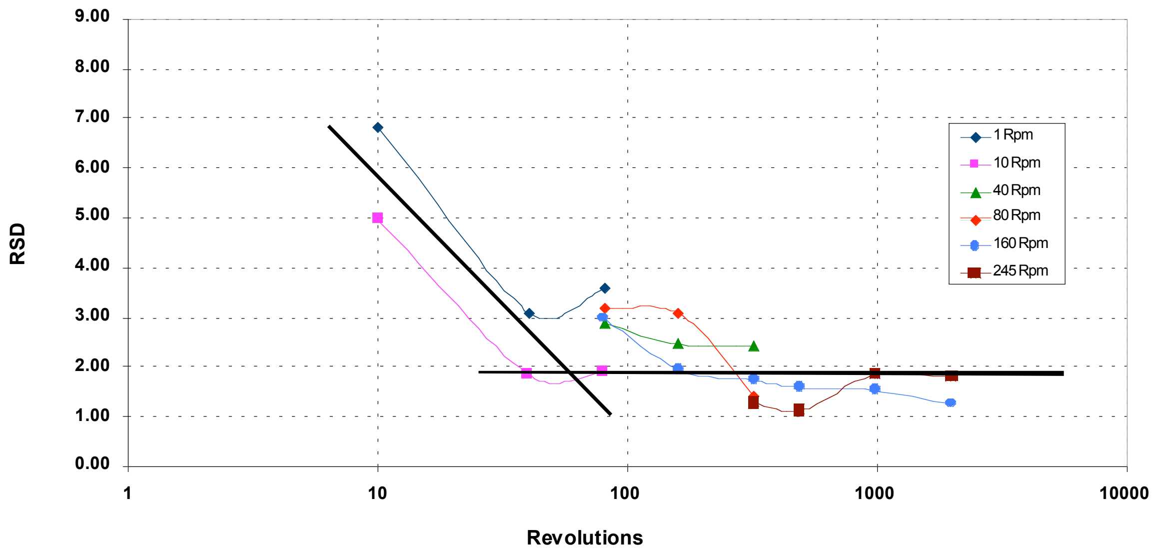

Figure 5-4: RSD curves representing content uniformity for pre-blends with 1% lubricant concentration sheared under different environments as in Table 5-3

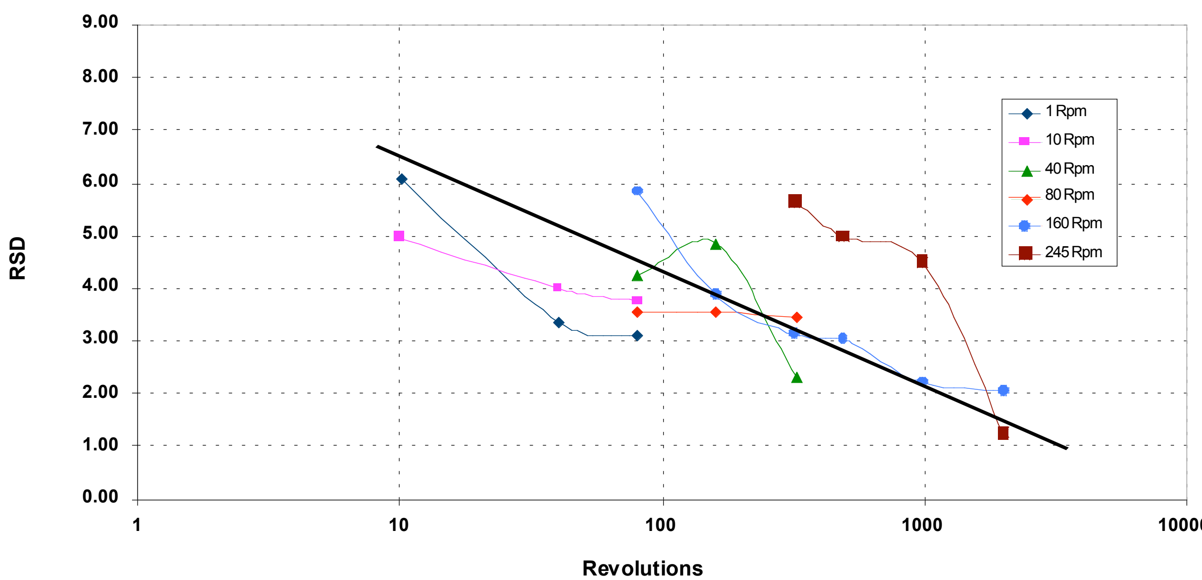

Figure 5-5: RSD curves representing content uniformity for pre-blends with 2% lubricant concentration sheared under different environments as in Table 5-3

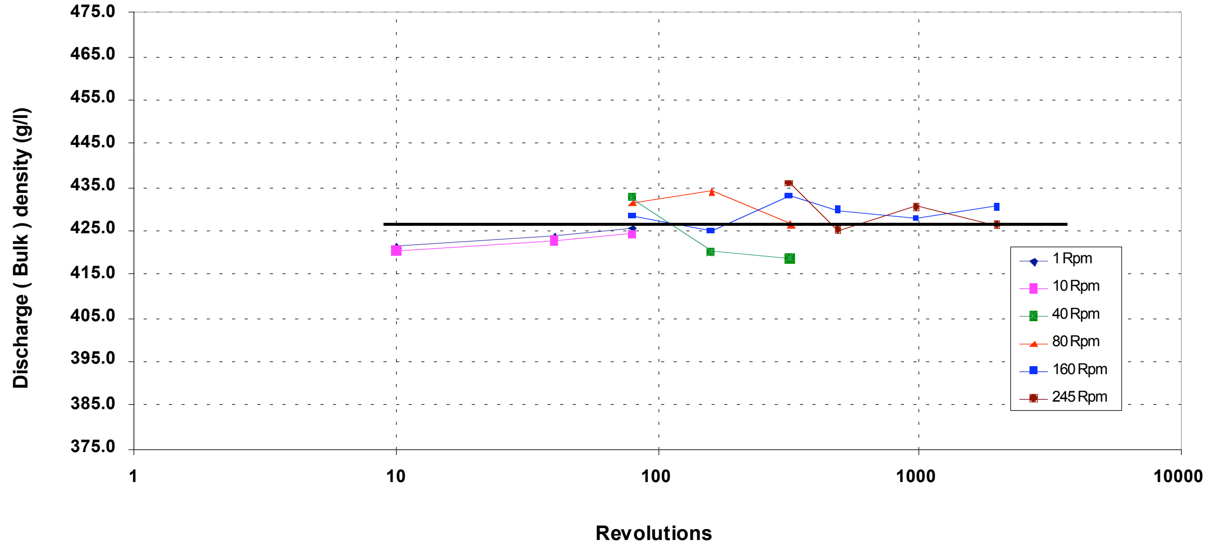

Figure 5-6: Density of sheared pre-blends with no lubrication

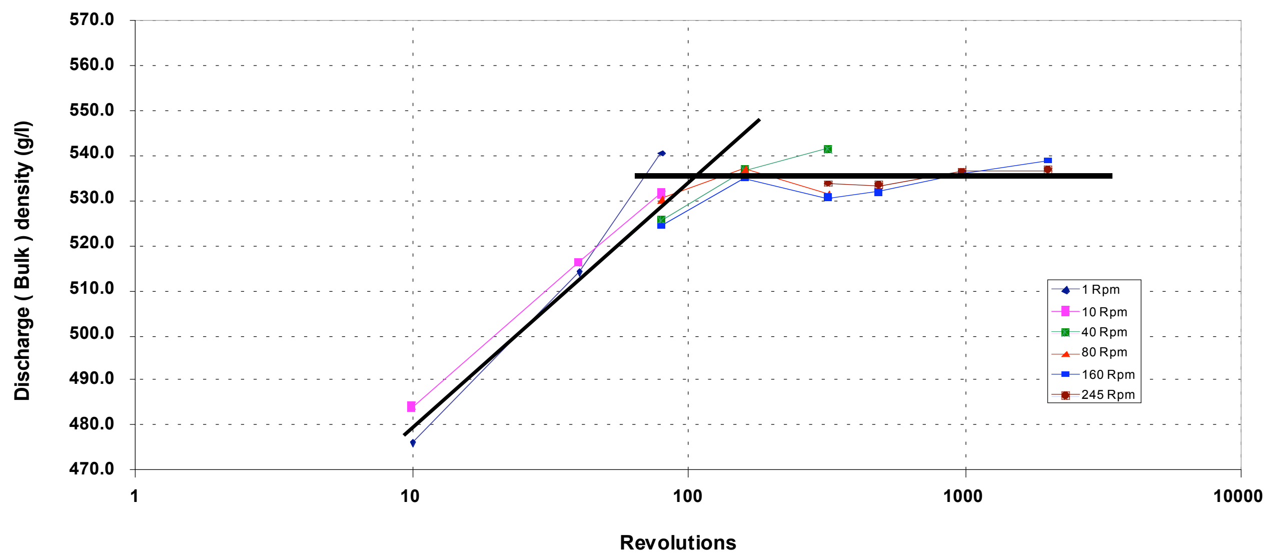

Figure 5-7: Density of sheared pre-blends with 1% MgSt as lubricant.

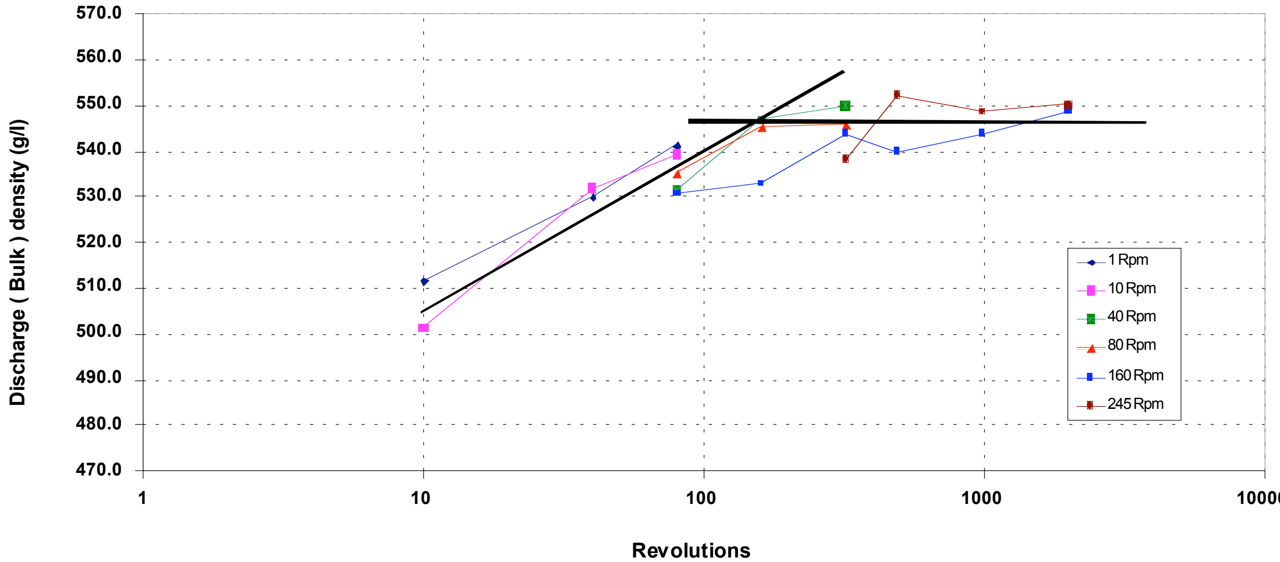

Figure 5-8: Density of sheared pre-blends with 2% MgSt as lubricant.

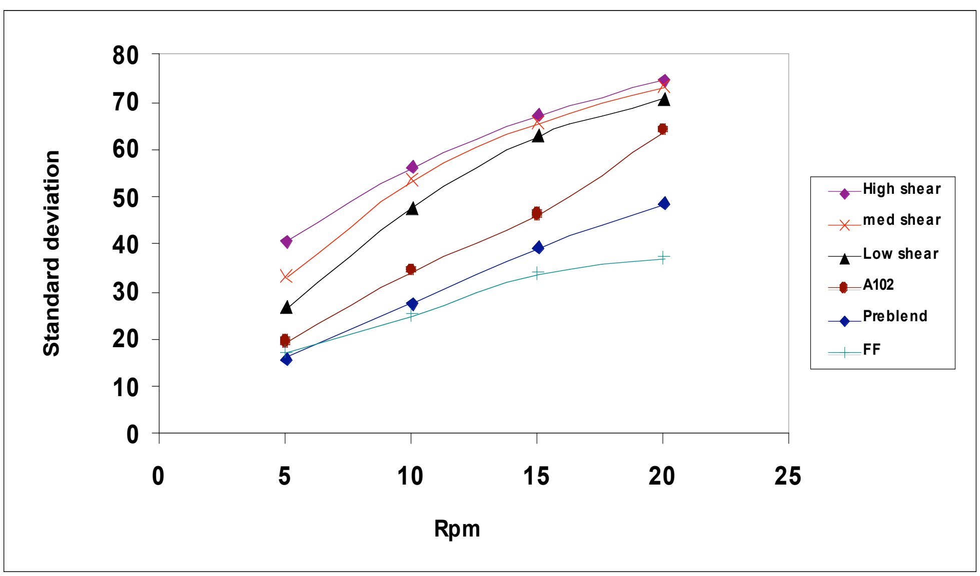

Figure 5-9-a: Standard deviation of GDR signal for powders and pre-blends when exposed to controlled shear environments. Higher RSD values correspond to worse flowability

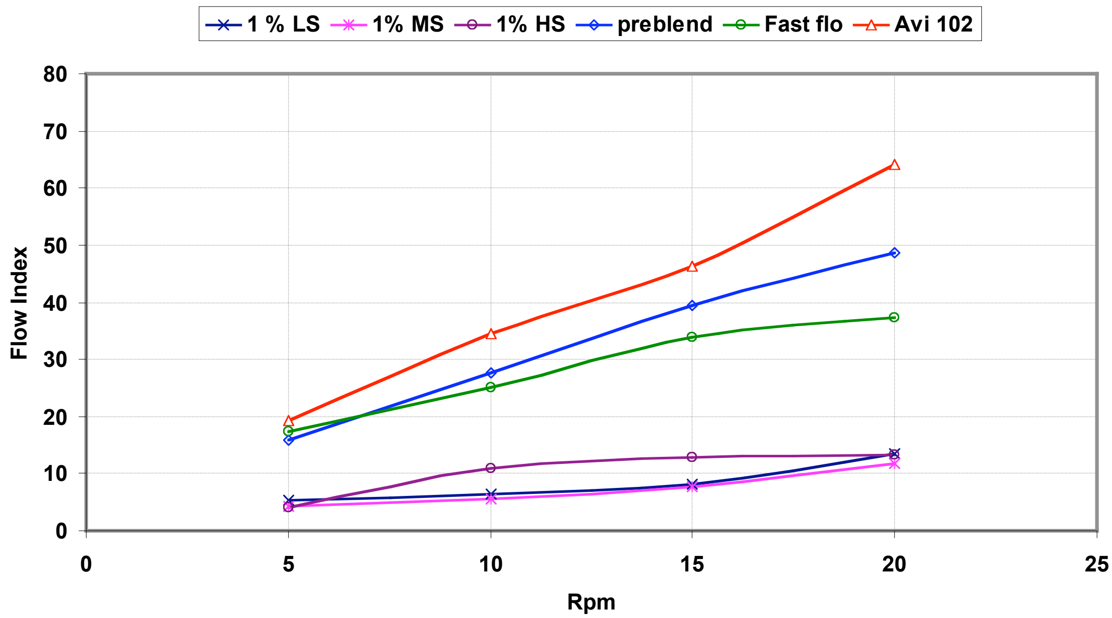

Figure 5-9-b: Flow indexes for powders and lubricated pre-blends when exposed to controlled shear environments

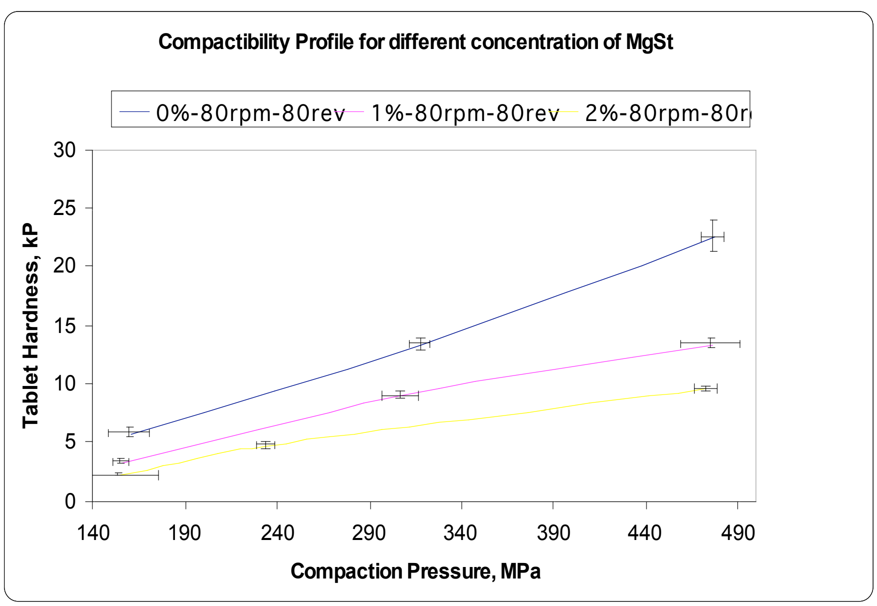

Figure 5-10: Effect of lubricant concentration on tablet hardness

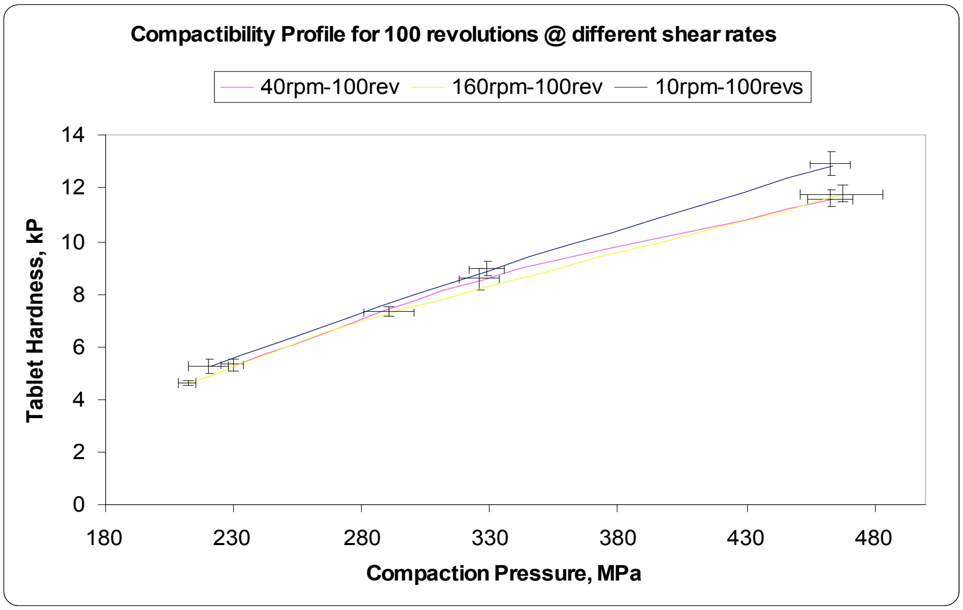

Figure 5-11-a: Effect of shear rate on tablet hardness

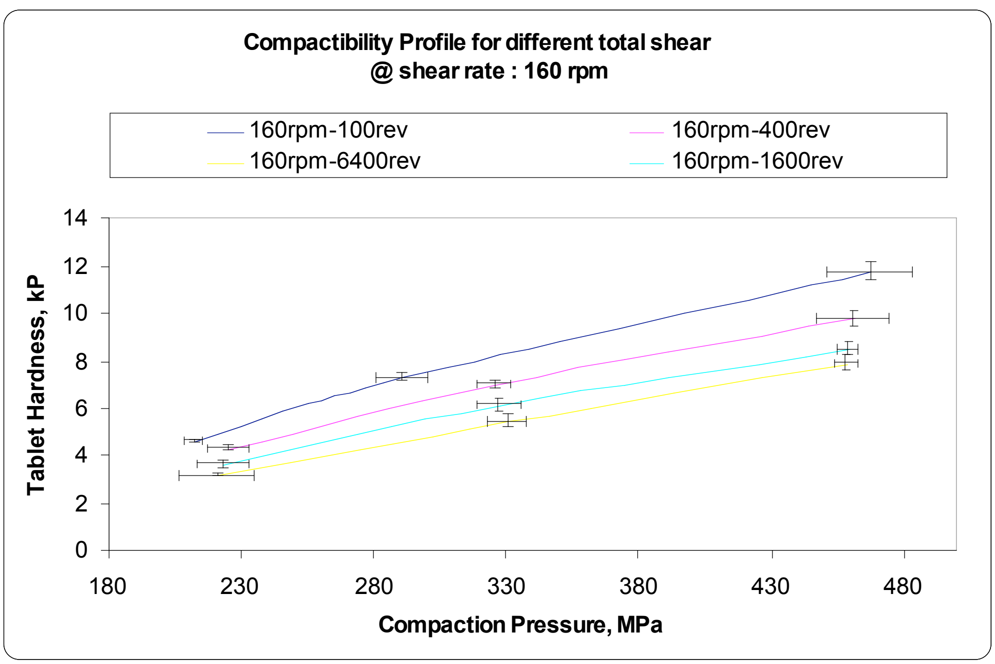

Figure 5-11-b: Effect of strain on tablet hardness

Name	Size and morphology	Vendor, City, State
Fast-Flo Lactose	~100μ, spherical	Foremost farms, Newark, NJ
Avicel PH 102 Microcrystalline cellulose	~90μ, needle-like	FMC, Rothschild, WI
Magnesium Stearate	~20 μ, irregular	Mallinckrodt, St Louis, MO

Table 5-1: Materials used in the experiment

Pre-blend	MgSt %	Fast Flo Lactose %	Avicel 102 %
Mixture 1	0	60	40
Mixture 2	1	59	40
Mixture 3	2	58	40

Table 5-2: Mixtures

total # revs (total shear units) →

rpm (shear rate) ↓

	10 rev (267)	40 rev (1,068)	80 rev (2,136)	160 rev (4,272)	320 rev (8,544)	490 rev (13,083)	980 rev (26166)	2000 rev (53,400)
1 rpm ($0.45\ s^{-1}$)	X	X	X					
10 rpm ($4.45\ s^{-1}$)	X	X	X					
40 rpm ($17.8\ s^{-1}$)			X	X	X			
80 rpm ($35.6\ s^{-1}$)			X	X	X			
160 rpm ($71.2\ s^{-1}$)			X	X	X	X	X	X
245 rpm ($109.03\ s^{-1}$)					X	X	X	X

Table 5-3: Grid showing the shear environments under which the experiments were performed

Shear rates (RPM) ↓

Revolutions →

	25	100	400	1600	6400
10	X	X	X	X	
40		X	X	X	
160		X	X	X	X

Table 5-4: Grid showing the shear environments from which tablets are made and tested for hardness.

CHAPTER VI

MEASURING HYDROPHOBICITY OF SHEARED LUBRICATED PHARMACEUTICAL BLENDS

Summary

This chapter studies the contribution of lubricant concentration, shear rate, and strain to the hydrophobicity of pharmaceutical formulations. This blend property is critical because it affects the dissolution and the drug release rates of powder formulations, tablets, and capsules, the mechanical properties of tablets, and the performance of tablet coating operations. Graphical and statistical results show that, in the absence of lubricant, the hydrophobicity of powders does not change substantially as a function of shear rate or strain. However, when lubricant is present (concentrations studied here range between 0.5% and 2%), hydrophobicity increases as a function of strain, shear rate, and lubricant concentration. At low strain values, the increment is slow, and for larger strain values, the hydrophobicity increment becomes very rapid. With the help of a statistical analysis, the onset of the steep increment can be established.

6-1 Introduction

As mentioned in Chapter 2, Lubricants are added to pharmaceutical formulations to improve flowability [1, 2], to facilitate tablet ejection, and to minimize tablet defects [3]. However, the most common lubricant, magnesium stearate, is very hydrophobic and can alter blend hydrophobicity (also known as wettability), and therefore, the dissolution and coating of tablets [4, 5]. Tablet dissolution is a critical variable because it determines the drug release rate, and ultimately, drug bioavailability [6-8]; many important product regulations focus on tablet dissolution [9-11]. This tablet property is determined by the characteristics of the granular material used and by variables of the tableting and coating processes. Powder hydrophobicity is also a key variable for granulation processes. Poor wetting of the substrate typically leads to weak, porous granules and inadequate binder distribution (wetting of the API is particularly important). As a result, granule flow and tablet mechanical properties can be compromised [12-16]. Hence, the method for material characterization presented here is critical for optimizing the quality of many pharmaceutical products.

Tablet dissolution is typically correlated with the type and concentration of lubricant, and especially with the powder mixing time [17-19]. There are other tablet parameters such as structure and composition that also affect dissolution [20]. For example, the addition of surfactants can offset a long dissolution time [21, 22]. However, it is possible to control wettability by understanding mixing of lubricants, which might be preferable to increasing the formulation complexity by using surfactants or other components to aid tablet dissolution. Another reason to study material properties is that the variety of tablet dissolution tests, with different hydrodynamic behavior [23-25], can add complexity to the interpretation of the results of a lubrication process. Then, in some cases, it can be difficult to establish whether a change in the tablet dissolution profile originates in the actual change in tablet property or in a variability of the dissolution test itself. Powder hydrophobicity is what ultimately determines the dissolution properties of the tablets.

The effect of lubricant mixing time on tablet dissolution depends on the magnitude of the shear rate (determined by the blender scale and its operation speed) and strain (determined by the length of the blending operation). Often, the magnitude of these two variables in a blender is unknown, and tablet dissolution is correlated with the type of blender (i.e. scale, shape, intensifier bars, etc) and its operation method (i.e. fill level, speed of rotation, etc) [26-28]. Studies in various blenders show that as the mixing time for magnesium stearate increases, there is an increase in the disintegration time and a decrease in drug dissolution for tablets [17-19, 26-28].

In order to study the effects of shear rate, strain, and lubricant concentration on blend hydrophobicity (or wetability), the controlled shear environment and experimental conditions described in Chapter 4 are used. The Materials and Methods section describes the composition of formulations, the method to prepare them under shear controlled conditions, and the method to measure their hydrophobicity (Washburn). The Washburn technique measures the contact angle of water saturated with excipients and the lubricated substrate. The Results section discusses the effects of shear rate and strain, for lubricated and un-lubricated formulations, on hydrophobicity. Then, a graphical representation that compiles the effects of shear rate, strain, and lubricant concentration on formulation hydrophobicity is presented. Finally, a statistical study of the experimental results is performed to establish the effect of each of those variables and their interactions. The Conclusion summarizes the results and provides guidelines to apply this technique to practical situations.

6-2 Materials and Methods

6-2-1 Formulations

The materials used in all experiments reported here are a mixture of lactose, microcrystalline cellulose, and different amounts of magnesium stearate (Table 6-1). These materials are some of the most common pharmaceutical excipients and in the interest of brevity their SEM images are not included in this chapter but can be found in "Handbook of Pharmaceutical excipients" [26].

Four mixtures are prepared with the following proportions on mass basis:

- Mixture 1: Lactose (60%), Avicel (40%), MgSt (0%).
- Mixture 2: Lactose (59.5%), Avicel (40%), MgSt (0.5%).
- Mixture 3: Lactose (59%), Avicel (40%), MgSt (1%).
- Mixture 4: Lactose (58%), Avicel (40%), MgSt (2%).

6-2-2 Instrument: Controlled shear environment (described in Chapter 4)

6-2-3 Procedure to prepare formulations under controlled shear conditions

The procedure to prepare lubricated formulations in the controlled shear environment is identical to that described in Chapter 4. That is preparing a lubricated pre-blend in the V-blender that is later exposed to any of the shear conditions expressed in Table 4-2 using the controlled shear environment. In the lubrication studies, the reasons to follow this procedure are different. If the controlled shear environment is loaded with the excipients and the lubricant in a stratified manner, it takes a long time to achieve lubricant homogeneity throughout the controlled shear environment. Homogeneity is critical because if ingredients are not pre-blended, some parts of the blend will have a high concentration of lubricant and others will have a low concentration of lubricant while being sheared, making the lubrication process uneven; unless this is avoided results could be misleading.

A homogeneous pre-blend of the lubricant or API and the excipients is prepared as explained in previous chapter (Section 5-2-1).

6-2-4 Washburn technique

Washburn described the phenomenon of liquid rising into the lattice of a powder bed due to capillary action [30, 31], and developed a technique that measures the speed at which a fluid permeates through a powder bed to study the hydrophobicity (or contact angle) of many type of materials. In his paper, he shows that the volume of fluid that penetrates the powder bed is a function of the square root of time (Eq. 6-1). This technique has been thoroughly used for drugs and pharmaceutical excipients [15, 32].

$$V = k'\left(\frac{\gamma}{\eta}\right)^{1/2} t^{1/2} \qquad \text{(Eq. 6-1)}$$

In the present study, the powder (50 grams) is poured into a chromatographic column with the bottom made of sintered glass (Figure 6-1-a) and densified during one minute using the tap density tester (VanKel, Model 50-1200). The bottom of the column is immersed into a large container of solution saturated with all soluble blend components, with the level of liquid barely above the sintered glass (Figure 6-1-b). The column is held by a support beam positioned on a scale (Adventurer Pro, Ohaus) connected to a computer with a data collecting system (Balance Talk, Labtronics, Inc.), as shown in Figure 6-1-c. The scale is tared, and the system collects data as the fluid permeates into the powder bed. Figures 6-2-a, 6-2-b, 6-2-c, and 6-2-d are plots of the weight of fluid that permeates into the column as a function of time.

Subsequently, these data are plotted as time versus mass of solution squared, and as a result, straight lines (Figures 6-3-a, 6-3-b, 6-3-c, and 6-3-d) whose slope represents the term (□ / C □^{2} □ cos)□ are obtained. □, □ and □ are the viscosity, the density, and the surface tension of the solution, respectively; C is a proportionality constant characteristic of the column and the powder packing, and □ is the contact angle. For notation simplicity, the term (□ / C □^{2} □ cos)□ is represented as □ in this paper. The constant C can be determined performing wetting experiments using n-hexane, which has a very low surface tension, and so (cos □) is equal to one. The value of the slope is used for the subsequent analysis of the effect of shear rate, strain, and lubricant concentration on hydrophobicity.

6-3 Results

6-3-1 Design of Experiment

The shear rates and strain values tested are the same as in Section 4-3-1, for the reason that those are the values expected in industrial units. The design is therefore a two-factorial experiment, with lubricant concentration and "shear treatment" as variables, and each hydrophobicity measurement repeated twice. The experiment is completely randomized. Table 6-1 compiles the hydrophobicity values □ values for all the "shear treatments" and lubricant concentrations examined. There are two experimental values for each condition studied, yielding a total of 80 experiments.

The average value for each of the forty conditions tested is plotted in Figure 6-4. Figure 6-4 presents the value of the term □ as a function of the lubricant concentration, and each curve corresponds to one of the ten shear treatments indicated in Table 4-1. The solid lines curves at the bottom correspond to the minimum level of strain (10 revolutions), and different shear rates (2 rpm and 40 rpm). The dashed lines curves correspond to a larger amount of strain (80 revolutions), and different shear rates (2 rpm, 40 rpm, and 160 rpm). The curves with dot lines correspond to a larger amount of strain (320 revolutions), and different shear rates (40 rpm, 160 rpm, and 245 rpm). Finally, the blurry lines on top correspond blends prepared using 2000 revolutions and two different shear rates (160 rpm, 245 rpm). The Washburn technique can not measure the value of □ for the blends with 1% and 2% magnesium stearate, prepared in the controlled shear environment operating at 245 rpm for 2000 revolutions because the solution does not permeate the powder bed at all. In the statistical analysis, the shear treatments which consist of 2000 revolutions are not included because some of them did not yield measurable values.

The number of measurements used for statistical analysis (60 values) still gives enough degrees of freedom to run a two-factor ANOVA and determine the effects of shear treatment (df=7), lubricant concentration (df=3), and also their possible interaction (df=21). The results of this test (Table 6-2) show that, for a significance p level of 0.05, shear treatment (p=0) and lubricant concentration (p=0) affect blend hydrophobicity. Additionally, there is significant interaction between these variables, and this is evident in

Figure 6-4 because the lines for the different shear treatments are not parallel and they cross each other at low lubricant concentration.

6-3-2 Effect of shear rate and strain on blend hydrophobicity

The previous two-factor ANOVA showed that shear treatment affects blend hydrophobicity. However, in Figure 6-4, it can be seen that in the absence of lubricant, all the hydrophobicity values are very similar. A plot of the average value of the term □ as a function of strain (number of revolutions), using curves that correspond to different shear rates (speed of the cylinder of the controlled shear environment) for the blend without lubricant shows that □ values are very similar and in the range 0.01-1 (Figure 6-5-a). In fact, an ANOVA test shows that the hydrophobicity of the formulation without lubricant does not change as a function of the shear treatment. The number of measurements used for statistical analysis (16 values) gives enough degrees of freedom to run a one-factor ANOVA and determine the effects of shear treatment (df=7). The results of this test (Table) show that, for a significance p level of 0.05, shear treatment (p=0.381) does not affect blend hydrophobicity.

On the other hand, when lubricant is present, shear treatment changes the hydrophobicity significantly. Figures 6-5-b, 6-5-c, and 6-5-d present the results for a 0.5%, 1%, and 2% MgSt concentration, where the term □ is plotted as a function of strain (number of revolutions), using curves that correspond to different shear rates (speed of the cylinder of the controlled shear environment). In general, the term □ increases as a function of strain, and such increase is a ~10^4 fold after the blend is exposed to 2000 revolutions of the controlled shear environment. One-factor ANOVA tests for the dataset for each lubricant concentration indicate that the shear treatment affects blend hydrophobicity (Table 6-3).

Figures 6-5-b, 6-5-c, and 6-5-d show curves that grow as a function of the total number of revolutions (strain), however, the curves that correspond to different shear rates lie close to each other. In order to determine whether shear rate has any influence on hydrophobicity, the average □ values for all the lubricated blends (0.5%, 1%, and 2%) prepared using the same number of revolutions (strain) and different rpm of the controlled shear environment must be compared. Two-factor ANOVA tests (lubricant concentration and shear rate) are carried out for blends prepared using 10, 80, and 320 revolutions of the controlled shear environment.

Table 6-3 shows that after 10 revolutions, the hydrophobicity of the blends prepared using 2rpm and 40rpm are significantly different (p=0.027). The number of measurements available for the lubricant concentrations of 0.5%, 1%, and 2% (12 values) gives enough degrees of freedom to run a two-factor ANOVA and determine the effects of shear rate (df=1) and lubricant concentration (df=2) on hydrophobicity and also their interaction (df=2).

Table 6-4 shows that after 80 revolutions, the hydrophobicity of the blends prepared using 2rpm, 40rpm, and 160rpm are significantly different (p=0.002) and Table 6-5 shows that after 320 revolutions, the hydrophobicity of the blends prepared using 40rpm, 160rpm, and 245rpm are significantly different (p=0.003). The number of measurements available for the lubricant concentrations of 0.5%, 1%, and 2% (18 values) gives enough degrees of freedom to run these two-factor ANOVA and determine the effects of shear rate (df=2) and lubricant concentration (df=2) on hydrophobicity and also their interaction (df=4). The results of these tests (Tables 6-4, 6-5, and 6-6) show that, for a significance p level of 0.05, shear rate affects blend hydrophobicity.

6-3-3. Effect of lubricant concentration on hydrophobicity

Figure 6-4 also shows the blend hydrophobicity for any shear treatment increases as a function of lubricant concentration, and most curves increase from left to right. In general, there is a steep increase in blend hydrophobicity when lubricant concentration goes from 0% to 0.5%, and a slower and constant increase when lubricant concentration goes from 0.5% to 2%. In order to establish the statistical significance of the effect of lubricant concentration on blend hydrophobicity, one-factor ANOVA tests are run for each of eight shear treatment (the sets at 2000 revolutions were not tested), using the data available for 0.5%, 1%, and 2% lubricant concentrations. The data in each set (6 values) gives enough degrees of freedom to study the effect of lubricant concentration (df=2). Seven tests yield p values much lower than 0.05, which indicates that lubricant concentration affects blend hydrophobicity (Table 6-6).

6-3-4. An application: determining when to stop the lubrication process

Hydrophobicity of lubricated blends grows as a function of strain and shear rate. Figures 6-5-b, 6-5-c, and 6-5-d show that, at low strain values (less than 100 revolutions), the increase in hydrophobicity is generally low, and that for larger strain values, hydrophobicity increases at much larger rates until the blend becomes waterproof. An interesting analysis is to determine the onset of such steep hydrophobicity increment.

Tukey's method (*w*) can be used to established what "shear treatments" are significantly different for each lubricant concentration.

The *w* values for the data set at each lubricant concentration are indicated on the right column of Table 6-7. Table 6-8 presents the average hydrophobicity values □ for all the shear treatments and lubricant concentrations. For each lubricant concentration (columns), one can look for the shear treatments that are substantially different, that is smaller than *w*. After organizing the averages from smallest to largest, in increasing order, one underlines the pairs that are smaller that *w*. For a 0.5% magnesium stearate concentration, the treatment "245 rpm -320 revs" is substantially larger than "160 rpm -320 revs" (and the other treatments), indicating that shear leads to a steep increase in hydrophobicity before 320 revolutions of the controlled shear environment. For 1% and 2%, the treatment "160 rpm -320 revs" is substantially larger than "40 rpm -320 revs" (and the other treatments), also that shear leads to a steep increase in hydrophobicity before 320 revolutions of the controlled shear environment. In conclusion, a strain equivalent to less than 320 revolutions of the controlled shear environment leads to a steep increase in hydrophobicity. Additionally, for high lubricant concentrations (1% and 2%), the steep increment occurs at lower shear rates (160 rpm) than for low lubricant concentration blends (0.5%), for which the increment occurs at 245 rpm.

6-4 Conclusions

This paper examines the effect of lubricant content, shear rate and strain on the hydrophobicity of lubricated formulations. A new controlled shear environment allows to uniformly expose blends to controlled combinations of shear rate and strain. Blend hydrophobicity is measured using the Washburn method. The entire procedure is highly reliable and gives reproducible results. The relevance of the present study is that it constitutes a step towards building predictive methods for dissolution, drug release, and other properties of products (i.e. tablet hardness, coating, etc).

The results, which are compiled in Figure 6-4, show that the hydrophobicity of lubricated blends increases as a function of strain, shear rate, and lubricant concentration.

The results presented in the current chapter constitute, to our knowledge, the first attempt to correlate the effect of processing variables such as shear rate and strain with hydrophobicity of a blend. Given that the focus of regulations is the final product (tablet or capsules), it is not surprising that most of the previous studies focused on the effects of processing variables on tablet dissolution. However, dissolution is obviously the result of the product processing history and composition. The type of approach provided by this chapter constitutes the first step towards building a predictive method for dissolution, drug release, and other characteristics (coating) of tablets or capsules. The contribution to tablet dissolution made by every unit of the manufacturing process could be ideally assessed using the current methodology.

This methodology has been used in previous chapters to study successfully the effect of shear rate and strain other blend properties. The next section will summarize these findings and will device an integral plan to use them towards understanding what factors lead to the mean values and the variability observed in product quality assessment.

REFERENCES

1- Velasco, M.V.; Munoz-Ruiz, A.; Monedero, M.C.; Jimenez-Castellanos, M.R. Study of flowability of powders. Effect of the addition of lubricants. *Drug Development and Industrial Pharmacy* 21 (1995), p. 2385.

2- Faqih, A.M.; Mehrotra A.; Hammond S.V.; Muzzio F.J. Effect of moisture and magnesium stearate concentration on flow properties of cohesive granular materials. *International Journal of Pharmaceutics* 336 (2007), p.338.

3- Miller, T.A.; York, P. Pharmaceutical tablet lubrication. *International Journal of Pharmaceutics* 41 (1988), p. 1.

4- Rizk S.; Guyot J.C.; Duru C.; Gaudy D. Influence of lubricant properties on compression behavior and drug dissolution rate of scleroglucan hydrophilic matrix. *International Journal of Pharmaceutics* 126 (1995), p. 57.

5- Desai, D.S.; Rubitski, B.A.; Varia, S.A.; Newman, A.W. Physical interactions of magnesium stearate with starch-derived disintegrants and their effects on capsule and tablet dissolution. *International Journal of Pharmaceutics* 91 (1993), p. 217.

6- Cao, Q.R.; Choi, Y.W.; Cui, J.H.; Lee, B.J. Formulation, release characteristics and bioavailability of novel monolithic hydroxypropylmethylcellulose matrix tablets containing acetaminophen. *Journal of Controlled Release* 108 (2005), p. 351.

7- Eddington, N.D.; Ashraf M.; Augsburger L.L.; Leslie J.L.; Fossler, M.J.; Lesko L.J.; Shah, V.P.; Rekhi, G.S. Identification of formulation and manufacturing variables that influence in vitro dissolution and in vivo bioavailability of propranolol hydrochloride tablets. *Pharmaceutical Development and Technology* 3 (1998), p. 535.

8- Rubinstein M.H.; Eastwood B.A. The effect of lubricant type and concentration on the bioavailability of frusemide from 40mg tablets. *The Journal of Pharmacy and Pharmacology* (1978), Suppl., 12 p.

9- FDA guidance for Industry: dissolution testing of immediate release solid oral dosage forms, August 1997; extended release solid oral dosage forms: development, evaluation and application of in vitro/in vivo correlations, September 1997. www.fda.gov/cder/guidance/1713bp1.pdf

10- Siewert, M.; Dressman, J.; Brown, C.K.; Shah, V.P. FIP/AAPS Guidelines to Dissolution/in Vitro Release Testing of Novel/Special Dosage Forms. *AAPS PharmSciTech*. 4 (2003).

11- FDA Guidance for Industry: Bioavailability and Bioequivalence Studies for Orally Administered Drug Products—General Considerations. October 2000.

12- Rowe, R.C. Correlation between predicted binder spreading coefficients and measured granule and tablet properties in the granulation of paracetamol. *International Journal of Pharmaceutics* 58 (1990), p. 209.

13- Buckton, G.; Newton, J.M. Assessment of the wettability and surface energy of a pharmaceutical powder by liquid penetration. *The Journal of Pharmacy and Pharmacology* 37 (1985), p. 605.

14- Zhang, D.; Flory, J.H.; Panmai, S.; Batra, U.; Kaufman, M.J. Wettability of pharmaceutical solids: its measurement and influence on wet granulation. *Colloids and Surfaces A: Physicochemical and Engineering Aspects* 206 (2002), p. 547.

15- Muster, T.H.; Prestidge, C.A. Water adsorption kinetics and contact angles of pharmaceutical powders. *Journal of Pharmaceutical Sciences* 94 (2002), p. 861.

16- Johnson, J.R.; Wang, L.H.; Gordon, M.S.; Chowhan, Z.T. Effect of formulation solubility and hygroscopicity on disintegrant efficiency in tablets prepared by wet granulation, in terms of dissolution. *Journal of Pharmaceutical Sciences* 80 (1991), p. 469.

17- Chowhan, Z.T.; Chi, L.H. Drug-excipient interactions resulting from powder mixing. IV: Role of lubricants and their effect on in vitro dissolution. *Journal of Pharmaceutical Sciences* 75 (1986), p. 542.

18- Kikuta, J.I.; Kitamori, N. Effect of mixing time on the lubricating properties of magnesium stearate and the final characteristics of the compressed tablets. *Drug Development and Industrial Pharmacy* 20 (1994), p. 343.

19- Sheskey, P.J.; Robb, R.T.; Moore, R.D.; Boyce, B.M. Effects of lubricant level, method of mixing, and duration of mixing on a controlled-release matrix tablet containing hydroxypropyl methylcellulose. *Drug Development and Industrial Pharmacy* 21 (1995), p. 2151.

20- Van Veen, B.; Pajander, J.; Zuurman, K.; Lappalainen, R.; Poso, A.; Frijlink, H.W.; Ketolainen, J.; van Veen, B. The effect of powder blend and tablet structure on drug release mechanisms of hydrophobic starch acetate matrix tablets. *European Journal of Pharmaceutics and Biopharmaceutics* 61 (2005), p.149.

21- Wang, L.H.; Chowhan, Z.T. Drug-excipient interactions resulting from powder mixing. Part V: Role of sodium lauryl sulfate. *International Journal of Pharmaceutics* 60 (1990), p. 61.

22- Ong, J.T.H.; Chowhan, Z.T.; Samuels, G.J. Drug-excipient interactions resulting from powder mixing. VI: Role of various surfactants. *International Journal of Pharmaceutics* 96 (1993), p. 231.

23- Hurtado y de la Pena et al. Comparison of Dissolution Profiles for Albendazole Tablets Using USP Apparatus 2 and 4. *Drug Development and Industrial Pharmacy* 29 (2003), p.777.

24- Morihara, M.; Aoyagi, N.; Kaniwa, N.; Katori, N.; Kojim, S.; Morihara. Hydrodynamic Flows Around Tablets in Different Pharmacopeial Dissolution Tests. *Drug Development and Industrial Pharmacy* 28 (2002), p.655

25- Kukura, J.; Arratia, P.E.; Szalia, E.S.; Muzzio, F.J. Engineering tools for understanding the hydrodynamics of dissolution tests. *Drug Development and Industrial Pharmacy* 29 (2003), p. 231.

26- Otsuka, M.; Jian, G.; Matsuda, Y. Effects of mixer and mixing time on the pharmaceutical properties of theophylline tablets containing various kinds of lactose as diluents. *Drug Development and Industrial Pharmacy* 19 (1993), p. 333.

27- Shah, A.C.; Mlodozeniec, A.R. Mechanism of surface lubrication: Influence of duration of lubricant-excipient mixing on processing characteristics of powders and properties of compressed tablets. *Journal of Pharmaceutical Sciences* 66 (1977), p. 1377.

28- Ullah, I.; Wiley, G.J.; Agharkar, S.N. Analysis and simulation of capsule dissolution problem encountered during product scale-up. *Drug Development and Industrial Pharmacy* 18 (1992), p. 895.

29- Mehrotra, A.; Llusa, M.; Faqih, A.; Levin, M.; Muzzio, F.J. Influence of shear intensity and total shear on properties of blends and tablets of lactose and cellulose lubricated with magnesium stearate. *International Journal of Pharmaceutics* 336 (2007), p. 284.

30- Washburn, E.W. The Dynamics of Capillary Flow. *Physical Review* 17 (1921), p. 374.

31- Hiemenz, P.C. Principles of Colloid & Surface Chemistry, 3rd Edition.

32- Prestidge, C.A.; Tsatouhas, G. Wettability studies of morphine sulfate powders. *International Journal of Pharmaceutics* 198 (2000), p. 201.

Figure 6-1-a

Figure 6-1-b

Figure 6-1-c

Figure 6-1-a: Chromatographic column, loaded with the powder, in the tap density tester. Figure 6-1-b: Chromatographic column submerged in the solution container. Figure 6-1-c: Setting to measure and record the increase in weigh of the chromatographic column.

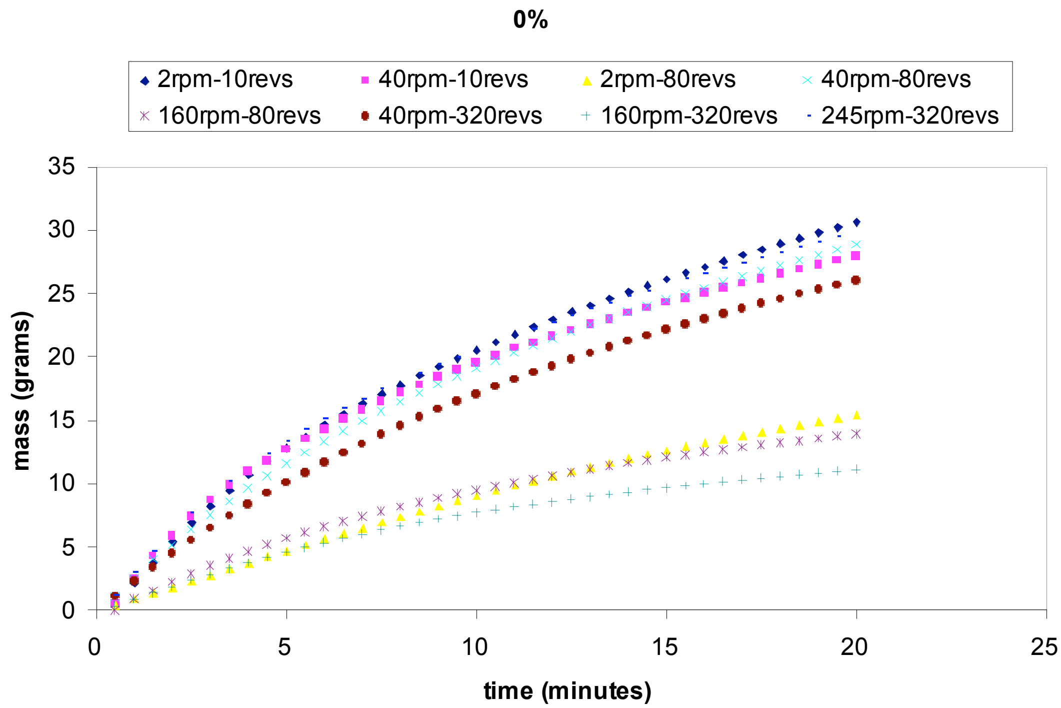

Figure 6-2-a: Amount of fluid that permeates through the powder bed (0% MgSt)

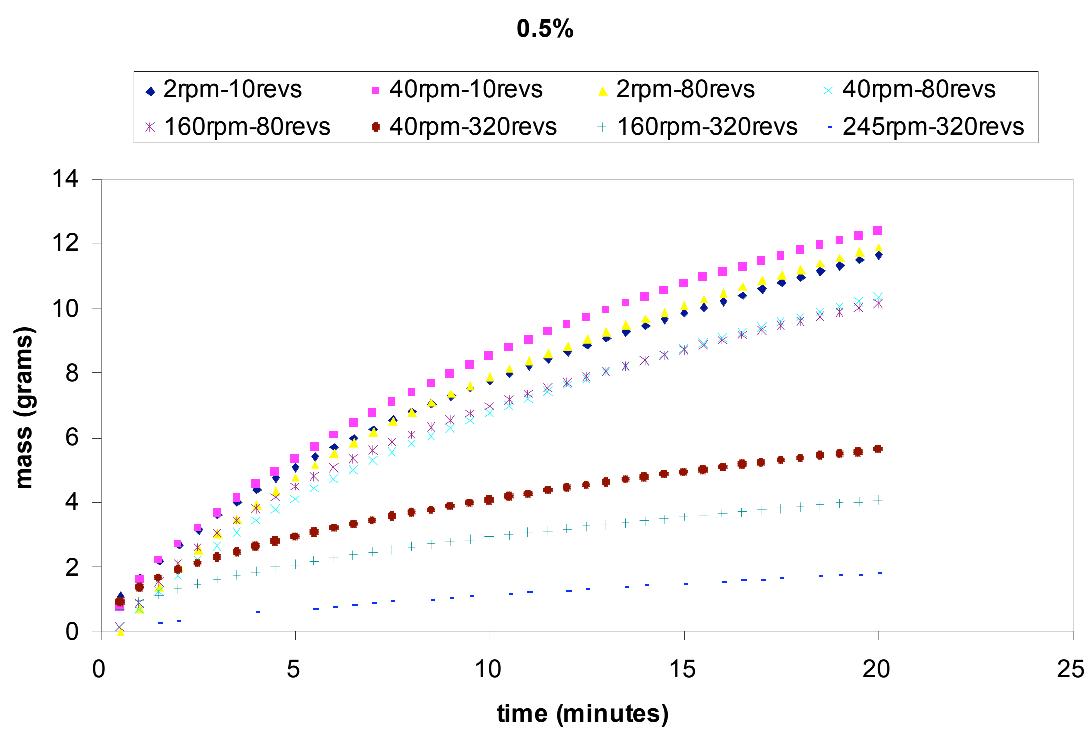

.

Figure 6-2-b: Amount of fluid that permeates through the powder bed (0.5% MgSt)

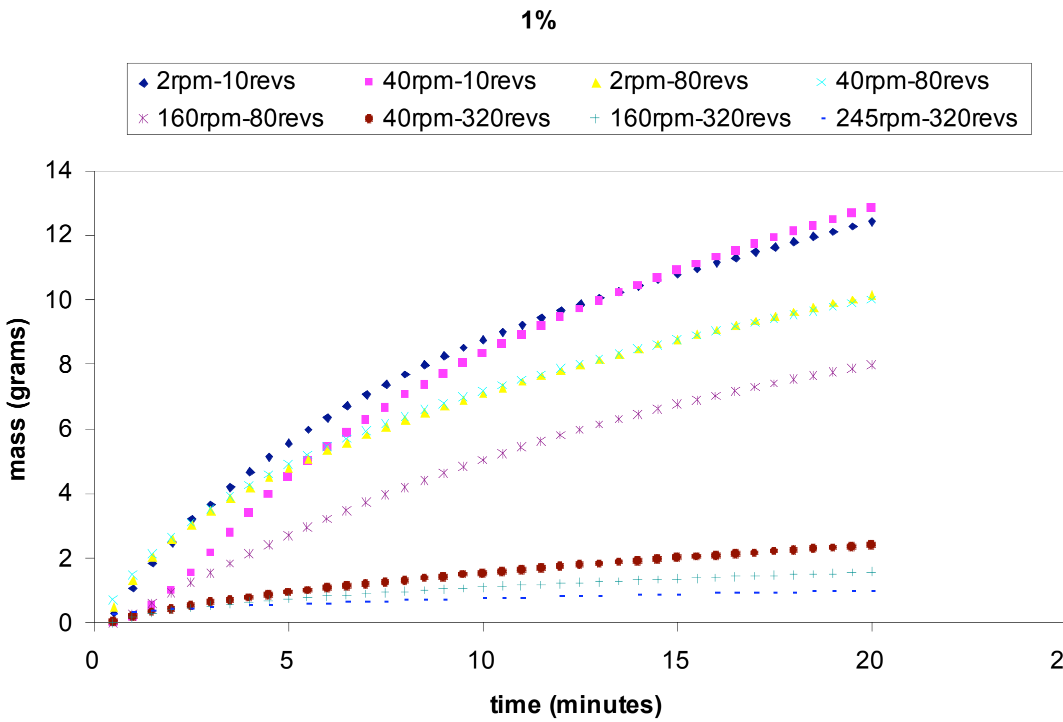

Figure 6-2-c: Amount of fluid that permeates through the powder bed (1% MgSt)

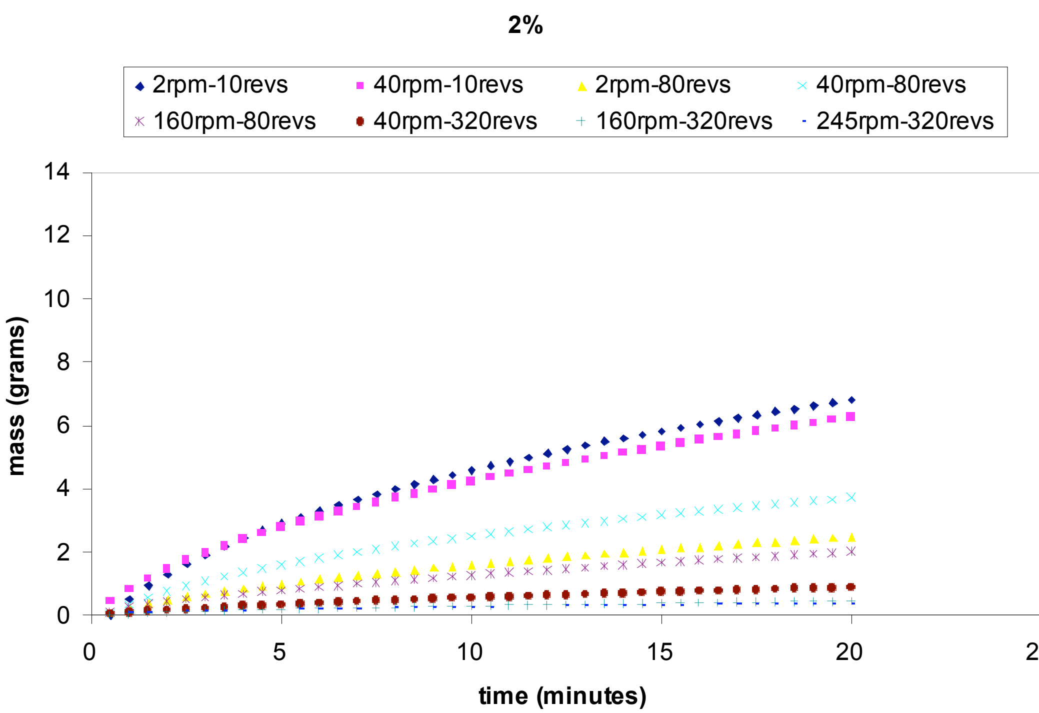

Figures 6-2-d: Amount of fluid that permeates through the powder bed (2% MgSt)

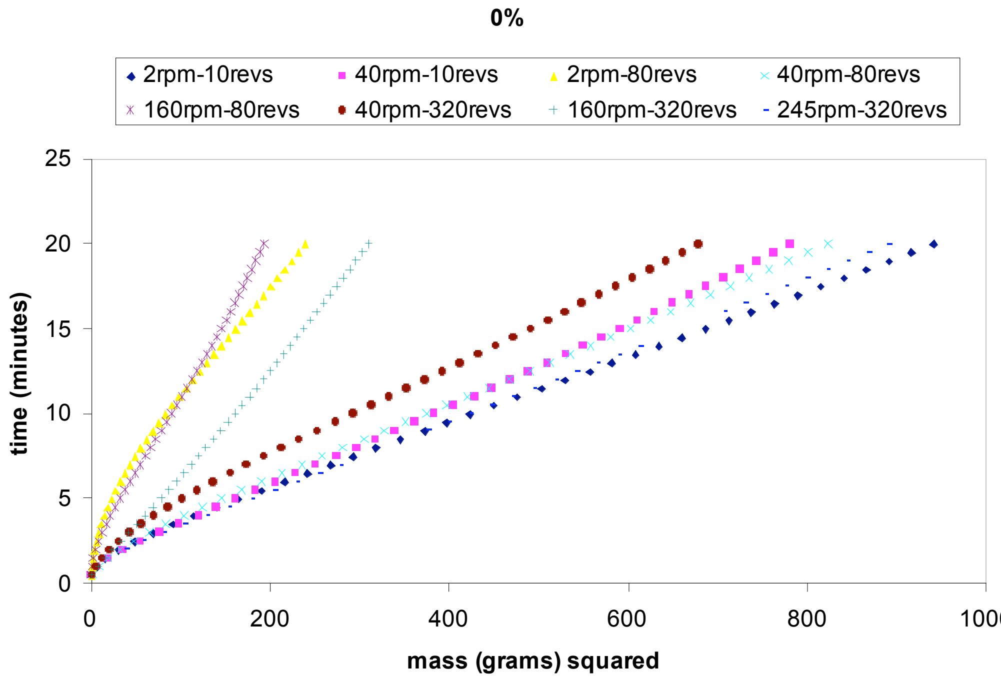

Figures 6-3-a: Plotting the data as time versus mass of fluid squared (0% MgSt)

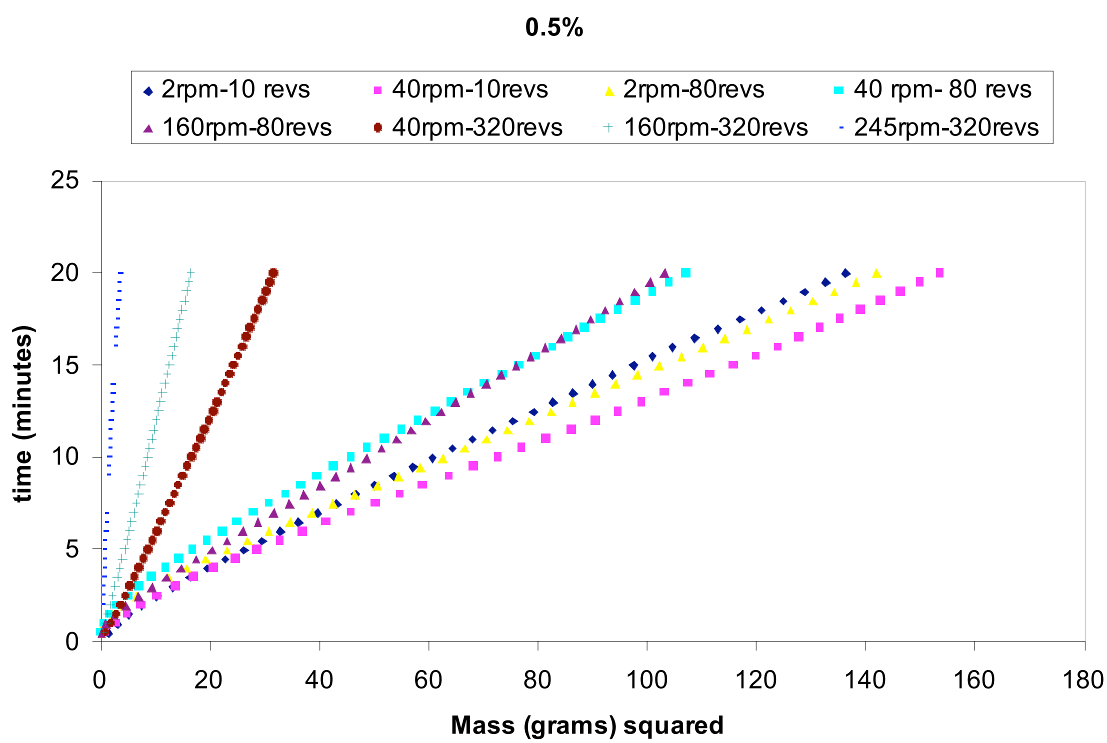

Figures 6-3-b: Plotting the data as time versus mass of fluid squared (0.5% MgSt)

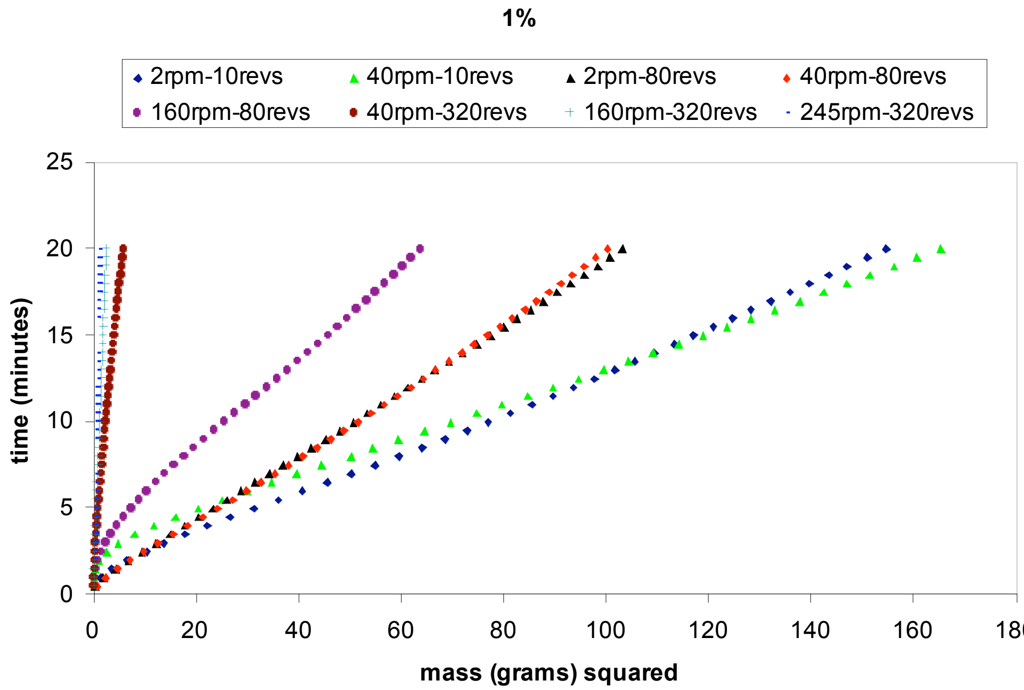

Figures 6-3-c: Plotting the data as time versus mass of fluid squared (1% MgSt)

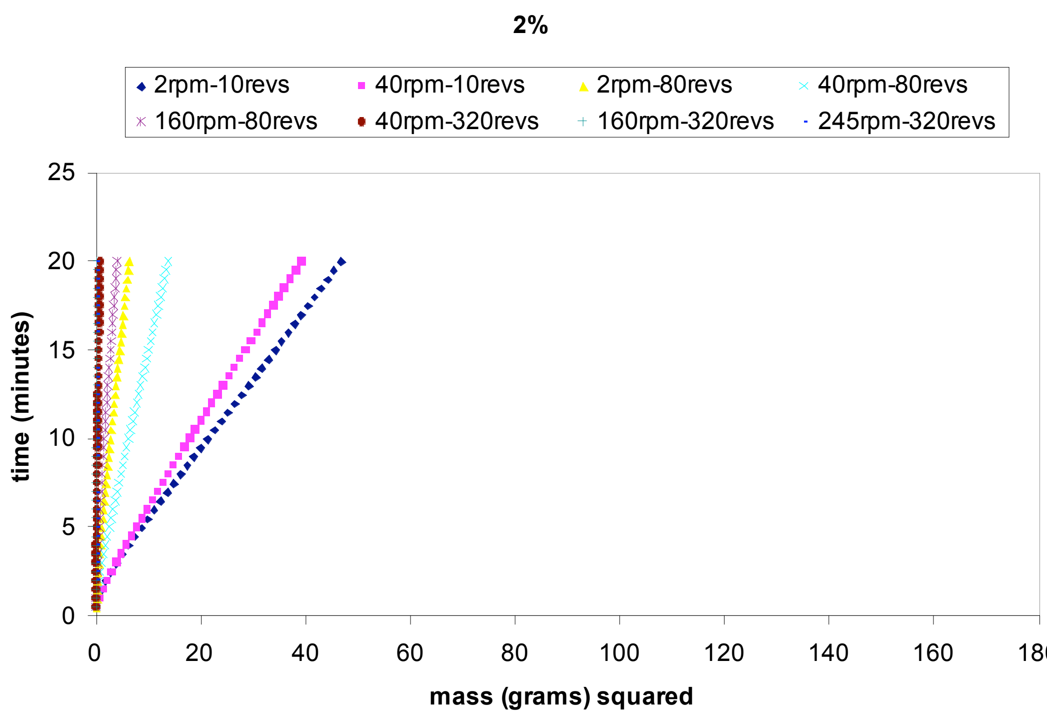

Figures 6-3-d: Plotting the data as time versus mass of fluid squared (2% MgSt)

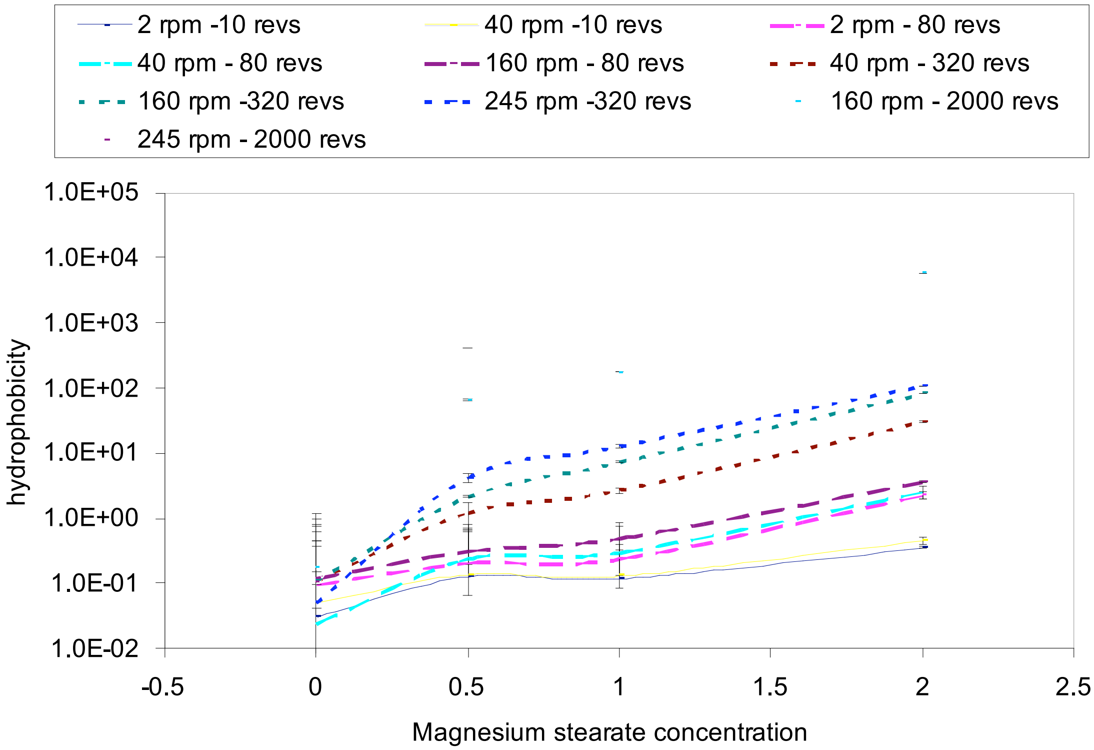

Figure 6-4: Effect of lubricant content, shear rate, and strain on the magnitude of □

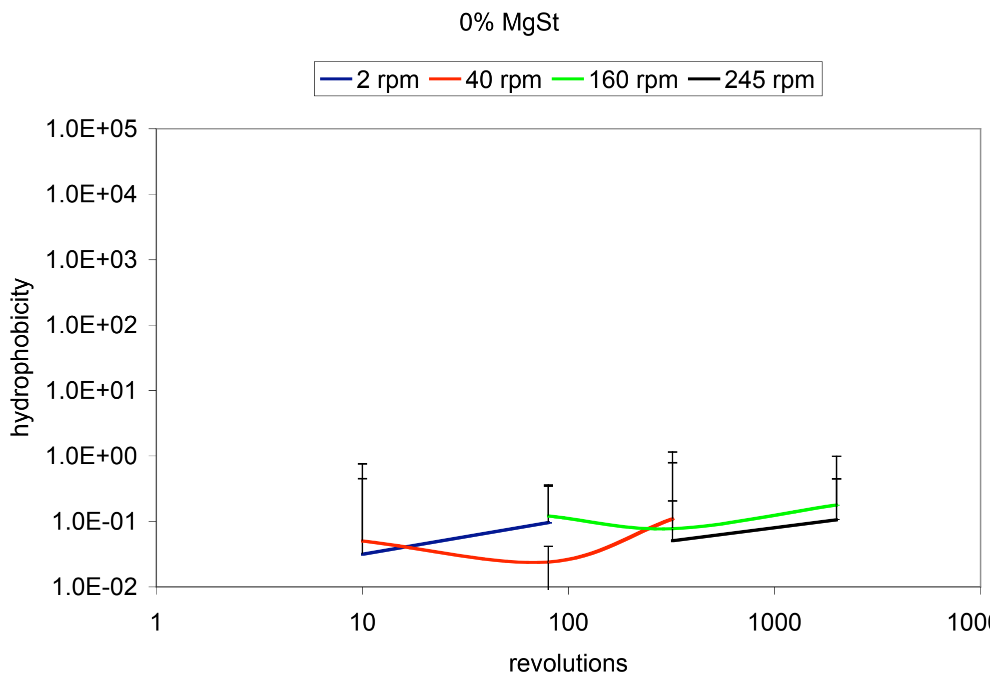

Figures 6-5-a: Effect of shear rate and strain on the magnitude of □ for a blend with 0% magnesium stearate

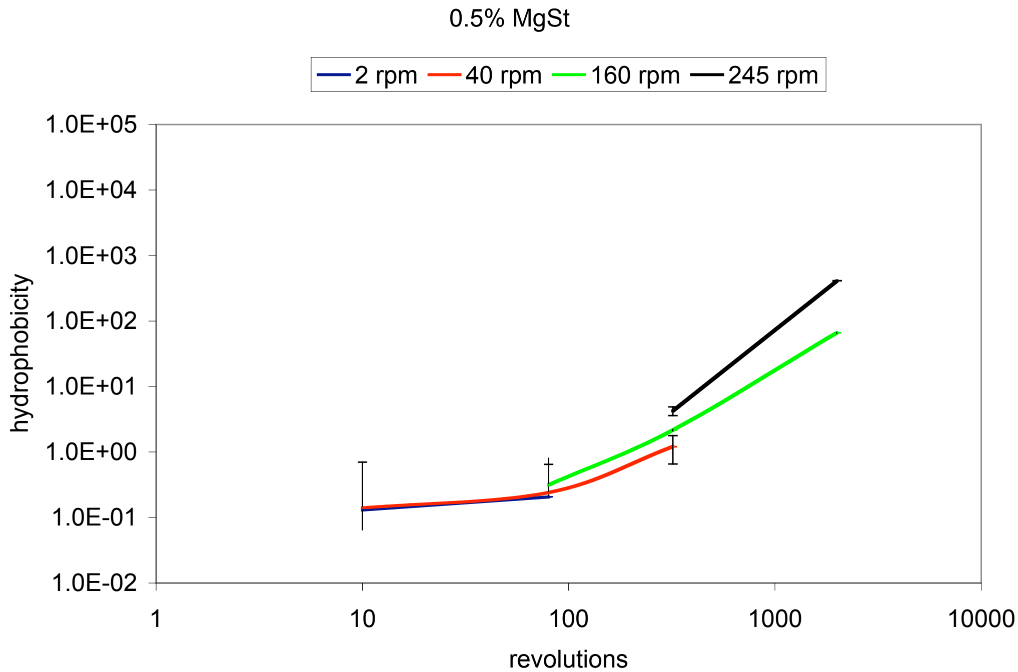

Figures 6-5-b: Effect of shear rate and strain on the magnitude of for a blend with 0.5% magnesium stearate

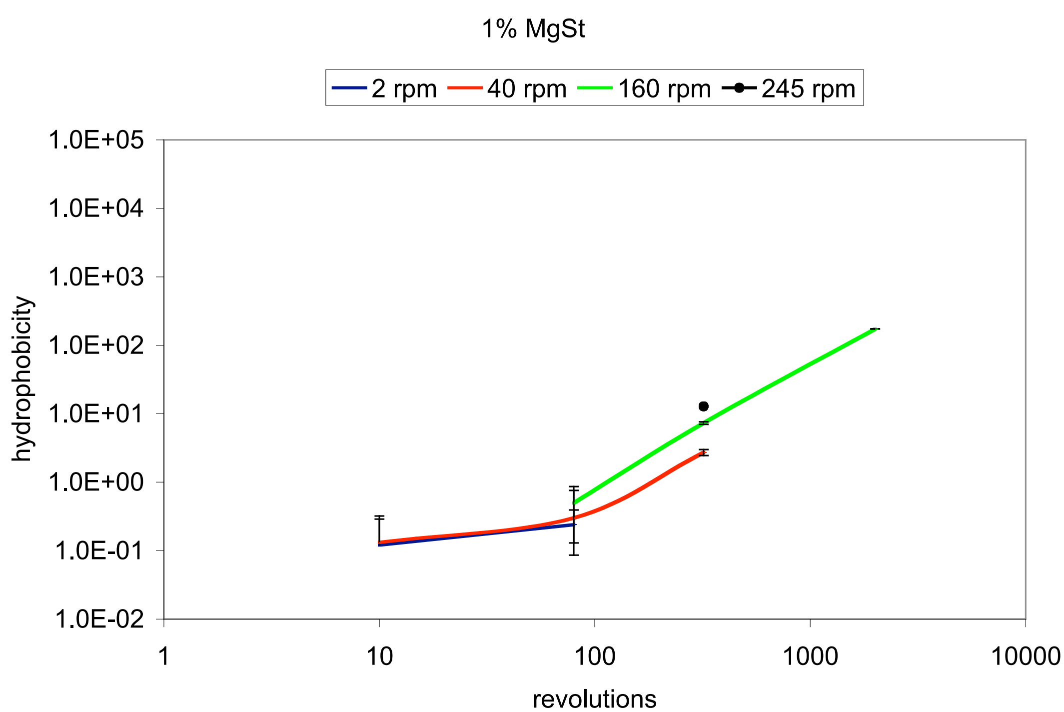

Figures 6-5-c: Effect of shear rate and strain on the magnitude of for a blend with 1% magnesium stearate

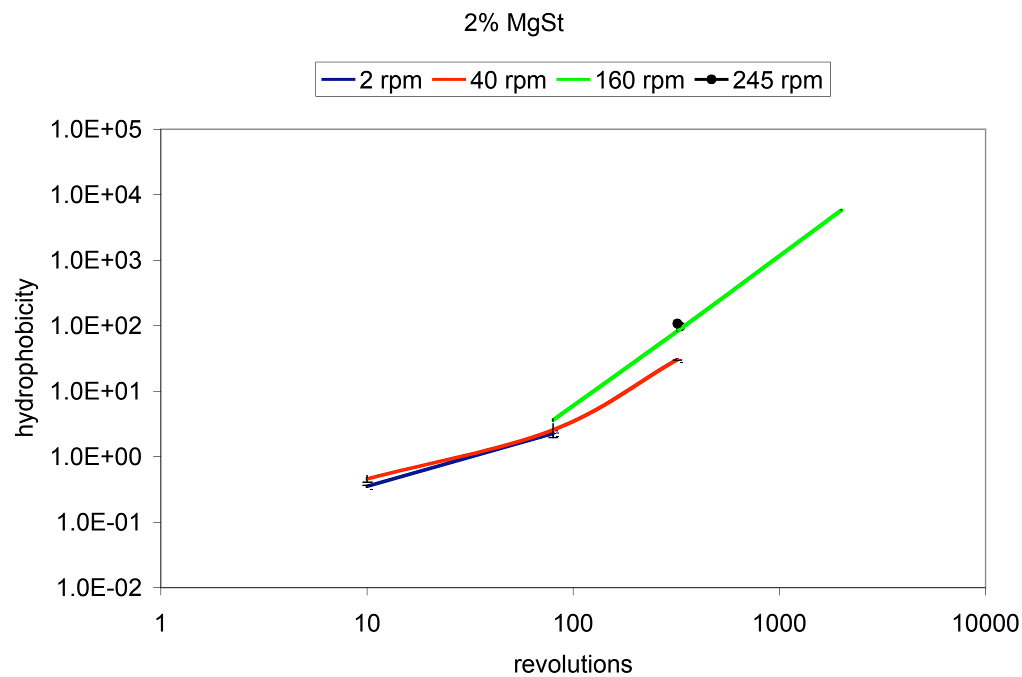

Figures 6-5-d: Effect of shear rate and strain on the magnitude of for a blend with 2% magnesium stearate

	0% MgSt	0.5% MgSt	1% MgSt	2% MgSt
2 rpm -10 revs	0.022, 0.041	0.136, 0.124	0.137, 0.103	0.356, 0.351
40 rpm -10 revs	0.025, 0.075	0.128, 0.224	0.117, 0.146	0.475, 0.441
2 rpm – 80 revs	0.078, 0.114	0.142, 0.172	0.213, 0.265	2.798, 2.262
40 rpm - 80 revs	0.024, 0.024	0.171, 0.309	0.203, 0.397	2.0, 1.377
160 rpm - 80 revs	0.141, 0.102	0.267, 0.192	0.569, 0.627	3.315, 3.909
40 rpm - 320 revs	0.029, 0.189	0.734, 1.691	3.521, 2.774	17.05, 43.77
160 rpm -320 revs	0.070, 0.084	2.203, 2.107	8.815, 8.351	90.5, 75.31
245 rpm -320 revs	0.024, 0.077	4.280, 6.951	5.7, 10.317	123.8, 92.33
160 rpm - 2000 revs	0.212, 0.145	35.328, 39.9	128.89, 217.97	10912, 758.78
245 rpm - 2000 revs	0.046, 0.058	34.328, 23.66	NA, NA	NA, NA

Table 6-1: Compilation of values for the group

Source	DF	Seq SS	Adj SS	Adj MS	F	P
shear treatment-	7	8149.7	8149.7	1164.2	37.90	0.000
Lub	3	9084.7	9084.7	3028.2	98.58	0.000
shear treatment-*Lub	21	17854.0	17854.0	850.2	27.68	0.000
Error	32	983.0	983.0	30.7		
Total	63	36071.4				

Table 6-2: ANOVA test run on the experimental values for all conditions

Source	DF	Seq SS	Adj SS	Adj MS	F	P
10 revs	1	0.008802	0.008802	0.008802	8.46	0.027
lub_	2	0.190304	0.190304	0.095152	91.45	0.000
10 revs*lub_	2	0.004469	0.004469	0.002235	2.15	0.198
Error	6	0.006243	0.006243	0.001041		
Total	11	0.209819				

Table 6-3: ANOVA test run to determine the effect of shear rates on samples with lubricant concentrations 0.5%, 1%, and 2%, and 10 revolutions of the controlled shear environment (10 revolutions)

Source	DF	Seq SS	Adj SS	Adj MS	F	P
80 revs	2	1.7030	1.7030	0.8515	13.96	0.002
lubricant	2	21.5483	21.5483	10.7741	176.65	0.000
80 revs*lubricant	4	2.1719	2.1719	0.5430	8.90	0.003
Error	9	0.5489	0.5489	0.0610		
Total	17	25.9722				

Table 6-4: ANOVA test run to determine the effect of shear rates on samples with lubricant concentrations 0.5%, 1%, and 2%, and 80 revolutions of the controlled shear environment (80 revolutions)

Source	DF	Seq SS	Adj SS	Adj MS	F	P
320 revs	2	2624.0	2624.0	1312.0	12.02	0.003
lub_	2	19083.7	19083.7	9541.9	87.41	0.000
320 revs*lub_	4	3712.8	3712.8	928.2	8.50	0.004
Error	9	982.4	982.4	109.2		
Total	17	26402.8				

Table 6-5: ANOVA test run to determine the effect of shear rates on samples with lubricant concentrations 0.5%, 1%, and 2%, and 320 revolutions of the controlled shear environment (320 revolutions)

	ANOVA (p values)
2 rpm -10 revs	0.001
40 rpm -10 revs	0.009
2 rpm - 80 revs	0.003
40 rpm - 80 revs	0.021
160 rpm – 80 revs	0.001
40 rpm – 320 revs	0.126
160 rpm -320 revs	0.002
245 rpm -320 revs	0.007

Table 6-6: ANOVA values for the different shear treatments (except one case, the critical value is exceeded, indicating the influence of lubricant concentration on hydrophobicity)

	Observed F	Critical F	*w* (Tukey's)
0%	2.344	F.01,9,10 = 4.94	NA
0.5%	14.431	F.01,7,8 = 6.18	2.81
1%	19.092	F.01,7,8 = 6.18	4.01
2%	30.427	F.01,7,8 = 6.18	43.52

Table 6-7: ANOVA values for the different lubricant concentrations, they indicate that shear treatment plays a role (except in the absence of lubricant)

	0.5%	1%	2%
2 rpm -10 revs	0.1303	0.1201	0.3531
40 rpm -10 revs	0.176	0.1318	0.4582
2 rpm - 80 revs	0.1571	0.239	2.5301
40 rpm - 80 revs	0.2401	0.3001	1.6886
160 rpm – 80 revs	0.22925	0.59815	3.6121
40 rpm – 320 revs	1.2125	3.1475	30.4095
160 rpm -320 revs	2.15485	***8.5827***	***82.887***
245 rpm -320 revs	***5.6155***	***8.0085***	***108.0705***

Table 6-8: Influence of shear treatment on hydrophobicity

CHAPTER VII

CONCLUSIONS

7-1. Introduction

The aim of the conclusion section is to present and summarize the results of previous chapters, now organized around the major groups of factors that contribute to the product performance. Figure 2-1 shows all those groups of factors, however, the results of this dissertation can be classified and will be discussed in this chapter within three of them (Raw materials, Blending and Lubrication). From the perspective of each of these sections, there is a discussion about how the results of previous chapters can be used to contribute to the improvement of manufacturing practices. Also, those results are presented as a feasibility study to generate additional research projects with a high probability to improve the product performance.

As suggested by the title of this dissertation, the general aim is to understand the effects of shear on different properties of the blend that will conform the final product. Shear is selected because it is known to affect all the main quality parameters for tablets and capsules: drug uniformity content, tablet hardness, and dissolution. The two subsequent sections on Blending and Lubrication will focus mainly on the issue of shear. The smaller section for Raw Materials, will address the effects of type of excipient, relative humidity, and electrostatic charging, on API de-agglomeration and content uniformity.

7-2. Blending

One of the main problems with blending units is that the magnitude of shear rates is unknown and mainly non-uniform. However, the current technology does not allow for an assessment of their shear conditions, and therefore, blending processes are still studied from the perspective of variables such as blender design, tumbling speed, operation parameters (baffles, impeller, fill level, etc), and residence time. This dissertation studies the effects of these parameters on API homogeneity and de-agglomeration. The API agglomeration problem is selected because it is probably the main source for content uniformity variability in the final products.

In Chapter II, a number of experiments are designed to produce large experimental data, and using statistical methods, determine the effects of fill level, blender scale, and baffles on the API homogeneity and de-agglomeration. The results show that for blenders without moving internals:

- Higher fill levels have a higher probability of presenting agglomerates.
- Larger blenders present less agglomerates.
- Baffles: do not affect the de-agglomeration performance of blenders.

The de-agglomeration capability of a blender may be enhanced by a moving internal (impeller) but it will depend on its design and placement.

Chapter II also compares the advantages of two types of blending protocol that guarantee the absence of agglomerates in the final blends. One includes a pre-blending step of API and excipients in a high shear unit, which minimizes the possibility of API agglomerates re-forming in the blend. The second type consists of exposing the entire final blend to the high shear rates of a mill. Both protocols guarantee the absence of agglomerates in the final blend, and the homogeneity of the final blend may still be favorably affected by larger scales of the blender.

Because of the inability to establish shear rate in blenders, a new shear controlled environment is used to investigate the correlation between API de-agglomeration and shear rate and strain (Chapter IV). The degree of API agglomeration in a formulation decreases as a function of strain and shear rate. The type of excipient affect only the de-agglomeration rate of the finest APAP grade. However, the API grade influences the degree of API agglomeration in the blend, especially at low strain values (or short mixing times), and the coarser types present a larger number of agglomerates.

The problems of using blender parameters instead of shear rate and strain arise for situations such as process design, process transfer, ingredient replacement, blender scale-up, etc. All these situations are critical for the lubrication process, as explained in the next section.

7-4 Lubrication

The controlled shear environment is also used to study the effect of shear rate and strain on several properties of lubricated blends and tablets. Strain affects blend flow, density, hydrophobicity, and tablet hardness when magnesium stearate is present in the formulation. Shear rate affects blend hydrophobicity, however its effects on other blend properties seems to be negligible. Additionally, changes in these properties correlate with the evolution of lubricant homogeneity. When there is no lubricant in the formulation, shear deteriorates powder flow. However it does not affect its density or hydrophobicity.

Hence, shear improves or deteriorates flow properties, according to the presence or absence of magnesium stearate. Magnesium stearate acts as a glidant, improving the flow of the blend, and as a lubricant, facilitating the tableting operation.

Tablet hardness, for tablets made out of lubricated blends, is affected mainly by strain and in less extent by shear rate. The effect of these two variables on tablet dissolution has not been tested. However, it is expected that tablet dissolution will be mainly determined by the powder hydrophobicity. The changes in most of these properties are also sensitive to lubricant concentration. Because not only the composition, but also the characteristics of the raw materials affect the product performance, we devote an area in this dissertation.

7-3. Raw materials

There are many parameters of raw materials that affect product performance: particle size distribution, particle morphology, moisture content, and the electrical charge of excipients, drugs, and other additives, determine their tendencies to segregate, agglomerate, adhere to each other, form ordered mixtures, random mixtures, etc. The results in Chapter IV show that the type of excipient and the drug grade may affect the drug de-agglomeration process. The results show that, in general, a coarser the drug is easier to de-agglomerate. The morphology of the excipient (needle-like versus round particles) plays a role in the de-agglomeration of the finer drug grade.

Moisture and electrical charge are probably the main factors that determine the ability of particles to form agglomerates. As shown in Chapter II, API agglomerates re-form when their particles are in contact with each other, and the factors leading to agglomeration are humidity content in the case of NaCl, and electrical charge in the case of APAP. The APAP is sieved before its addition to the blender, and in such process, it can acquire electrical charge. Preblending these APIs with a portion of excipients in a high shear unit can minimize agglomerate re-forming.

7-5. Future projects

The expectation of regulating agencies and consumer organizations is that pharmaceutical manufacturing becomes more flexible and robust. However, major impediments are identified towards achieving this aim:

- Shear rates are unknown in blenders.
- Lack of correlations and understanding among processing variables, particle surface characteristics, and product performance.

The research presented in this dissertation provides the basis to study and overcome these problems:

7-5-1. Assessing the shear conditions of blending units

As already mentioned, the shear rates in most blenders are unknown and sometimes non-uniform. However, other units such as the controlled shear environment uniformly expose a blend to a known shear rate and strain. An attempt to establish the shear conditions in blenders would be to use the values for the some properties (hydrophobicity, density) measured at the outcome of the controlled shear environment could be potentially used in combination with the values obtained in the outcome of blending units to establish the shear conditions in the latter. The results of a lubrication process are more amenable to carry out such statistical comparison between blenders and controlled shear environment. The reason is that an extensive property, at least in the sample size of interest, such as density or hydrophobicity is analyzed. A process such as the API de-agglomeration in blenders and in the controlled shear environment may be more difficult to establish a comparison between their shear conditions because the agglomerate is a local event that, in many cases, goes undetected.

This type of study would involve the methodic sampling of a large number of units, of different scales, and with a variety of operating conditions and materials. Finally, the results would be statistically compared with those of the controlled shear environment.

7-5-2. Particle surface characteristics and dissolution

Published research shows that tablet hardness is affected by lubrication because the magnesium stearate particles insert between carrier (i.e. excipient) particles and alter their inter-particle forces. The results on blend hydrophobicity are evidence that surface properties of particles are modified, and they are expected to affect the disintegration and the dissolution of tablets. Tablet hardness and blend hydrophobicity depend on the particle surface characteristics, and they can be correlated with shear rate, strain, and lubricant concentration for a simple formulation of excipients and lubricant. However, when a drug is added into the formulation, the effect of shear rate, strain, lubricant, and drug concentration on tablet hardness, dissolution, and drug release are more difficult to anticipate. For example, when the API particle size distribution (PSD) is much smaller than the excipient particle size, an ordered mixture can be formed, and when API PSD is in the range of the excipient size, a random mixture is likely to be formed. An issue to be investigated is how the dissolution of random and ordered mixtures is affected by shear rate, strain, and lubricant content. One can hypothesize that, for ordered mixtures, the lubricant either coats the ensemble excipient-API, or that the lubricant particles will insert on the excipient surface, in between API particles. The hypothesis for a random mixture can be that the lubricant adheres indistinctly, or preferentially to the surface of excipients and API. The experiment proposed is to prepare different blends and test drug dissolution from a lubricated blend, and additionally perform surface characterization with adequate techniques. Additionally, tablets should be made and their dissolution and mechanical properties examined.

Since all these tablet properties are a function of the particle surface characteristics, it is possible to think that a method that characterizes particle surface on-line could be the basis and one of the elements to predict the product performance. Some preliminary tests on the electrical properties of particles have been carried out. For example, the impedance of a lubricated powder bed seems to be dependent on the lubricant concentration as well as on the shear treatment.

7-6. Closing remarks

Finding a solution to the two previous issues will facilitate the development of predictive correlations that will allow designing a process and selecting materials to produce a product with desired characteristics. The controlled shear environment should be used to study the correlation between processing conditions, particle surface characteristics, blend microstructure, and product performance for increasingly complex formulations. In other words, the controlled shear environment can be used as a formulation tool, to optimize the amount of excipients and additives used in a given product, or as a process development tool, to determine the optimum shear rate and the strain for a given product. The results presented in this dissertation are clear examples of these uses and open new possibilities for the improvement of the pharmaceutical manufacturing.

Curriculum Vita

Marcos Llusá

EDUCATION

B.S. Chemical Engineering May 1997
National University of Rio Cuarto, Argentina
M.S. Chemical Engineering May 2002
Department of Chemical and Biochemical Engineering, Rutgers University.
Ph.D. Chemical Engineering May 2008
Department of Chemical and Biochemical Engineering, Rutgers University

WORK EXPERIENCE

Research Assistant March 1996 – March 1997
Department of Chemistry, National University of Rio Cuarto, Argentina
Field Engineer October 1997 – February 1999
TOTAL, Tierra del Fuego, Argentina
Research Assistant June 2002 – May 2008
Department of Chemical Engineering, Rutgers University

PUBLICATIONS

1. F.J. Muzzio, M. Levin, K.R. Morris, M. Ierapetritou, P. Portillo, A. Alexander, Marcos Llusá, J.L.P. Soh, R.J. McCann. A forward-looking approach to process scale-up for solid dose manufacturing. Chapter to be published in the "Pharmaceutical Dosage Forms - Tablets Volume III", 3rd Edition, 2008, Stephen W. Hoag and Larry L. Augsburger Editors.

2. M. Llusá, F.J. Muzzio. Introduction to studies in granular mixing. Submitted to *Chemical Engineering Education*. October 2007.

3. M. Llusá, K. Sturm, O. Sudah, H. Stamato, D. J. Goldfarb, H. Ramachandruni, S. Hammond, M.R. Smith, and F. J. Muzzio. Mitigating API agglomeration. Submitted to International Journal of Pharmaceutics. October 2007.

4. M. Llusá, F.J. Muzzio. A quantitative method for reconstructing blend composition distributions in the presence of agglomerates. Accepted for publication *Journal of Pharmaceutical Innovation,* May 2007.

5. F.J. Muzzio, M. Llusá, C.L. Goodridge, Nhat-Hang Duong, E. Shen. Evaluating the mixing performance of a ribbon blender. Accepted for publication in *Powder Technology*, July 2007.

6. M. Llusá, A. Mehrotra, A.M. Faqih, M. Levin and F.J. Muzzio. Influence of shear intensity and total shear on properties of lubricated pharmaceutical blends and tablets. *International Journal of Pharmaceutics* (2006).

7. M. Llusá, F.J. Muzzio. The Effect of Shear Mixing on the Blending of Cohesive Lubricants and Drugs. *Pharmaceutical Technology,* Dec 1, 2005.

8. G.M. Morales, M. Llusá, M.C. Miras and C. Barbero. Effects of high hydrochloric acid concentration on aniline chemical polymerization. *Polymer,* Volume 38, Issue 20, Pages 5247-5250, 1997.